Organization 1600 Bldg/Room REM

United States Patent and Trademark Office
P.O. Box 1450
Alexandria, VA 22313-1450
If Undeliverable Return in Ten Days

OFFICIAL BUSINESS
PENALTY FOR PRIVATE USE, $300

RETURNED FOR POSTAGE

AN EQUAL OPPORTUNITY EMPLOYER

2_87

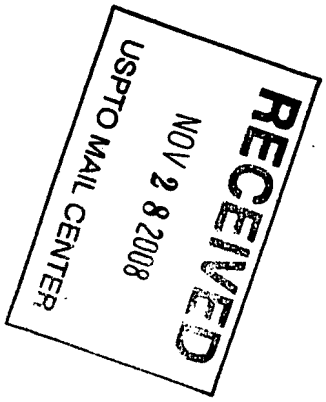

UNITED STATES PATENT AND TRADEMARK OFFICE

UNITED STATES DEPARTMENT OF COMMERCE
United States Patent and Trademark Office
Address: COMMISSIONER FOR PATENTS
P.O. Box 1450
Alexandria, Virginia 22313-1450
www.uspto.gov

APPLICATION NO.	FILING DATE	FIRST NAMED INVENTOR	ATTORNEY DOCKET NO.	CONFIRMATION NO.
10/814,634	04/01/2004	Tania Kastelic	608352000100	8704

25226 7590 11/26/2008

MORRISON & FOERSTER LLP
755 PAGE MILL RD
PALO ALTO, CA 94304-1018

EXAMINER	
QIAN, CELINE X	

ART UNIT	PAPER NUMBER
1636	

MAIL DATE	DELIVERY MODE
11/26/2008	PAPER

Please find below and/or attached an Office communication concerning this application or proceeding.

The time period for reply, if any, is set in the attached communication.

Office Action Summary	Application No.	Applicant(s)	
	10/814,634	KASTELIC ET AL.	
	Examiner	Art Unit	
	CELINE X. QIAN	1636	

-- The MAILING DATE of this communication appears on the cover sheet with the correspondence address --

Period for Reply

A SHORTENED STATUTORY PERIOD FOR REPLY IS SET TO EXPIRE 3 MONTH(S) OR THIRTY (30) DAYS, WHICHEVER IS LONGER, FROM THE MAILING DATE OF THIS COMMUNICATION.

- Extensions of time may be available under the provisions of 37 CFR 1.136(a). In no event, however, may a reply be timely filed after SIX (6) MONTHS from the mailing date of this communication.
- If NO period for reply is specified above, the maximum statutory period will apply and will expire SIX (6) MONTHS from the mailing date of this communication.
- Failure to reply within the set or extended period for reply will, by statute, cause the application to become ABANDONED (35 U.S.C. § 133). Any reply received by the Office later than three months after the mailing date of this communication, even if timely filed, may reduce any earned patent term adjustment. See 37 CFR 1.704(b).

Status

1)☒ Responsive to communication(s) filed on *05 June 2008*.

2a)☒ This action is **FINAL**. 2b)☐ This action is non-final.

3)☐ Since this application is in condition for allowance except for formal matters, prosecution as to the merits is closed in accordance with the practice under *Ex parte Quayle*, 1935 C.D. 11, 453 O.G. 213.

Disposition of Claims

4)☒ Claim(s) *9,10,13-15,24-36 and 38-49* is/are pending in the application.

4a) Of the above claim(s) *10,13 and 14* is/are withdrawn from consideration.

5)☐ Claim(s) _____ is/are allowed.

6)☒ Claim(s) *9,15,24-36 and 38-49* is/are rejected.

7)☐ Claim(s) _____ is/are objected to.

8)☐ Claim(s) _____ are subject to restriction and/or election requirement.

Application Papers

9)☐ The specification is objected to by the Examiner.

10)☒ The drawing(s) filed on *01 April 2004* is/are: a)☒ accepted or b)☐ objected to by the Examiner.

Applicant may not request that any objection to the drawing(s) be held in abeyance. See 37 CFR 1.85(a).

Replacement drawing sheet(s) including the correction is required if the drawing(s) is objected to. See 37 CFR 1.121(d).

11)☐ The oath or declaration is objected to by the Examiner. Note the attached Office Action or form PTO-152.

Priority under 35 U.S.C. § 119

12)☐ Acknowledgment is made of a claim for foreign priority under 35 U.S.C. § 119(a)-(d) or (f).

a)☐ All b)☐ Some * c)☐ None of:

1.☐ Certified copies of the priority documents have been received.

2.☐ Certified copies of the priority documents have been received in Application No. _____.

3.☐ Copies of the certified copies of the priority documents have been received in this National Stage application from the International Bureau (PCT Rule 17.2(a)).

* See the attached detailed Office action for a list of the certified copies not received.

Attachment(s)

1) ☒ Notice of References Cited (PTO-892)
2) ☐ Notice of Draftsperson's Patent Drawing Review (PTO-948)
3) ☐ Information Disclosure Statement(s) (PTO/SB/08) Paper No(s)/Mail Date _____.
4) ☐ Interview Summary (PTO-413) Paper No(s)/Mail Date. _____ .
5) ☐ Notice of Informal Patent Application
6) ☐ Other: _____.

DETAILED ACTION

Claims 9, 10, 13-15, 24-36, 38-49 are pending in the application. Claims 10, 13 and 14 are withdrawn from consideration for being directed to non-elected subject matter. Claims 9, 15, 24-36 and 38-49 are currently under examination.

Response to Amendment

The rejection of claims 9, 15, 23-29 under 35 U.S.C.112 1st paragraph has been withdrawn in light of Applicant's amendment.

The rejection of claims 30-39 under 35 U.S.C.112 2nd paragraph has been withdrawn in light of Applicant's amendment.

The rejection of claims 9, 24-27, 29-34, 36-39 under 35 U.S.C.102 (b) has been withdrawn in light of Applicants' amendment.

Claims 9, 15, 24-36, 38-49 are rejected under 35 U.S.C.103 (a) for reason discussed below, necessitated by Applicant's amendment.

New Grounds of Rejection Necessitated by Amendment

Claim Rejections - 35 USC § 103

The following is a quotation of 35 U.S.C. 103(a) which forms the basis for all obviousness rejections set forth in this Office action:

> (a) A patent may not be obtained though the invention is not identically disclosed or described as set forth in section 102 of this title, if the differences between the subject matter sought to be patented and the prior art are such that the subject matter as a whole would have been obvious at the time the invention was made to a person having ordinary skill in the art to which said subject matter pertains. Patentability shall not be negatived by the manner in which the invention was made.

This application currently names joint inventors. In considering patentability of the claims under 35 U.S.C. 103(a), the examiner presumes that the subject matter of the various claims was commonly owned at the time any inventions covered therein were made absent any

evidence to the contrary. Applicant is advised of the obligation under 37 CFR 1.56 to point out the inventor and invention dates of each claim that was not commonly owned at the time a later invention was made in order for the examiner to consider the applicability of 35 U.S.C. 103(c) and potential 35 U.S.C. 102(e), (f) or (g) prior art under 35 U.S.C. 103(a).

Claims 9, 15, 24-27, 29-34, 36, 38-41 and 49 are rejected under 35 U.S.C. 103(a) as being unpatentable over Zubiaga et al., in view of Banholzer et al.

Zubiaga et al. disclose an expression vector comprising *c-fos* promoter operatively linked to globin gene, wherein several ARE isolated from *c-fos* is inserted into 3'UTR of the globin gene, pBBB+ARE, resulting in sets of cell lines comprises different expression constructs. Zubiaga et al. also disclose a control plasmid pBΔARE, in which it comprises the 53bp 3' UTR from c-fos inserted downstream of β-globin stop codon (see page 2220, 2nd col., Result section, 1st paragraph). Zubiaga et al. also disclose that a plasmid pRSV-lacZ, comprising a gene coding for expression of lacZ, 5'and 3'UTR for expression of said gene without mRNA instability sequence (see page 2221, 1st col., 2nd paragraph, lines 4-9), which serves as an internal control for correction for variations in transfection efficiency. Zubiaga et al. further disclose a second control plasmid pGB-ARE contains a fragment from GAPDH coding sequence inserted in frame within the 5' half of the globin coding region, and same elements from pBBB+ARE (see page 2221, bridging paragraph). Lastly, Zubiaga et al. disclose that the internal control construct, the second control plasmid pGB-ARE and the expression plasmid pBBB+ARE are co-transfected into NIH-3T3 cells (see page 2221, 1st col., 2nd paragraph, lines 1-4), and plasmid constructs comprising different ARE sequence are transfected separately into NIH-3T3 cells (see for example, Figure 1). Zubiaga et al. do not teach an assay system for screening compounds which

destabilize mRNA that comprises a cell line as claimed in claim 9 and a test compound, and wherein the cell line is stably transfected.

Banholzer et al. disclose that rapamycin promotes degradation of IL-3 transcripts at posttranscriptional level via 3' UTR (see page 3257, 2nd col., 1st paragraph). Banholzer et al. disclose two cell lines stably transfected with IL-3 expression system either with (VD1-M1) or without (VD1-M1ΔAU) mRNA instability sequence (3' UTR) (see page 3256, 1st col., lines 1-3). Banholzer et al. teach that the cell lines V2D1, V3D6 are autocrine tumor cell lines, as such the cell lines are of native cell type in which the IL3 RNA instability sequence is produced (see page 3255, 2nd col., Result section: 1st paragraph). Banholzer et al. also disclose that following rapamycin and FK506 treatment, endogenous and exogenous wild type IL-3 decayed with very similar kinetics (see Figure 3b, left panel) whereas the exogenous mutant IL-3 mRNA level is not affected by either compound (Figure 3b, right panel, and 3c). The method and assay system disclosed by Banholzer et al. identifies rapamycin and FK506 as compounds that induce mRNA degradation.

It would have been obvious for one of ordinary skill in the art to develop an assay system as taught by Banholzer that is able to screen compounds such as rapalogs for their ability to modulating the mRNA instability sequence. Based on the teaching of Zubiaga, the ordinary skilled in the art would have been motivated to screening compounds that would affect ARE sequence instability using the heterologous expression construct as disclosed in Zubiaga et al. One of ordinary skill in the art would also be motivated to use stably transfected cell lines because they are easy to maintain such that one does not have to do transfection every time to test a compound. The level of skill in the art is high. Absent evidence from the contrary, one of

ordinary skilled in the art would have reasonable expectation of success to use the cell line taught by Zubiaga as a system to test compounds and make the cell line a stably transfected cell for said purpose. Therefore, the claimed invention would have been *prima facie* obvious at the time the invention was made.

Claims 28 and 35 are rejected under 35 U.S.C. 103(a) as being unpatentable over Zubiaga et al., in view of Banzohler et al., as applied to claims 9, 15, 24-27, 29-34, 36, 38, 39, 41 and 49, and further in view of Lemm and Ross (Molecular and Cellular Biology, 2002, Vol 22, No.12, pages 3959-3969).

The teachings of Zubiaga and Banzholer et al. are discussed above. However, Zubiaga and Banzholer et al. references do not teach a coding region instability determinant as the instability sequence.

Lemm and Ross teach a 249 nucleotide coding region from c-myc destabilizes c-myc mRNA. Lemm and Ross also teach that said nucleotide sequence destabilizes beta-globin mRNA when inserted in frame within the coding region of said beta-globin gene (see page 3959, 2nd col., 2nd paragraph).

The obviousness of making a stably transfected cell line comprising constructs coding for a protein with instability sequences and use said cell line to identify compound that affect stability of the sequences were discussed above. It would have been obvious to one of ordinary skill in the art to use the cell lines with constructs that have instability sequence as taught by Zubiaga et al. and/or Banzholer to test compounds that affect coding region instability determinants (CRD) from c-myc based on the combined teaching of Zubiaga, Banzholer and Lemm and Ross. The ordinary artisan would insert the CRD into the expression construct as

taught by either Zubiaga or Banzholer and determine whether such instability is modulate by any compound such as the Rapamycin destabilizes IL-3 mRNA. All the claimed elements were known in prior art and one skilled in the art could have combined the elements as claimed by known methods with no change in their respective functions, and the combination would have yielded predictable results to one of ordinary skill in the art at the time the invention was made. Absent evidence from the contrary, the ordinary artisan would have reasonable expectation of success to insert the CRD into a construct which can then be stably transfected into a cell line for testing compounds. Therefore, the invention would have been *prima facie* obvious to one of ordinary skill in the art at the time the invention was made.

As for the priority date for claims 28 and 35, it does not enjoy the priority to the 09/869,159 application because the limitation of "DNA corresponding to one or more CRD from the coding region of said naturally occurring genes" is not described in the '159 application. The instant application is a CIP of the '159 application, and the newly presented material in the instant application has priority date of the instant application, which is 4/1/04. Therefore, the Lemm and Ross references published in 2002 is considered as prior art for this reason.

Claim 43 and 47 are rejected under 35 U.S.C. 103(a) as being unpatentable over Zubiaga et al., in view of Banzohler et al., as applied to claims 9, 15, 24-27, 29-34, 36, 38, 39, 41 and 49, and further in view of Kastelic et al (Cytokine, 1996. Vol. 8, No. 10, pages 751-761).

The teachings of Zubiaga and Banzholer et al. are discussed above. However, Zubiaga and Banzholer et al. references do not teach the instability sequence is from the gene coding for IL-1β.

Kastelic et al. teach IL-1β, IL-6 and TNF-α mRNA comprises instability sequence AUUUA, in the 3' UTR (see page 757, Table 1). Kastelic et al. further teach that said AU elements are sufficient to confer the destabilizing effect of radicicol analogue A in an reporter gene expression system (see page 758, 1st col., 2nd paragraph).

The obviousness of making a stably transfected cell line comprising constructs coding for a protein with instability sequences and use said cell line to identify compound that affect stability of the sequences were discussed above. It would have been obvious to one of ordinary skill in the art to use the cell lines with constructs that have instability sequence as taught by Zubiaga et al. and/or Banzholer to test compounds that affect the AUUUA mRNA instability sequence from IL-1β and TNF-α based on the combined teaching of Zubiaga, Banzholer and Kastelic et al. The ordinary artisan would insert the AUUUA instability sequence from IL-1β and TNF-α into the expression construct as taught by either Zubiaga or Banzholer and determine whether such instability is modulate by any compound other than radicicol analogue A. All the claimed elements were known in prior art and one skilled in the art could have combined the elements as claimed by known methods with no change in their respective functions, and the combination would have yielded predictable results to one of ordinary skill in the art at the time the invention was made. Absent evidence from the contrary, the ordinary artisan would have reasonable expectation of success to insert the AUUUA instability sequence from IL-1β and TNF-α into a construct which can then be stably transfected into a cell line for testing compounds. Therefore, the invention would have been *prima facie* obvious to one of ordinary skill in the art at the time the invention was made.

Claim 48 is rejected under 35 U.S.C. 103(a) as being unpatentable over Zubiaga et al., in view of Banzohler et al., as applied to claims 9, 15, 24-27, 29-34, 36, 38, 39, 41 and 49, and further in view of Levy et al (JBC, 1996, Vol. 271, No. 5, pages 2746-2753).

The teachings of Zubiaga and Banzholer et al. are discussed above. However, Zubiaga and Banzholer et al. references do not teach the instability sequence is from the gene coding for VEGF.

Levy et al. teach 3'UTR from the VEGF coding sequence comprises AU rich sequences that may be responsible for the increased expression of VEGF in response to hypoxia (see page 2749, 2nd col., 4th paragraph), wherein deletion of the sequences increases the mRNA stability (see page 2748, 1st col., last paragraph).

The obviousness of making a stably transfected cell line comprising constructs coding for a protein with instability sequences and use said cell line to identify compound that affect stability of the sequences were discussed above. It would have been obvious to one of ordinary skill in the art to use the cell lines with constructs that have instability sequence as taught by Zubiaga et al. and/or Banzholer to test compounds that affect the AUUUA mRNA instability sequence from VEGF based on the combined teaching of Zubiaga, Banzholer and Levy et al. The ordinary artisan would insert the AUUUA instability sequence from VEGF into the expression construct as taught by either Zubiaga or Banzholer and determine whether such instability is modulate by test compounds similar to the effect of hypoxia. All the claimed elements were known in prior art and one skilled in the art could have combined the elements as claimed by known methods with no change in their respective functions, and the combination would have yielded predictable results to one of ordinary skill in the art at the time the invention

was made. Absent evidence from the contrary, the ordinary artisan would have reasonable expectation of success to insert the AUUUA instability sequence from VEGF into a construct which can then be stably transfected into a cell line for testing compounds. Therefore, the invention would have been *prima facie* obvious to one of ordinary skill in the art at the time the invention was made.

Claim 44 is rejected under 35 U.S.C. 103(a) as being unpatentable over Zubiaga et al., in view of Banzohler et al., as applied to claims 9, 15, 24-27, 29-34, 36, 38, 39, 41 and 49, and further in view of Rajagopalan et al (Journal of Neurochem. 2000. Vol74, pages 52-59).

The teachings of Zubiaga and Banzholer et al. are discussed above. However, Zubiaga and Banzholer et al. references do not teach the instability sequence is from the gene coding for APP.

Ragagopalan et al. teach that a 29 nt nucleotide in the 3'UTR of the APP gene confers instability of the APP mRNA, wherein its function may be inhibited by a combination of growth factors (see abstract, and page 55, 2nd col., through page 56, 1st col. and Figure 3).

The obviousness of making a stably transfected cell line comprising constructs coding for a protein with instability sequences and use said cell line to identify compound that affect stability of the sequences were discussed above. It would have been obvious to one of ordinary skill in the art to use the cell lines with constructs that have instability sequence as taught by Zubiaga et al. and/or Banzholer to test compounds that affect the 29nt mRNA instability sequence from APP based on the combined teaching of Zubiaga, Banzholer and Rajagopalan et al. The ordinary artisan would insert the 29nt instability sequence from APP into the expression construct as taught by either Zubiaga or Banzholer and determine whether such instability is

modulate by test compounds similar to the effect of growth factors. All the claimed elements were known in prior art and one skilled in the art could have combined the elements as claimed by known methods with no change in their respective functions, and the combination would have yielded predictable results to one of ordinary skill in the art at the time the invention was made. Absent evidence from the contrary, the ordinary artisan would have reasonable expectation of success to insert the 29nt instability sequence from APP into a construct which can then be stably transfected into a cell line for testing compounds. Therefore, the invention would have been *prima facie* obvious to one of ordinary skill in the art at the time the invention was made.

The priority date for claim 44 is determined as 4/1/04, which is the filing date of the instant application. This claim does not enjoy the priority to the 09/869,159 application because the limitation of "mRNA instability sequence from APP gene" is not described in the '159 application. The instant application is a CIP of the '159 application, and the newly presented material in the instant application has priority date of the instant application, which is 4/1/04. Therefore, the Rajagopalan reference published in 2000 qualifies as prior art.

Claim 45 is rejected under 35 U.S.C. 103(a) as being unpatentable over Zubiaga et al., in view of Banzohler et al., as applied to claims 9, 15, 24-27, 29-34, 36, 38, 39, 41 and 49, and further in view of Capaccioli et al. (Oncogene, 1996, Vol.13, pages 106-115).

The teachings of Zubiaga and Banzholer et al. are discussed above. However, Zubiaga and Banzholer et al. references do not teach the instability sequence is from the gene coding for bcl-2α.

Capaccioli et al. teach that bcl-2/Ig H expression is up-regulated in t(14,18) cells by treating cells with antisenses to the hybrid gene. Capaccioli et al. also teach that there is an AU

rich region at the 5' end of the 3' UTR of the bcl-2/IgH gene which might be masked by the antisense, such that the expression is increased. Capaccioli et al. teach that this AU motif is repeated in this region and highly conserved in mouse, chicken and human bcl-2 genes (see page 112, 2nd col.)

The obviousness of making a stably transfected cell line comprising constructs coding for a protein with instability sequences and use said cell line to identify compound that affect stability of the sequences were discussed above. It would have been obvious to one of ordinary skill in the art to use the cell lines with constructs that have instability sequence as taught by Zubiaga et al. and/or Banzholer to test compounds that affect the AU rich motif mRNA instability sequence from bcl-2 based on the combined teaching of Zubiaga, Banzholer and Capaccioli et al. The ordinary artisan would insert the AU rich instability sequence from bcl-2 gene into the expression construct as taught by either Zubiaga or Banzholer and determine whether such instability is modulate by test compounds or other factors that would regulate post transcriptional bcl-2 gene expression. All the claimed elements were known in prior art and one skilled in the art could have combined the elements as claimed by known methods with no change in their respective functions, and the combination would have yielded predictable results to one of ordinary skill in the art at the time the invention was made. Absent evidence from the contrary, the ordinary artisan would have reasonable expectation of success to insert the AU rich instability sequence from bcl-2 into a construct which can then be stably transfected into a cell line for testing compounds. Therefore, the invention would have been *prima facie* obvious to one of ordinary skill in the art at the time the invention was made.

Claim 46 is rejected under 35 U.S.C. 103(a) as being unpatentable over Zubiaga et al., in view of Banzohler et al., as applied to claims 9, 15, 24-27, 29-34, 36, 38, 39, 41 and 49, and further in view of Yeilding et al (Molecular and Cellular Biology, 1996.Vol. 16, No. 7, pages 3511-3522).

The teachings of Zubiaga and Banzholer et al. are discussed above. However, Zubiaga and Banzholer et al. references do not teach the instability sequence is from the gene coding for VEGF.

Yeilding et al. teach that the 3'UTR and exon 3 of the c-myc gene coding sequence comprises sequences that are responsible for maintaining low level of mRNA during myoblast differentiation (see page bridging paragraph from page 3513-3514), wherein deletion of the sequences increases the mRNA stability (see page 3517, 1st col-2nd col., and bridging paragraph of page 3518-3519).

The obviousness of making a stably transfected cell line comprising constructs coding for a protein with instability sequences and use said cell line to identify compound that affect stability of the sequences were discussed above. It would have been obvious to one of ordinary skill in the art to use the cell lines with constructs that have instability sequence as taught by Zubiaga et al. and/or Banzholer to test compounds that affect the mRNA instability sequence from c-myc based on the combined teaching of Zubiaga, Banzholer and Yielding et al. The ordinary artisan would insert the 3'UTR or the exon 3 instability sequence from c-myc into the expression construct as taught by either Zubiaga or Banzholer and determine whether such instability is modulate by test compounds similar that regulates c-myc expression. All the claimed elements were known in prior art and one skilled in the art could have combined the

elements as claimed by known methods with no change in their respective functions, and the combination would have yielded predictable results to one of ordinary skill in the art at the time the invention was made. Absent evidence from the contrary, the ordinary artisan would have reasonable expectation of success to insert the instability sequences from c-myc into a construct which can then be stably transfected into a cell line for testing compounds. Therefore, the invention would have been *prima facie* obvious to one of ordinary skill in the art at the time the invention was made.

Claim 42 is rejected under 35 U.S.C. 103(a) as being unpatentable over Zubiaga et al., in view of Banzohler et al., as applied to claims 9, 15, 24-27, 29-34, 36, 38, 39, 41 and 49, and further in view of Zhang et al (Biochemical and Biophysical Research Communications, 1996. Vol. 227, No.3, pages 707-711).

The teachings of Zubiaga and Banzholer et al. are discussed above. However, Zubiaga and Banzholer et al. references do not teach the detectable signal is detected directly.

Zhang et al. teach several reporter genes, such as secreted alkaline phosphatase, B-gal, firefly luciferase, CAT and GFP can be used in *in vivo* reporter assays (see page 707, 3rd paragraph). Zhang et al. further teach that GFP is an important reporter because it has advantages over other reporter for not requiring additional cofactors, substrates, or additional gene products. Zhang et al. further teach the generation of a humanized EGFP that has great sensitivity and stability (see bridging paragraph of 708 and 709).

It would have been obvious to one of ordinary skill in the art to develop a method of screening compound that modulate mRNA instability by using an expression cassette comprising a reporter in which the signal may be directly measured such as GFP reporter gene and a mRNA

instability sequence inserted into 3'UTR of said reporter gene based on the teaching of Banhozler et al., Zubiaga et al., and Zhang et al. Banhozler et al. has demonstrated that compounds such as rapamycin can be tested for its ability to affect mRNA instability in a construct comprising the mRNA sequence down stream of the AP gene. Since the ARE instability region has already been identified as taught in Zubiaga et al., it can be inserted to 3'UTR of any known gene, including a reporter gene such as GFP. One of ordinary skill in the art would have been motivated to do so because the advantages offered by a GFP reporter over measuring mRNA stability by Northern blot, such as the non-invasive nature of direct measurement of fluorescent intensity. The level of skill in the art of molecular cloning is high. Absent evidence from the contrary, one of ordinary skill in the art would have reasonable expectation of success to make a stably transfected cell line comprising an expression cassette comprising a GFP reporter and mRNA instability sequence to screen for compounds that modulate mRNA instability. All the claimed elements were known in prior art and one skilled in the art could have combined the elements as claimed by known methods with no change in their respective functions, and the combination would have yielded predictable results to one of ordinary skill in the art at the time the invention was made. Therefore, the invention would have been *prima facie* obvious to one of ordinary skill of art at the time the invention was made.

Conclusion

No claims are allowed.

Applicant's amendment necessitated the new ground(s) of rejection presented in this Office action. Accordingly, **THIS ACTION IS MADE FINAL**. See MPEP § 706.07(a). Applicant is reminded of the extension of time policy as set forth in 37 CFR 1.136(a).

A shortened statutory period for reply to this final action is set to expire THREE MONTHS from the mailing date of this action. In the event a first reply is filed within TWO MONTHS of the mailing date of this final action and the advisory action is not mailed until after the end of the THREE-MONTH shortened statutory period, then the shortened statutory period will expire on the date the advisory action is mailed, and any extension fee pursuant to 37 CFR 1.136(a) will be calculated from the mailing date of the advisory action. In no event, however, will the statutory period for reply expire later than SIX MONTHS from the date of this final action.

Any inquiry concerning this communication or earlier communications from the examiner should be directed to CELINE X. QIAN whose telephone number is (571)272-0777. The examiner can normally be reached on 10-6:30 M-F.

If attempts to reach the examiner by telephone are unsuccessful, the examiner's supervisor, Joe Woitach Ph.D. can be reached on 571-272-0739. The fax phone number for the organization where this application or proceeding is assigned is 571-273-8300.

Information regarding the status of an application may be obtained from the Patent Application Information Retrieval (PAIR) system. Status information for published applications may be obtained from either Private PAIR or Public PAIR. Status information for unpublished applications is available through Private PAIR only. For more information about the PAIR system, see http://pair-direct.uspto.gov. Should you have questions on access to the Private PAIR system, contact the Electronic Business Center (EBC) at 866-217-9197 (toll-free). If you would like assistance from a USPTO Customer Service Representative or access to the automated information system, call 800-786-9199 (IN USA OR CANADA) or 571-272-1000.

/Celine X Qian Ph.D./
Primary Examiner, Art Unit 1636

Notice of References Cited	Application/Control No. 10/814,634	Applicant(s)/Patent Under Reexamination KASTELIC ET AL.	
	Examiner CELINE X. QIAN	Art Unit 1636	Page 1 of 2

U.S. PATENT DOCUMENTS

*		Document Number Country Code-Number-Kind Code	Date MM-YYYY	Name	Classification
	A	US-			
	B	US-			
	C	US-			
	D	US-			
	E	US-			
	F	US-			
	G	US-			
	H	US-			
	I	US-			
	J	US-			
	K	US-			
	L	US-			
	M	US-			

FOREIGN PATENT DOCUMENTS

*		Document Number Country Code-Number-Kind Code	Date MM-YYYY	Country	Name	Classification
	N					
	O					
	P					
	Q					
	R					
	S					
	T					

NON-PATENT DOCUMENTS

*		Include as applicable: Author, Title Date, Publisher, Edition or Volume, Pertinent Pages)
	U	Kastelic et al (Cytokine, 1996. Vol. 8, No. 10, pages 751-761).
	V	Levy et al (JBC, 1996, Vol. 271, No. 5, pages 2746-2753).
	W	Rajagopalan et al (Journal of Neurochem. 2000. Vol74, pages 52-59).
	X	Capaccioli et al. (Oncogene, 1996, Vol.13, pages 106-115).

*A copy of this reference is not being furnished with this Office action. (See MPEP § 707.05(a).)
Dates in MM-YYYY format are publication dates. Classifications may be US or foreign.

Notice of References Cited	Application/Control No. 10/814,634	Applicant(s)/Patent Under Reexamination KASTELIC ET AL.	
	Examiner CELINE X. QIAN	Art Unit 1636	Page 2 of 2

U.S. PATENT DOCUMENTS

*		Document Number Country Code-Number-Kind Code	Date MM-YYYY	Name	Classification
	A	US-			
	B	US-			
	C	US-			
	D	US-			
	E	US-			
	F	US-			
	G	US-			
	H	US-			
	I	US-			
	J	US-			
	K	US-			
	L	US-			
	M	US-			

FOREIGN PATENT DOCUMENTS

*		Document Number Country Code-Number-Kind Code	Date MM-YYYY	Country	Name	Classification
	N					
	O					
	P					
	Q					
	R					
	S					
	T					

NON-PATENT DOCUMENTS

*		Include as applicable: Author, Title Date, Publisher, Edition or Volume, Pertinent Pages)
	U	Yeilding et al (Molecular and Cellular Biology, 1996.Vol. 16, No. 7, pages 3511-3522).
	V	Zhang et al (Biochemical and Biophysical Research Communications, 1996. Vol. 227, No.3, pages 707-711).
	W	
	X	

*A copy of this reference is not being furnished with this Office action. (See MPEP § 707.05(a).)
Dates in MM-YYYY format are publication dates. Classifications may be US or foreign.

INDUCTION OF RAPID IL-1β mRNA DEGRADATION IN THP-1 CELLS MEDIATED THROUGH THE AU-RICH REGION IN THE 3′UTR BY A RADICICOL ANALOGUE

Tania Kastelic, Jörg Schnyder, Albert Leutwiler, René Traber[1]
Bruno Streit, Heinz Niggli, Andrew MacKenzie, Dominique Cheneval

A radicicol analogue (analogue A) was found to inhibit interleukin 1 beta (IL-1β) and tumour necrosis factor alpha (TNF-α) secretion from THP-1 cells. If added to cells activated by interferon gamma and lipopolysaccharide, radicicol analogue A not only inhibited the secretion of IL-1β but also induced an extremely rapid degradation of IL-1β, IL-6 and TNF-α mRNA to undetectable levels within 5–8 h. This degradation is independent of translation and of the signal inducing transcription. The common feature of these genes is the inclusion of one or more copies of the mRNA-instability sequence, AUUUA, in the 3′ untranslated region. Indeed, no destabilizing effect of radicicol analogue A could be observed on mRNA derived from the expression of an IL-1β construct lacking the AUUUA motifs of the 3′UTR. The effect of radicicol analogue A on protein/mRNA interaction and on post-translational modifications of cytoplasmic proteins is described. This class of compound constitutes a valuable tool for the further elucidation of the mechanism of mRNA degradation of cytokines and proto-oncogenes.

Interleukin 1 beta (IL-1β) is a major mediator of inflammation.[1,2] Together with tumour necrosis factor alpha (TNF-α), it contributes to the pathogenesis of inflammation and tissue destruction, e.g. in the joints of arthritis patients. IL-1β is synthesized primarily by monocytes as an inactive p33 precursor which is cleaved by the interleukin 1 beta-converting enzyme (ICE), to yield mature IL-1β.[3] Proof of the central role of these cytokines in inflammation is provided by the findings that IL-1 receptor antagonist (IL-1ra), soluble IL-1 receptor (IL-1sr) or antibodies to IL-1 and TNF-α, all block acute and chronic inflammatory responses in animal models.[4–7] Because IL-1β and TNF-α are both regulated at the transcriptional and translational level,[8,9] reduction in IL-1β levels represents an alternative means of inhibiting the inflammatory response.

THP-1 cells, after differentiation with interferon gamma (IFN-γ), mimic native monocyte-derived macrophages in several respects,[9,10] most importantly, in becoming responsive to both lipopolysaccharide (LPS) and phorbol-12-myristate-13-acetate (PMA), which stimulate the secretion of mature IL-1β and TNF-α. THP-1 cells provide a valuable model system for studying the mechanisms involved in cytokine processing and secretion.

It has become evident that besides being regulated at the transcriptional level, many eukaryotic genes are also regulated by the stability/instability of their mRNA. The mechanism of mRNA degradation and the existence of instability sequence determinants, only recently became the subject of detailed studies (for a review see Ref. 11). Several types of sequence elements have been identified which modulate mRNA decay rates, which can vary from minutes to over 24 h in an eukaryotic cell.[12] In 1986, Caput *et al.*[13] reported the identification of a sequence (TTATTTAT) in the 3′ untranslated region (3′UTR), common to inflammatory mediators and other transiently expressed genes, such as the immediate early gene, c-*fos*. Shaw and Kamen reported that these conserved AU-rich elements (AREs) in the 3′UTR, confer selective mRNA degradation.[14] Recently, TTATTTATT was determined to be the minimal consensus sequence necessary to confer instability.[15] However, neighbouring elements or the metabolic state of the cell type in which the gene is expressed, may also play a role.[16] Moreover, instability of granulocyte-macrophage colony-stimulating factor (GM-CSF) mRNA conferred by the AU motif requires active transcription and the presence of the AU motif in the 3′ UTR, between stop codon and polyA tail.[17] The AREs represent binding sites for both nuclear and cytoplasmic proteins.[17–26]

From the Sandoz Research Institute Berne, Inflammation, Monbijoustrasse 115 CH-3007 Bern, Switzerland and [1]Sandoz Pharma Ltd. CH-4002 Basel, Switzerland
Correspondence to: Dominique Cheneval
Received 8 February 1996; accepted for publication 15 May 1996

1043-4666/96/100751 + 11 $25.00/0

KEY WORDS: AUUUA motif/mRNA degradation/radicicol/THP-1/3′UTR

CYTOKINE, Vol. 8, No. 10 (October 1996: 751–761)

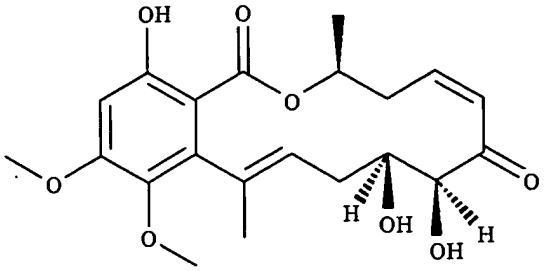

Figure 1. Chemical Structure of radicicol analogue A

The results presented here seem to indicate that the effects of radicicol analogue A seen on IL-1β mRNA and protein levels in THP-1 cells, are due to post-transcriptional regulation. We describe the rapid decay of IL-1β mRNA seen after addition of radicicol analogue A, and investigations into the mechanism of action of this compound.

RESULTS

Inhibition of the secretion of mature IL-1β from THP-1 cells

Radicicol analogue A, $C_{20}H_{24}O_8$, ((7*S*,12*S*,13*S*)-(9Z15E)-4,12,13-trihydroxy-1,2-dimethoxy-7-methyl-8,12,13,14-tetrahydro-7[H]-6-oxabenzocyclotetradecene-5,11-dione) (Fig. 1), was isolated from the fungus strain F/87-2509.04 after finding IL-1β inhibitory activity in a human monocyte/rabbit chondrocyte co-culture test.[27] This compound also inhibited the secretion of mature IL-1β from THP-1 cells. IC_{50} was 50 and 30 nM for IL-1β and TNF-α, respectively. After stimulation with IFN-γ and LPS, a lag of about 16 h occurred before IL-1β secretion significantly increased and reached maximal levels around 48 h. When added 5 min prior to IFN-γ, radicicol analogue A (1 μM) greatly reduced the levels of IL-1β secreted, and increased the lag to approximately 24 h after addition of LPS (Fig. 2). IL-1β mRNA levels in untreated cells, started to rise 2 h after LPS addition and reached a maximum at 16–24 h. However, in the presence of radicicol analogue A, mRNA expression was not detected until 16 h after LPS addition and was significantly reduced (Fig. 2, inset). Even though radicicol analogue A strongly inhibited the secretion up to about 24 h, the effect after this time was weakening. This appears to be due to a loss or consumption of the compound, because a second addition of compound at later times restored full inhibition. The inhibition of IL-1β mRNA accumulation was concentration dependent and could be observed at concentrations of

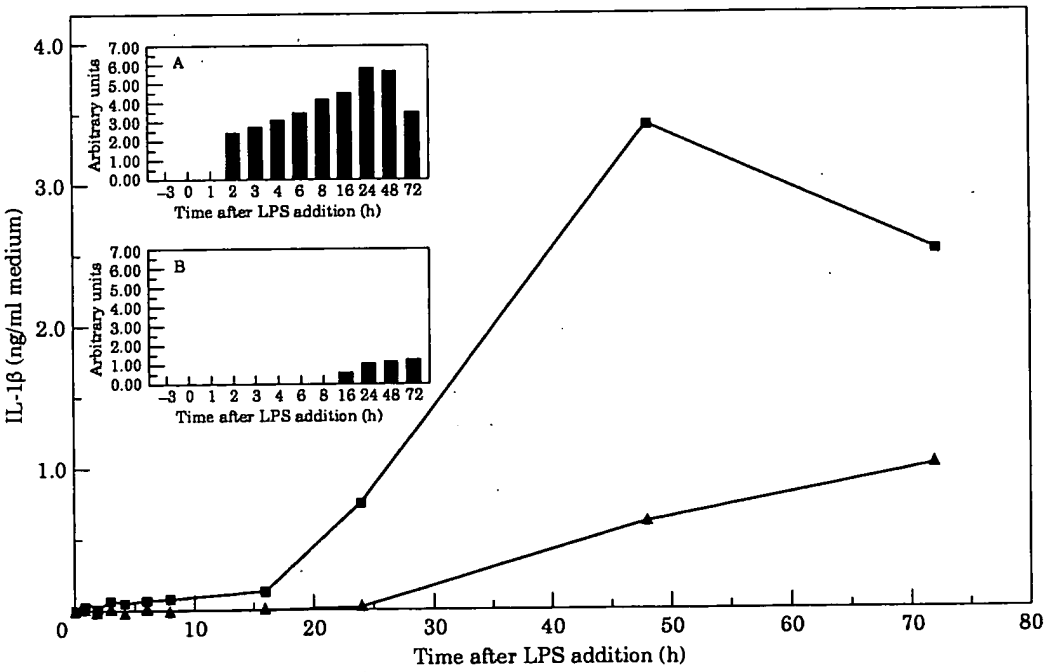

Figure 2. IL-1β secretion from THP-1 cells and IL-1β mRNA levels in THP-1 cells during differentiation in the absence and presence of radicicol analogue A.

Time course of IL-1β secretion from THP-1 cells measured by ELISA. The time indicated represents hours after LPS addition (see Materials and Methods). Cell media were harvested and centrifuged in an Eppendorf centrifuge for 5 min (12 000 × *g*). The supernatants were then assayed for IL-1β by ELISA. (■), no treatment; (▲), 1 μM radicicol analogue A added 5 min prior to IFN-γ addition. Insets: Total RNA was harvested at the indicated times and analysed for IL-1β mRNA by RT-PCR amplification and normalized to β-actin (see Materials and Methods). Time course of IL-1β gene expression during the differentiation of THP-1 cells in the absence (inset A) and the presence (inset B) of 1 μM radicicol analogue A.

radicicol analogue A in the nanomolar range (data not shown).

Induction of IL-1β mRNA degradation by radicicol analogue A

As shown in Figure 3A, radicicol analogue A when added 16 h after LPS stimulation, virtually abolished IL-1β secretion from THP-1 cells. In fact, this inhibition occurred even if radicicol analogue A was added as late as 24 h after LPS addition. To investigate this effect further, we treated THP-1 cells with actinomycin D 16 h after LPS addition and monitored IL-1β secretion at subsequent times. As depicted in Figure 3B, IL-1β release continues to increase after the addition of actinomycin D, presumably due to translation of mRNA present at the time of addition. Secretion completely stopped after adding cycloheximide (CHX). In this respect, CHX and radicicol analogue A behave similarly. In order to determine whether the effect of radicicol analogue A is simply due to an inhibition of transcription and the observed mRNA decrease reflects the normal half-life of IL-1β mRNA in THP-1 cells under our cell culture conditions, the effects of adding actinomycin D 16 h after LPS addition were compared. Based on IL-1β mRNA analysis in differentiated cells, maximal levels of IL-1β mRNA were present at this time. Eight hours after the addition of actinomycin D, the mRNA level for IL-1β was reduced to about 80% of its control value in contrast to the complete disappearance seen with radicicol analogue A at 1 μM (Fig. 4). Under these conditions, β-actin mRNA was unaffected (not shown).

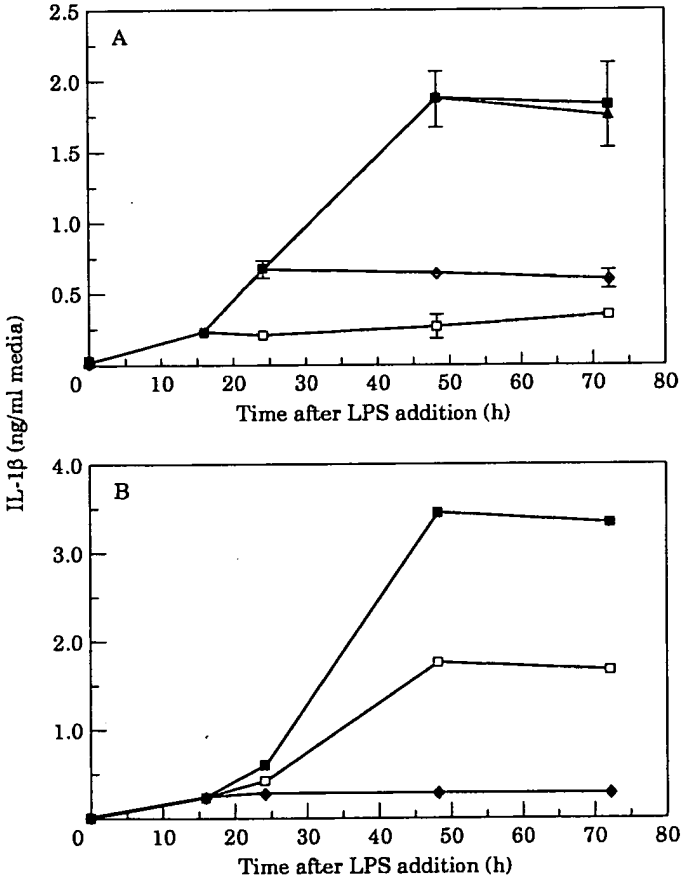

Figure 3. IL-1β secretion from THP-1 cells.

(A) After addition of radicicol analogue A. IL-1β secretion measured by ELISA is shown when radicicol analogue A (1 μM) is added at various times after the addition of LPS during the differentiation of THP-1 cells. (□), radicicol analogue A added at time = 16 h; (◆), radicicol analogue A added at time = 24 h; (▲), radicicol analogue A added at time = 48 h; (■), control, no compound added. (mean ± SD; $n = 3$, not shown when $P < 0.05$). (B) IL-1β secretion from THP-1 cells after addition of transcription and translation inhibitors. IL-1β secretion was measured by ELISA either after actinomycin D (10 μg/ml), (□), or cycloheximide (20 μM), (◆), were added to differentiating THP-1 cells 16 h after LPS addition. (■), control cells, no compound added. The figure represents a typical result of three experiments.

CYTOKINE, Vol. 8, No. 10 (October 1996: 751–761)

After actinomycin D treatment, mRNA continued to decrease to undetectable levels by 56 h. However, treatment with radicicol analogue A led to a re-appearance of IL-1β message by 56 h almost to the level seen in untreated cells, consistent with the loss of effect observed at the protein level described above. IL-1β mRNA appears to be very stable after addition of actinomycin D whereas radiciol analogue A induces a rapid disappearance of message. mRNA half-lives were determined to be 15 and 2 h for actinomycin D and radicicol analogue A, respectively. proIL-1β protein levels remained high for longer than 5 h after addition of radicicol analogue A, even though the mRNA for IL-1β had disappeared. Only after 8 h was a decrease in the level of proIL-1β protein in the presence of radicicol analogue A observed, most likely reflecting proIL-1β protein half-life (results not shown). In untreated control cells, the level of proIL-1β protein remained constant up to 32 h after LPS stimulation. However, as seen in Figure 3A, secretion of mature IL-1β, in the presence of radicicol analogue A, stopped immediately, raising the question of why processing and subsequent secretion of proIL-1β does not continue if the effect of radicicol analogue A is on mRNA degradation alone. One possible explanation relates to the observation that radicicol analogue A also inhibits the autocatalytic processing of p45 ICE to its active p10/p20 subunits (Ref. 28, P. Ramage and D. Cheneval unpublished observation). It is possible that the inhibition of post-translational processing and secretion might be functionally linked to the mRNA degradation effects of radicicol analogue A. Although a number of radicicol analogues were found to be capable of inhibiting IL-1β secretion from THP-1 cells, most of them had no effect on mRNA stability, suggesting two independent activities of radicicol analogue A (results not shown). Structural differences in the radicicol family apparently are able to determine different mechanisms of action. A number of recent reports conclude that RNA degradation is coupled to ongoing translation.[15–17] Even though CHX leads to a slight increase in mRNA levels for IL-1β (Fig. 4B, middle panel), radicicol analogue A could still induce mRNA degradation effectively in the presence of CHX, indicating that radicicol analogue A overrides any possible requirement for ongoing translation. PMA, which was reported to stabilize IL-1β mRNA in THP-1 cells,[29] also increased the half-life of GM-CSF mRNA compared to phytohaemagglutinin stimulated cells.[14] Interested to learn if PMA could compensate for the degradation induced by radicicol analogue A, THP-1 cells were stimulated with PMA instead of IFN-γ. Figure 4C shows that PMA had no effect on the efficacy of radicicol analogue A, suggesting that the mechanism of IL-1β mRNA degradation by radicicol analogue A is independent of the stimulant used. Since we had previously found that radicicol analogue A also inhibited the secretion of TNF-α and IL-6 from THP-1 cells, RT-PCR analysis of the same total RNA used in the experiment described in Figure 4A and B, was performed for TNF-α and IL-6 mRNA levels. Figure 5A shows the results of this analysis compared to the effect seen on IL-1β mRNA. Because a common feature of the genes shown in Figure 5A is the presence of an AU-rich mRNA instability sequence in the 3′ UTR, we decided to analyse a set of genes not containing this motif. As shown in Figure 5B, none of these genes were sensitive to radicicol analogue A.

Radicicol analogue A exerts its effect on IL-1β mRNA through the ARE in the 3′UTR

The correlation between a mRNA destabilizing effect of radicicol analogue A and the presence of an ARE, could be strengthened further by analysing a number of other ARE-containing genes (Table 1). However, molecular proof could only be obtained by a more detailed analysis of the role of the 3′UTR. In order to achieve this, a cDNA encoding human IL-1β containing 344 bp of 3′UTR which lacked the AUUUA rich domain (Fig. 6), was obtained by RT-PCR amplification of total RNA isolated from THP-1 cells. A mammalian expression vector (see Materials and Methods section) containing the IL-1β cDNA lacking the ARE-containing 3′UTR (pHD-neo2-hIL-1β-3′UTR), was transfected into THP-1 cells and selected with G418 to obtain stable clones. When radicicol analogue A was added to LPS-stimulated THP-1 cells containing the construct, a rapid decrease of endogenous IL-1β mRNA was observed by the RNase protection method, whereas a sustained

Figure 4. IL-1β mRNA levels in THP-1 cells

(A) In the presence of radicicol analogue A. 16 h after adding LPS to IFN-γ differentiated THP-1 cells, either actinomycin D (20 μg/ml) or radicicol analogue A (compound A), 1 μM was added and total RNA was harvested at the indicated times thereafter. Northern blot analysis for IL-1β was then carried out and the results compared to untreated cells. Indicated times are hours after addition of either actinomycin D or radicicol analogue A. (B) IL-1β mRNA levels in THP-1 cells in the presence of CHX and radicicol analogue A. THP-1 cells were differentiated with IFN-γ and 16 h after LPS addition, 20 μM cycloheximide alone or in combination with the radicicol analogue A was added. 1, 2, 5 and 8 h later, total RNA was isolated and analysed for IL-1β by Northern blotting. (C) IL-1β mRNA levels in THP-1 stimulated by PMA. THP-1 cells were differentiated and stimulated by adding 5 ng/ml of PMA instead of IFN-γ + LPS 16 h after the addition of PMA, radicicol analogue A was added. 1, 2, 5 and 8 h later, total RNA was isolated and analysed for IL-1β by Northern blotting. a: control, no compound added; b: in the presence of radicicol analogue A 1 μM; c: methylene blue staining as a control for equal loading.

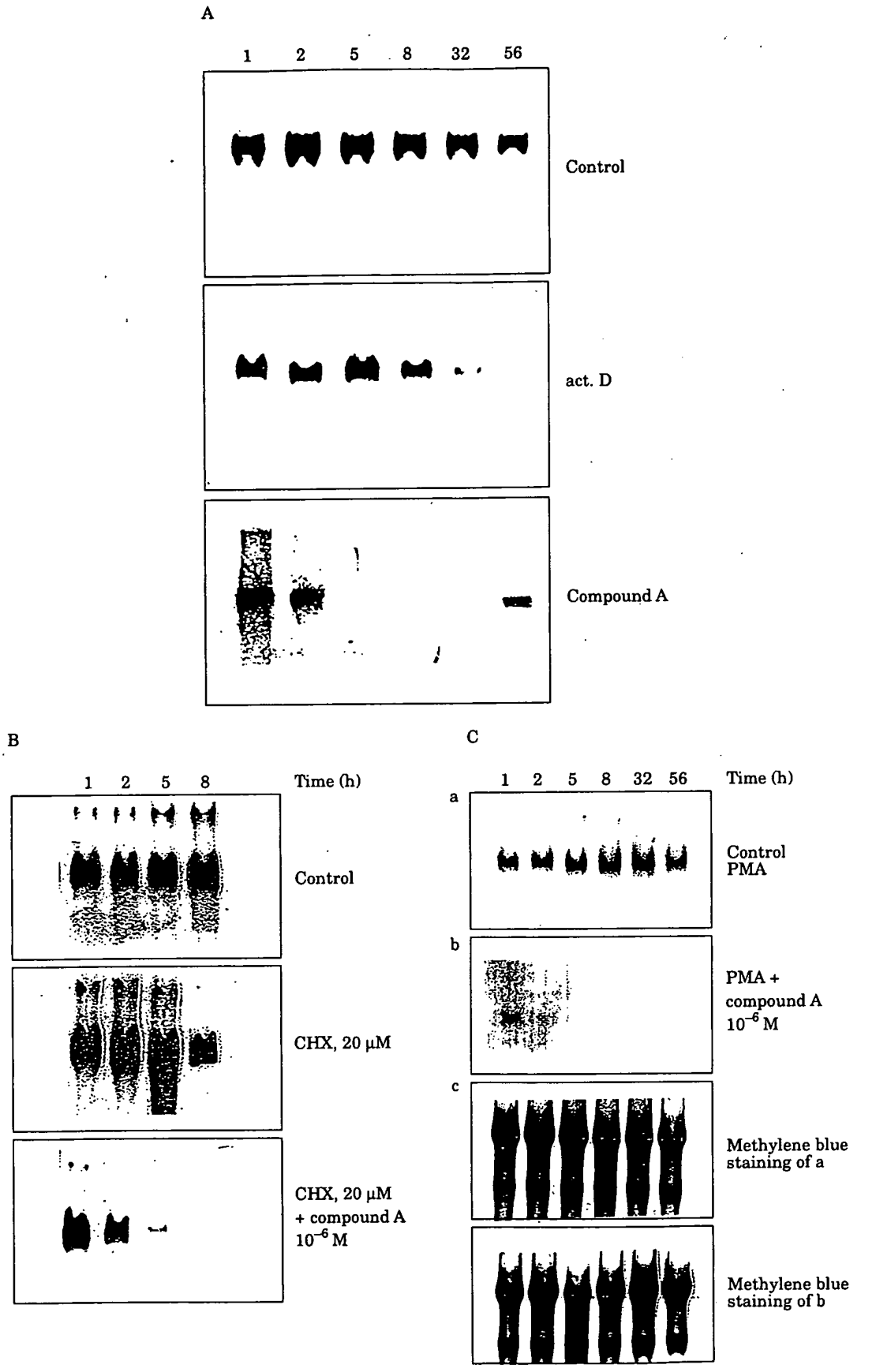

Figure 4—*caption opposite*

CYTOKINE, Vol. 8, No. 10 (October 1996: 751–761)

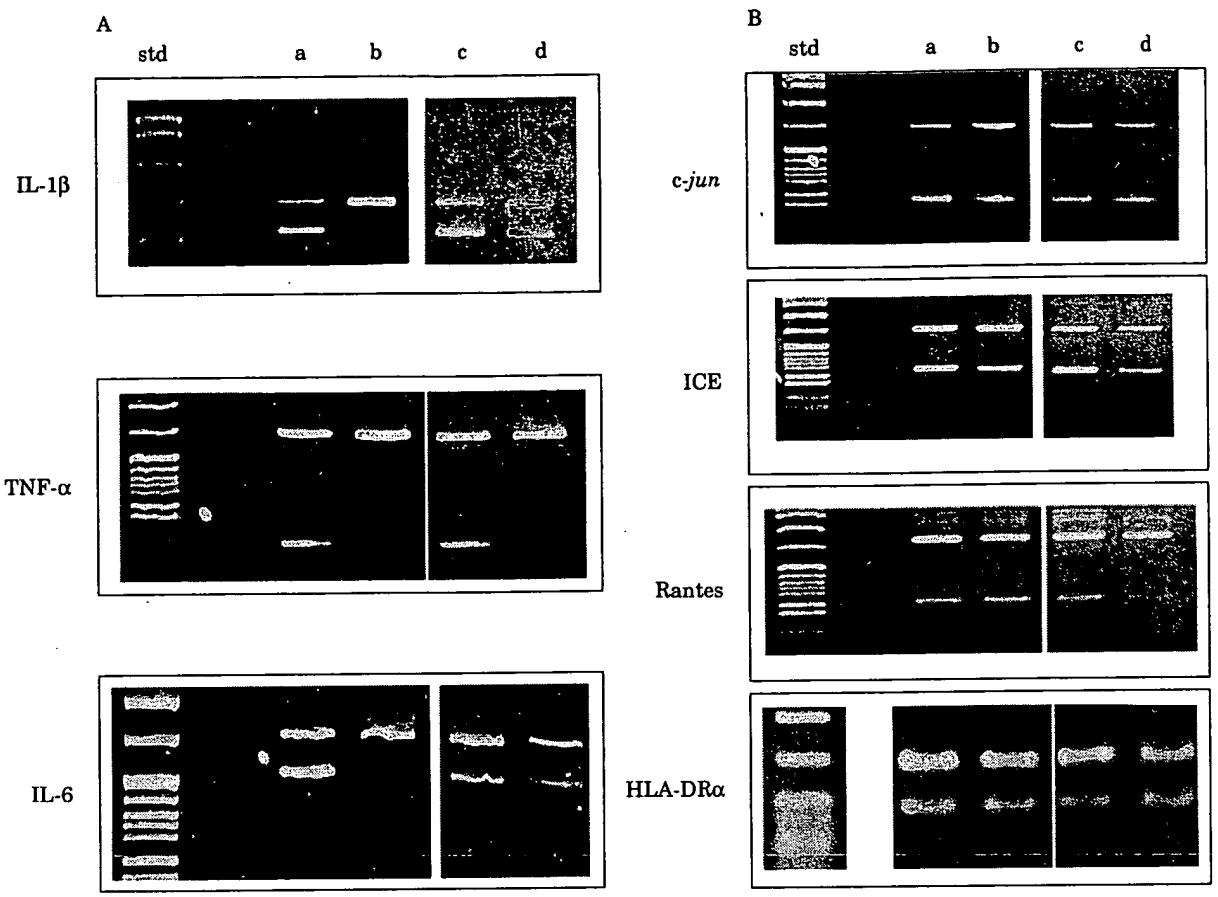

Figure 5. (A) RT-PCR analysis of total RNA for IL-1β, TNF-α, and IL-6. (B) RT-PCR analysis of total RNA for c-jun, ICE, Rantes and HLA-DRα.

std: molecular weight standard (*Msp*I digest of pBR322, NEB); a: control; b: radicicol analogue A, 1 μM; c: CHX, 20 μM; and d: actinomycin D, 20 μg/ml. Upper band: β-actin; lower band: gene as indicated on the left.

expression of exogenous mRNA was observed (Fig. 7). This result clearly shows that the effects of radicicol analogue A are mediated by the deleted portion of the 3′UTR containing the AU-rich region. Applying this method, we were able to show that all cell lines expressing exogenous mRNA lacking the AREs were not affected by radicicol analogue A, whereas endogenous IL-1β mRNA was rapidly degraded.

Influence of radicicol analogue A on the binding of protein(s) to the AU-rich region of the 3′UTR

Recently, a number of AUUUA binding proteins have been described, some of which have been implicated in RNA degradation. The authors were interested to know whether radicicol analogue A would directly influence binding of such a protein to this region. For this purpose, gel-shift assays were conducted using a riboprobe derived from the 240-bp end of the 3′UTR of IL-1β containing six AUUUA motifs. Interestingly, the appearance of an additional, LPS-independent band during the time course after IFN-γ-induced differentiation could be observed, which was not present in the extracts of undifferentiated cells. However, radicicol analogue A had no effect on the binding of cytoplasmic or nuclear proteins to the AU-rich region, either when added directly to the extracts or when extracts from cells treated with the radicicol analogue A were used (not shown), indicating an upstream effect on the mRNA binding of proteins. Radicicol analogue A was found to inhibit tyrosine phosphorylation of a number of proteins which are differentially expressed or differentially modified by a tyrosine kinase (Fig. 8). Based on these findings, we carried out supershift experiments using anti-phosphotyrosine antibodies. No further band shifts could be observed. Taken together, these results indicate that the effect of radicicol analogue A is not on direct protein/RNA interaction or on the state of phosphorylation of a protein/RNA complex at the AREs. Instead, it appears that radicicol analogue A modifies protein(s) which interact with AU-binding protein(s) but do not directly bind to the AREs. Whether the inhibitory effect on a tyrosine kinase is connected to the effects seen on mRNA, remains to be investigated.

TABLE 1. mRNA Instability Conferred by Radicicol Analogue A

mRNA	Containing AUUUA motifs	Sensitive to radicicol analogue A
IL-1β	yes	yes
TNF-α	yes	yes
IL-6	yes	yes
c-myc*	yes	yes
GM-CSF*	yes	yes
IL-2†	yes	yes
IL-3*	yes	yes
E-selectin‡	yes	yes
VCAM1‡	yes	yes
ICAM1‡	yes	yes
β-actin	no	no
HPRT	no	no
Rantes	no	no
c-jun	no	no
HLA-DRα	no	no
ICE	no	no

Shown are genes investigated on the basis of their sensitivity towards radicicol analogue A and a correlation to the presence of AU-rich motifs. *: mRNA steady state levels (G. Baumann, personal communication); ‡: observed in TNF-α stimulated HUVECS (D. Cheneval, G. Weitz, unpublished results); †: IL-2 reporter gene assay (G. Baumann, personal communication); ICE: IL-1β converting enzyme; HPRT: Hypoxanthine-guanine phosphoribosyl transferase; ICAM1: intercellular adhesion molecule 1; VCAM1: vascular cell adhesion molecule 1; HLA: human leukocyte antigen.

DISCUSSION

The underlying mechanism for the observation that radicicol analogue A inhibits mature IL-1β secretion from THP-1 cells seems to be the induction of mRNA instability. Radicicol analogue A (1 μM) causes a very rapid degradation of mRNA and an inhibition of secretion of mature IL-1β, which is probably due to the inhibition of p45 proICE autoprocessing. Changes in mRNA stability play an important role in modulating the level of expression of many eukaryotic genes (see Cleveland and Yen for review, Ref. 31). A number of compounds give precedence for lowering mRNA stability of cytokine and other gene transcripts, although their mechanism of action is unknown.[32-38] IL-1β mRNA stability has been reported to be decreased by dexamethasone,[32] an effect which could be inhibited by the glucocorticoid receptor antagonist, mefipristone (RU 486). This compound did not modify the effects of radicicol analogue A in the present system, indicating that its effects are not mediated by the glucocorticoid receptor (not shown). Cyclosporin A was also tested because Nair *et al.* recently reported that it mediated RNA degradation of IL-3 through the ARE.[39] Because it has been reported that radicicol[40] could act through tyrosine kinases,[41] tyrosine kinase inhibitors, such as herbimycin and genistein, were assayed for their effect on RNA degradation. However, of these compounds, only the radicicol analogs and to a lesser extent dexamethasone, had the ability to induce IL-1β mRNA degradation in THP-1 cells (results not shown).

Radicicol has recently been reported to reverse the transformation of *src*-transformed fibroblasts, an effect the authors correlated to the decrease of $p60^{src}$ autophosphorylation, as well as, other tyrosine-phosphorylated proteins.[42] In vitro, radicicol also inhibited autophosphorylation, as well as, transphosphorylation of $p60^{v\text{-}src}$.[43] Furthermore, a selective inhibition of Cox II (cyclooxygenase type II) but not Cox I expression, was reported for radicicol in LPS, but not PMA-stimulated macrophages.[43] Radicicol inhibited tyrosine phosphorylation of $p53/56^{lyn}$, a Src family tyrosine kinase and one of the major tyrosine-phosphorylation kinases in LPS-stimulated macrophages. Whether the inhibition of $p53/56^{lyn}$or another tyrosine kinase is responsible for the mRNA destabilizing effects of radicicol analogue A, is the subject of future studies. Radicicol itself was found to have IL-1β mRNA degrading abilities in our system, albeit less potent than radicicol analogue A. Radicicol analogue A also inhibited prostaglandin E_2 (PGE_2) release from THP-1 cells with an IC_{50} of

*GGACCAAAGG CGGCCAGGAT ATAACTGACT TCACCATGCA

ATTTGTGTCT TCCTAAAGAG AGCTGTACCC AGAGAGTCCT

GTGCTGAATG TGGACTCAAT CCCTAGGGCT GGCAGAAAGG

GAACAGAAAG GTTTTTGAGT ACGGCTATAG CCTGGACTTT

CCTGTTGTCT ACACCAATGC CCAACTGCCT GCCTTAGGGT

AGTGCTAAGA GGATCTCCTG TCCATCAGCC AGGACAGTCA

GCTCTCTCCT TTCAGGGCCA ATCCCAGCCC TTTTGTTGAG

CCAGGCCTCT CTCACCTCTC CTACTCACTT AAAGCCCGCC

TGACAGAAAC CAGGCCACAT TTTGGTTCTA AGAAACCCTC

CTCTGTCATT CGCTCCCACA TTCTGATGAG CAACCGCTTC

CCT**ATTTATTTATTTA**TTTG TTTGTTTGTT TTGATTCATT

GGTCTA***ATTTA*** TTCAAAGGG GGCAAGAAGT AGCAGTGTCT

GTAAAAGAGC CTAGTTTTTA ATAGCTATGG AATCAATTCA

ATTTGGACTG GTGTGCTCTC TTTAAATCAA GTCCTTTAAT

TAAGACTGAA AATATATAAG CTCAGATT***ATTTA***AATGGGA

AT***ATTTA***TAA ATGAGCAAAT ATCATACTGT TCAATGGTTC

TCA**AATAAA**C TTCACT

Figure 6. 3' Untranslated region of IL-1β mRNA.

The 3'UTR of human IL-1β is shown. AUUUA motifs are highlighted and italicized. The region downstream from the arrow was used for gel-retardation assays and was omitted in the construct used for THP-1 cell transfection and subsequent RNase protection assays (ΔAU-3'UTR). The region underlined was found to be sufficient to confer mRNA instability by the radicicol analogue A (results not shown).

CYTOKINE, Vol. 8, No. 10 (October 1996: 751–761)

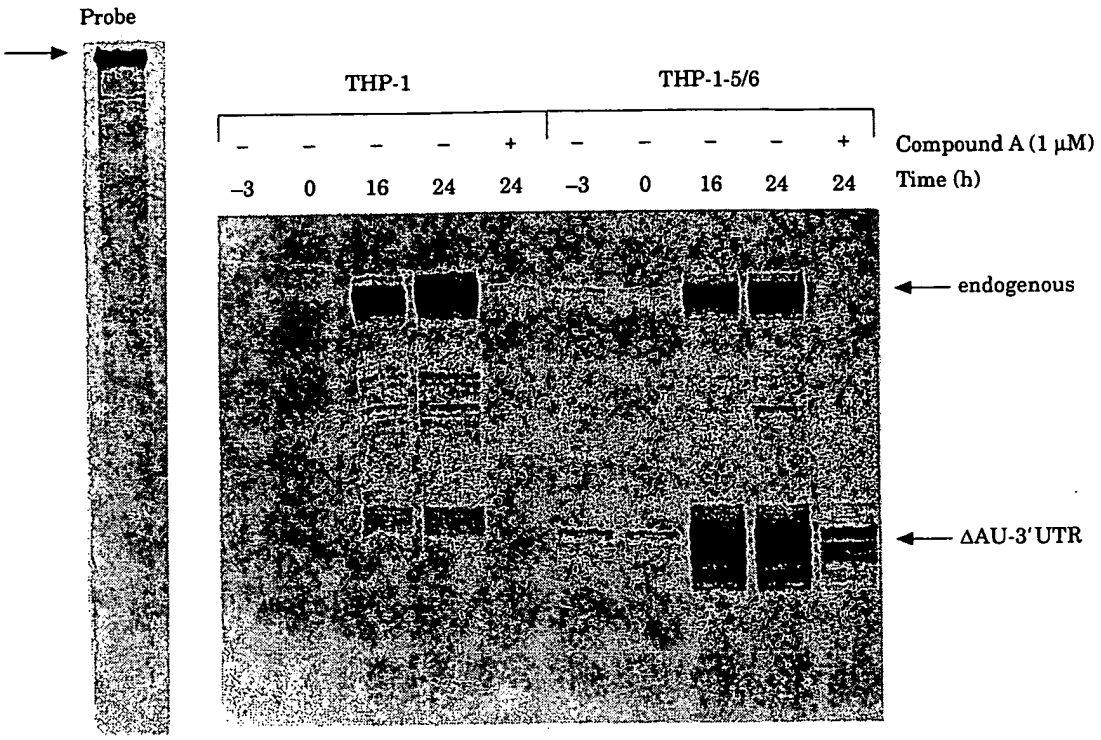

Figure 7. IL-1β RNase protection assay.

A mammalian expression vector for the human IL-1β cDNA containing only 344 bp of the IL-1β 3'UTR and lacking all six AUUUA motifs (ΔAU-3'UTR), was transfected into THP-1 cells. Total RNA was harvested at various times of stimulation (+/− 1 μM radicicol analogue A). Time of incubation with LPS is represented. IFN-γ was added at −3 h and radicicol analogue A was added at 16 h. The RNase protection result of one cell line (THP-1-5/6) is shown vs untransfected THP-1 cells.

120 nM and induced Cox II mRNA degradation in a similar manner as IL-1β (not shown). Radicicol analogue A did not inhibit cyclooxygenase at 10 μM. It seems possible however, that post-translational inhibition of IL-1β secretion or PGE_2 release and mRNA degradation occur by two different pathways because it was found that many other radicicol analogs were able to block IL-1β secretion but had no effect on mRNA stability.

It is interesting to note that all the genes so far shown to be affected in their mRNA accumulation or protein expression by radicicol analogue A, contain at least one copy of the consensus AUUUA sequence in the 3'UTR (Table 1), whereas all the genes which showed resistance to radicicol analogue A, do not. IL-1β contains six AUUUA elements, three of which are in tandem. Experiments with a luciferase gene expression system containing AU-rich elements of the IL-1β 3'UTR showed that a 30-bp stretch containing the three tandem penta-nucleotide motifs (Fig. 6), is sufficient to confer the destabilizing effect of radicicol analogue A (results not shown). Gel-retardation assays and UV-crosslinking experiments carried out with riboprobes derived from the AUUUA-containing region of IL-1β 3'UTR, indicate that radicicol analogue A has no effect on protein binding to mRNA at the ARE. However, it inhibits tyrosine phosphorylation of a number of differentially expressed proteins or inhibits a differentially expressed tyrosine kinase. An AUUUA-binding protein in THP-1 cells, was also differentially expressed or modified in IFN-γ-stimulated cells. The luciferase gene expression assay mentioned above, showed a significant decrease in luciferase activity induced by radicicol analogue A, only in differentiated cells. The fact that mRNA degradation by radicicol analogue A is seen only in differentiated cells, seems to indicate that at least part of the mRNA degrading machinery is expressed differentially or that this compound is able to block a differentiation-induced increase in IL-1β mRNA stability. This might explain why radicicol analogue A showed an effect independent of whether PMA or IFN-γ was used to induce this differentially expressed gene. Radicicol analogue A might influence post-translational modification(s) on protein(s) belonging to

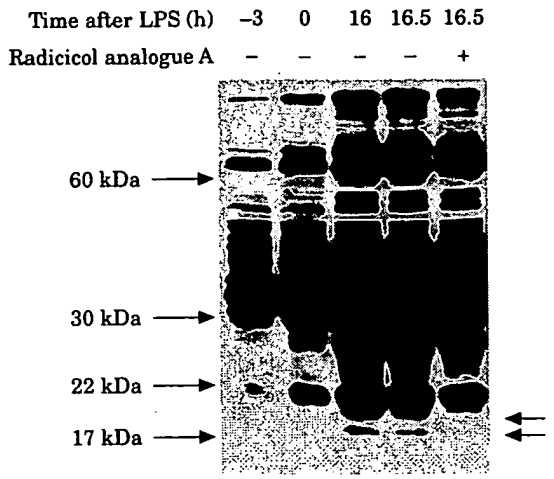

Figure 8. Western blot analysis using anti-tyrosine antibodies.

THP-1 cells were differentiated and radicicol analogue A (1 μM) was added 16 h after LPS addition. Whole cell extracts from various stages of differentiation were loaded on a 4–20% Novex SDS-PAGE gel and probed by Western blot analysis using anti-phosphotyrosine antibodies (Upstate Biotechnology Inc.). Indicated times are hours after addition of LPS. Arrows indicate proteins affected by radicicol analogue A.

a protein complex interacting with proteins binding to the ARE of IL-1β mRNA. In this manner, radicicol analogue A is able to override the differentiation-induced mRNA stabilization of IL-1β in THP-1 cells, rather than directly influencing mRNA binding of protein(s) to the AREs.

MATERIALS AND METHODS

Tissue culture

The human monocytic leukaemia cell line, THP-1, was grown in RPMI medium supplemented with 110 U/ml penicillin, 100 μg/ml streptomycin, 2 mM L-glutamine, 50 μM 2-mercaptoethanol and 2 g/l $NaHCO_3$. Heat-treated fetal bovine serum (FBS) (5%) was added before use. The cells were grown to a density of 5×10^5/ml and then stimulated with IFN-γ (100 U/ml). Three hours later, LPS (5 μg/ml) was added. This time point was designated time 0. Compounds were added either 5 min before adding IFN-γ or at various times after LPS addition.

ELISA

Enzyme-linked immunoabsorbent assays (ELISA) were carried out with commercially available kits obtained from Cayman Chemical Company (Ann Arbor, MI) according to the manufacturer's protocol.

RNA isolation and analysis

Total cellular RNA was isolated from THP-1 cells at different times after the initiation of differentiation using the guanidine isothiocyanate method of Chirgwin *et al.*[44] Each RNA sample (20 μg) was denatured and analysed on a 1% agarose gel containing 2.2 M formaldehyde. The gel was transferred to Hybond-N (Amersham, UK), UV-crosslinked by the Stratagene Stratalinker (1600 μJ × 100) and judged for equal loading of RNA by methylene blue staining. Blots were hybridized to a digoxigenin (DIG)-labelled DNA probe. Labelling and detection was carried out by the DIG kit (Boehringer Mannheim, Germany) according to the manufacturer's specifications. DNA probes were obtained by subcloning RT-PCR derived fragments of the genes of interest, into pGemT-vector (Promega, Madison, WI). For the RT-PCR analysis, 1 μg of total RNA was reverse transcribed using AMV reverse transcriptase (Life Sciences Inc., St Petersburg, FL), then amplified by the PCR method. Each PCR reaction also contained a set of β-actin primers as internal control.[45] The levels of the expected PCR product were compared to the constant levels of β-actin. The size of the PCR products was compared to *Msp*I digested pBR322 standards (New England Biolabs, Beverly, MA). PCR products were analysed on a 4% agarose gel. Nucleotide sequences for the oligonucleotide 5′ and 3′ primers, respectively, are shown in Table 2.

Cloning of the hIL-1β-3′UTR cDNA

Total RNA from THP-1 cells was harvested after IFN-γ/LPS stimulation (16 h after LPS addition). Based on the human IL-1β cDNA sequence (Genbank accession number K02770), 1 μg total RNA was RT-PCR amplified using the following upstream and downstream primers, respectively: 5′ GGG **GGT ACC** AAG TGT CTG AAG CAG CCA T and 5′ CCC **ATC GAT** AAG CGG TTG CTC ATC AGA AT. *Kpn*I and *Cla*I restriction sites, shown in bold, were incorporated into the primers. A *Kpn*I/*Cla*I restriction digest of the resulting ~1.2-kb RT-PCR product was then cloned into the *Kpn*I/*Cla*I of pGem7Zf(-) (Promega) and sequenced. The mammalian expression vector, pHD,[30] kindly provided by Dr Schütz (German Cancer Research

TABLE 2. Nucleotide sequences for the oligonucleotide 5′ and 3′ primers

	5′	3′
β-actin:	ATGGGTCAGAAGGATTCCTA	AGAGGCGTACAGGGATAGCAC
IL-1β:	GACACATGGGATAACGAGGCT	ACGCAGGACAGGTACAGATTC
TNF-α:	TCTCGAACCCCGAGTCACAA	TATCTCTCAGCTCCACACCA
IL-6:	AGTAACATGTGTGAAAGCAG	CAGGAACTGGATCAGGACTT
c-*jun*:	AGCCCTCGGCGAACCCCTCCT	CCCAAGATCCTGAAACAGAGC
ICE:	ACACGTCTTGCTCTCATTATC	AAATGCCTCCAGCTCTGTAGT
HLA-DRα:	GCCGAGTTCTATCTGAATCCT	ATTGGTGATCGGAGTATAGTT
Rantes:	5′: CTGGTTCCGGCGAGGTACCATGAAGGTCTCC	
	3′: CTCGCTCCGGCGACTCTCCATCCTAGCTCA	

Center, Heidelberg, Germany), was modified as follows. A Klenow blunt-ended *Xho*I/*Sal*I fragment from pMC1neo (Stratagene, La Jolla, CA) was subcloned into a Klenow blunt-ended, unique *Aat*II site in pHD, yielding pHD-neo. The *Xho*I site located in the multiple cloning site was next eliminated by religating a Klenow blunt-end *Xho*I digest of pHD-neo. The resulting plasmid, pHD-neo2, was linearized with *Kpn*I/*Cla*I then ligated to the *Kpn*I/*Cla*I hIL-1β cDNA, yielding a hIL-1β mammalian expression vector (pHD-neo2-hIL-1β-3′UTR) which contained only 344 bp of the hIL-1β 3′UTR and lacking all six AUUUA motifs.

Transfections

10^7 cells/ml in 1.3 mM KH_2PO_4, 7.36 mM Na_2HPO_4, 2.44 mM KCl, 124 mM NaCl, 5 mM glucose, 9.6 μM $MgCl_2$ and 16 μM $CaCl_2$, pH 7.2, were transfected with 20 μg of DNA in a Bio Rad Gene Pulser (250 V, 690 μF and indefinite resistance) using a 0.4 cm cuvette. Cells were subsequently cultured in RPMI medium supplemented as described above, containing 10% FBS and 600 μg/ml G418.

RNase protection of hIL-1β mRNA

RNase protection analysis was performed as described by Melton *et al.*[46] A 280-bp RT-PCR fragment derived from THP-1 cell mRNA corresponding to a portion of the IL-1β 3′UTR spanning four of the AUUUA motifs, was subcloned into pGEM7Zf(-) (pGEM-IL1β-RP). Using *Xba*I linearized pGEM-IL1β-RP, SP6 RNA polymerase and [α-^{33}P]UTP, a hIL-1β riboprobe was synthesized.

Acknowledgements

The authors wish to thank Drs G. Baumann and T. Payne for the critical reading of this manuscript. RU 486 was generously provided by Roussel Uclaf, France.

REFERENCES

1. Dinarello CA (1991) Interleukin-1 and interleukin-1 antagonism. Blood 77: 1627–1652.

2. Bevilacqua MP, Pober JS, Wheller ME, Cotran RS, Gimbrone MA (1985) Interleukin 1 acts on cultured human vascular endothelium to increase the adhesion of polymorphonuclear leukocytes, monocytes and related leukocyte cell lines. J Clin Invest 76: 2003–2011.

3. Thornberry NA, Bull HG, Calayacay JR, Chapman KT, Howard AD, Kostura MJ, Miller DK, Molineaux SM, Weidner JR, Aunins J, Elliston KO, Ayala JM, Casano FJ, Chin J, Ding GJ-F, Egger LA, Gaffney EP, Limjuco G, Palyha OC, Raju SM, Rolando AM, Salley JP, Yamin TT, Lee TD, Shively JE, MacCross M, Mumford RA, Schmidt JA, Tocci MJ (1992) A novel heterodimeric cysteine protease is required for interleukin-1β processing in monocytes. Nature 356: 786–774.

4. Wakabayashi G, Gelfando JA, Burke JF, Thompson RC, Dinarello CA (1991) A specific receptor antagonist for interleukin 1 prevents *Escherichia coli*-induced shock in rabbits. FASEB J 5:338–343.

5. Fanslow W, Sims JE, Sassenfeld H, Morrissey PJ, Gillis S, Dower SK, Widmer MB (1990) Regulation of alloreactivity *in vivo* by a soluble form of the interleukin-receptor. Science 248: 739–742.

6. McIntyre KW, Stepan GJ, Kolinsky KD, Benjamin WR, Plocinski JM, Daffka KL, Campen CA, Chizzonite RA, Kilian PL (1991) Inhibition of interleukin 1 (IL-1) binding and bioactivity *in vitro* and modulation of acute inflammation *in vivo* by IL-1 receptor antagonist and anti-IL-1 receptor monoclonal antibody. J Exp Med 173: 931–939.

7. Dinarello CA (1991) Inflammatory cytokines: interleukin-1 and tumor necrosis factor as effector molecules in autoimmune diseases. Curr Opin Immun 3: 941–948.

8. Beutler B, Krochin N, Milsark IW, Luedke C, Cerami A (1986) Control of cachectin (tumor necrosis factor) synthesis: mechanism of endotoxin resistance. Science 232: 977–980.

9. Fenton MJ, Vermeulen MW, Clark BD, Webb AC, Auron PE (1988) Human pro-IL-1β—gene expression in monocytic cells is regulated by two distinct pathways. J Immunol 140: 2267–2273.

10. Auwerx J (1991) The human leukemia cell line, THP-1: a multifacetted model for the study of monocyte-macrophage differentiation. Experientia 47: 22–30.

11. Sachs AB (1993) Messenger RNA degradation in eukaryotes. Cell 74: 413–421.

12. Peltz SW, Brewer G, Bernstein P, Hart PA, Ross J (1991) Regulation of mRNA turnover in eukaryotic cells. Crit Rev Euc Gene Expr 1: 99–126.

13. Caput D, Beutler B, Hartog D, Thayer R, Brown-Shimer S, Cerami A (1986) Identification of a common nucleotide sequence in the 3′-untranslated region of mRNA molecules specifying inflammatory mediators. Proc Natl Acad Sci USA 83: 1670–1674.

14. Shaw G, Kamen R (1986) A Conserved AU sequence from the 3′ untranslated region of GM-CSF mRNA mediates selective mRNA degradation. Cell 46: 659–667.

15. Zubiaga AM, Belasco JG, Greenberg ME (1995) The nonamer UUAUUUAAUU is the key AU-rich sequence motif that mediates mRNA degradation. Mol Cell Biol 15: 2219–2230.

16. Lindstein T, June CH, Ledbetter JA, Stella G, Thompson CB (1989) Regulation of lymphokine messenger RNA stability by a surface-mediated T cell activation pathway. Science 244: 339–343.

17. Savant-Bhonsale S, Cleveland DW (1992) Evidence for instability of mRNAs containing AUUUA motifs mediated through translation-dependent assembly of a >20S degradation complex. Genes & Development 6: 1927–1939.

18. Malter JS (1989) Identification of an AUUUA-specific messenger RNA binding protein. Science 244: 664–666.

19. Malter JS, Hong Y (1991) A redox switch and phosphorylation are involved in the post-translational up-regulation of the adenosine-uridine binding factor by phorbol ester and ionophore. J Biol Chem 266: 3167–3171.

20. Bickel M, IwaiY, Pluznik DH, Cohen R (1992) Binding of sequence-specific proteins to the adenosine- plus uridine- rich sequences of the murine granulocyte/macrophage colony-stimulating factor mRNA. Proc Natl Acad Sci USA 89: 10001–10005.

21. Bohjanen PR, Petryniak B, June CH, Thompson CB, Lindsten T (1992) AU RNA-binding factors differ in their binding specificities and affinities. J Biol Chem 267: 6302–6309.

22. Vakalopoulou E, Schaack J, Shenk T (1991) A 32-kilodalton protein binds to AU-rich domains in the 3′ untranslated region of rapidly degraded mRNAs. Mol Cell Biol 11: 3355–3364.

23. Levine TD, Gao F, King PH, Andrews LG, Keene JD (1993) Hel-N1: an autoimmune RNA-binding protein with specificity for 3′ uridylate-rich untranslated regions of growth factor mRNAs. Mol Cell Biol 13: 34940–3504.

24. You Y, Chen CA, Shyu A (1992) U-rich sequence-binding proteins (URBPs) interacting with a 20-nucleotide U-rich sequence in the 3′ untranslated region of c-fos mRNA may be involved in the first step of c-fos mRNA degradation. Mol Cell Biol 12: 2931–2940.

25. Schuler GA, Cole MD (1988) GM-CSF and oncogene mRNA stabilities are independently regulated in trans in a mouse monocytic tumor. Cell 55: 1115–1122.

26. Bohjanen PR, Petryniak B, June CH, Thompson CB, Lindsten T (1991) An inducible cytoplasmic factor (AU-B) binds selectively to AUUUA multimers in the 3′ untranslated region of lymphokine mRNA. Mol Cell Biol 11: 3288–3295.

27. Schnyder J, Payne T, Dinarello CA (1987) Human monocyte or recombinant interleukin 1's are specific for the secretion of a metalloproteinase from chondrocytes. J Immunol 138: 496–503.

28. Ramage P, Cheneval D, Chvei M, Graff P, Hemmig R, Heng R, Kocher H.-P, MacKenzie A, Memmert K, Revesz L, Wishart W (1995) Expression, refolding and autocatalytic proteolytic processing of the interleukin-1β converting enzyme precursor. J Biol Chem 270: 9378–9383.

29. Siljander P, Hurme M (1993) Continuous presence of phorbol ester is required for its IL-1β mRNA stabilizing effect. FEBS Lett 315: 81–84.

30. Müller G, Ruppert S, Schmid E, Schütz G (1988) Functional analysis of alternatively spliced tyrosinase gene transcripts. EMBO J 7: 2723–2730.

31. Cleveland DW, Yen TJ (1989) Multiple determinants of eukaryotic mRNA stability. New Biol 1: 121–126.

32. Lee SW, Tsou A-P, Chan H, Thomas J, Petrie K, Eugut EM, Allison AC (1988) Glucocorticoids selectively inhibit the transcription of the interleukin 1β gene and decrease the stability of interleukin 1β mRNA. Proc Natl Acad Sci USA 85: 1204–1208.

33. Gorospe M, Kumar S, Baglioni C (1993) Tumor necrosis factor increase stability of interleukin-1 mRNA by activating protein kinase C. J Biol Chem 268: 6214–6220.

34. Akeson AL, Woods CW, Mosher LB, Thomas CE, Jackson RL (1991) Inhibition of IL-1β expression in THP-1 cells by probucol and tocopherol. Atherosclerosis 86: 261–270.

35. Mahoney CW, Azzi A (1988) Vitamin E inhibits protein kinase C activity. Biochem Biophys Res Commun 154: 694–697.

36. Antrast J, Lasnier F, Pairault J (1991) Adipsin gene expression in 3T3-F442A adipocytes is posttranscriptionally down-regulated by retinoid acid. J Biol Chem 266: 1157–1161.

37. Moreira AL, Sampaio EP, Zmuidzinas A, Frindt P, Smith KA, Kaplan G (1993) Thalidomide exerts its inhibitory action on tumor necrosis factor α by enhancing mRNA degradation. J Exp Med 177: 1675–1680.

38. Distel R, Robinson GS, Spiegelman BM (1992) Fatty acid regulation of gene expression. J Biol Chem 267: 5937–5941.

39. Nair APK, Hahn S, Banholzer R, Hirsch HH, Moroni Ch (1994) Cyclosporin A inhibits growth of autocrine tumor cell lines by destabilizing interleukin-3 mRNA. Nature 369: 239–242.

40. Delmotte P, Delmotte-Plaquee J (1953) A new antifungal substance of fungal origin. Nature 171: 344.

41. Kwon HJ, Yoshida M, Fukui Y, Horinouchoi S, Beppu T (1992) Potent and specific inhibition of p60v-src protein kinase both *in vivo* and *in vitro* by radicicol. Cancer Res 52: 6926–6930.

42. Kwon HJ, Yoshida M, Abe K, Horinouchi S, Beppu T (1992) Radicicol, an agent inducing the reversal of transformed phenotypes of src-transformed fibroblasts. Biosci Biotech Biochem 56: 538–539.

43. Chanmugam P, Feng L, Liou S, Jang BC, Boudreau M, Yu G, Lee JH, Kwon HJ, Beppu T, Yoshida M, Xia Y, Wilson CB, Hwang D (1995) Radicicol, a protein tyrosine kinase inhibitor, supresses the expression of mitogen-inducible cyclooxygenase in macrophages stimulated with lipopolysaccharide and in experimental glomerulonephritis. J Biol Chem 270: 5418–5426.

44. Chirgwin JM, Przbybyla AE, MacDonald RJ, Rutter WJ (1979) Isolation of biologically active ribonucleic acid from sources enriched in ribonucleases. Biochemistry 18: 5294–5299.

45. Cheneval D, Christy RJ, Geiman D, Cornelius P, Lane MD (1991) Cell-free transcription directed by the 422 adipose P2 gene promoter: Activation by the CCAAT/enhancer binding protein. Proc Natl Acad Sci 88: 8465–8469.

46. Melton DA, Krieg PA, Rebagliati MR, Maniatis T, Zinn K, Green MR (1984) Efficient *in vitro* synthesis of biologically active RNA and RNA hybridization probes from plasmid containing a bacteriophage SP6 promoter. Nucleic Acids Res 12: 7035–7056.

THE JOURNAL OF BIOLOGICAL CHEMISTRY
Vol. 271, No. 5, Issue of February 2, pp. 2746–2753, 1996
Printed in U.S.A.

Post-transcriptional Regulation of Vascular Endothelial Growth Factor by Hypoxia*

(Received for publication, September 5, 1995, and in revised form, November 16, 1995)

Andrew P. Levy‡§, Nina S. Levy¶, and Mark A. Goldberg¶‖

From the ‡Cardiology and ¶Hematology-Oncology Divisions, Department of Medicine, Brigham and Women's Hospital, and Harvard Medical School, Boston, Massachusetts 02115

The major control point for the hypoxic induction of the vascular endothelial growth factor (VEGF) gene is the regulation of the steady-state level of the mRNA. We previously demonstrated a discrepancy between the transcription rate and the steady-state mRNA level induced by hypoxia. This led us to examine the post-transcriptional regulation of VEGF expression. Actinomycin D experiments revealed that hypoxia increased VEGF mRNA half-life from 43 ± 6 min to 106 ± 9 min. Using an *in vitro* mRNA degradation assay, the half-life of VEGF mRNA 3′-untranslated region (UTR) transcripts were also found to be increased when incubated with hypoxic *versus* normoxic extracts. Both cis-regulatory elements involved in VEGF mRNA degradation under normoxic conditions and in increased stabilization under hypoxic conditions were mapped using this degradation assay. A hypoxia-induced protein(s) was found that bound to the sequences in the VEGF 3′-UTR which mediated increased stability in the degradation assay. Furthermore, genistein, a tyrosine kinase inhibitor, blocked the hypoxia-induced stabilization of VEGF 3′-UTR transcripts and inhibited hypoxia-induced protein binding to the VEGF 3′-UTR. These findings demonstrate a significant post-transcriptional component to the regulation of VEGF.

Hypoxia has been shown to be an important stimulus for the new blood vessel formation seen in coronary artery disease (1), tumor angiogenesis (2), and diabetic neovascularization (3). VEGF,[1] also known as vascular permeability factor, is a potent angiogenic and endothelial cell-specific mitogen (4–6), which is regulated by hypoxia *in vitro* (2, 7, 8) and *in vivo* (2, 3, 9–11). The major control point for the hypoxic induction of the VEGF gene is the regulation of the steady-state level of mRNA (2, 8) which is determined by the relative rates of mRNA synthesis and decay.

We have previously demonstrated that hypoxia induces VEGF steady-state mRNA 25.0 ± 11.4 and 12.0 ± 0.6 fold in rat primary cardiac myocytes (8) and rat pheochromocytoma PC12 cells (12), respectively. However, nuclear runoff transcription assays demonstrated that the transcription rate for VEGF was increased only 3.1 ± 0.6-fold by hypoxia in the PC12 cells (12). Rat genomic sequences encoding VEGF were cloned and a 28-bp element in the 5′ promoter was identified that mediates a significant portion of this hypoxia-inducible transcription in transient expression assays. This element was shown to have sequence and protein binding similarities to the hypoxia-inducible factor 1 binding site within the erythropoietin (Epo) 3′ enhancer (12). These studies demonstrated that, while increased transcription rate can account for a portion of the increase in the steady-state level of VEGF mRNA in the PC12 cells, it does not account for all of the increase and suggested that a post-transcriptional mechanism plays a significant role in the hypoxic induction of VEGF mRNA, as well.

Post-transcriptional mechanisms of regulation have previously been suggested for Epo (13–15) and demonstrated for tyrosine hydroxylase (16), two other hypoxia-inducible genes. In the present study we examine the post-transcriptional regulation of VEGF mRNA expression under both normoxic and hypoxic conditions. We have employed several complementary techniques including actinomycin D chase experiments, *in vitro* mRNA degradation studies, and RNA electromobility shift assays.

MATERIALS AND METHODS

Cell Lines and Culture Conditions—PC12 rat pheochromocytoma cells were the generous gift of Dr. Eva J. Neer (Brigham and Women's Hospital, Boston, MA). H9c2 rat heart myocytes were obtained from the American Type Culture Collection (Rockville, MD) The cells were routinely grown in Dulbecco's modified Eagle's medium (DMEM) (Sigma) with 10% fetal bovine serum and used for all experiments at ~70% confluence. Cells were cultured under either normoxic conditions (5% CO_2, 21% O_2, 74% N_2) in a humidified Napco incubator at 37 °C or hypoxic conditions (5% CO_2, 1% O_2, 94% N_2) in an Espec triple gas incubator (Tabai-Espec Corp., Osaka, Japan). Genistein (Sigma) was prepared as a 100 mM stock in Me_2SO and added to cells 30 min prior to placement in the hypoxia chamber at a final concentration of 500 μM.

Cloning and Sequencing of Rat VEGF cDNA—2 × 10^6 bacteriophage clones from a λ gt11 oligo(dT)-primed PC12 cDNA library (Clontech, La Jolla, CA) were screened with two contiguous genomic fragments from the 3′-UTR of the VEGF gene (12), an 875-bp *Bam*HI-*Eco*RI fragment (nucleotide 756-1642, GenBank™ accession no. U22372) and a 256-bp *Eco*RI-*Eco*RI fragment (nucleotide 1642–1855, GenBank™ accession no. U22372). Distinct VEGF cDNA clones hybridizing to both probes were isolated. The cDNA insert from each clone was isolated on a *Kpn*I-*Sac*I fragment (which contained both λ gt11 and VEGF sequences) and cloned into the Bluescript vector (Stratagene). Sequencing of the cDNA inserts was performed by the dideoxy chain-termination method using Sequenase (Stratagene) initially with oligonucleotide primers (5′-CCATCTGCTGCACGCGGAAGAAGGC-3′ and 5′-CCTTACGCGAAATACGGGCAGACATG-3′) corresponding to the λ gt11 sequence adjacent to the insert and subsequently, in a progressive fashion, with oligonucleotides complementary to the sequences obtained

* This work was supported in part by National Institutes of Health Grants T32HL07604 and 1KO8HL03405-01 (to A. P. L.), 1F32HL08838-02 (to N. S. L.), and DK45098 (to M. A. G.), an American Heart Association Grant-in-Aid (to M. A. G.), and an American Heart Association Established Investigator Award (to M. A. G.). The costs of publication of this article were defrayed in part by the payment of page charges. This article must therefore be hereby marked "*advertisement*" in accordance with 18 U.S.C. Section 1734 solely to indicate this fact.

§ Current address: Whitaker Cardiovascular Institute, Evans Department of Medicine, Boston University School of Medicine, Boston, MA 02118.

‖ To whom correspondence and reprint requests should be addressed: Brigham and Women's Hospital, LMRC Rm. 222, 221 Longwood Ave., Boston, MA 02115. Tel.: 617-732-7646; Fax: 617-739-0748.

[1] The abbreviations used are: VEGF, vascular endothelial growth factor; bp, base pair; Epo, erythropoietin; UTR, untranslated region; DMEM, Dulbecco's modified Eagle's medium; kb, kilobase; EMSA, electromobility shift assay; PCR, polymerase chain reaction; TBE, Tris borate EDTA; IRE, iron responsive element.

from the respective clones. Both strands of all clones were sequenced.

In Vitro Cell-free RNA Degradation Assay—Cells were grown under either normoxic or hypoxic conditions and S100 cytoplasmic extracts were prepared according to the method of Wang *et al.* (17). Briefly, cells were washed twice with ice-cold phosphate-buffered saline and then scraped into 10 ml of phosphate-buffered saline. The cells were then pelleted and resuspended in 2 volumes of homogenization buffer (10 mM Tris-HCl, pH 7.4, 0.5 mM dithiothreitol, 10 mM KCl, and 1.5 mM $MgCl_2$) and lysed with 20 strokes in a Dounce homogenizer (pestle B). 0.1 volume of extraction buffer (1.5 M KCl, 15 mM $MgCl_2$, 100 mM Tris-HCl, pH 7.4, 5 mM dithiothreitol) was added, and the homogenate was centrifuged at 14,000 × *g* for 2 min to pellet nuclei. The supernatant from this step was harvested and centrifuged at 100,000 × *g* for 1 h at 4 °C. Cytoplasmic extracts were immediately frozen on dry ice and were stored at −70 °C. Protein concentrations were determined by Bradford protein assay (Bio-Rad) and were routinely 3–5 mg/ml. The entire procedure was performed at 4 °C.

[^{32}P]CTP-labeled, capped, and polyadenylated transcripts were synthesized *in vitro* (18). The *Eco*RI site of pSP64 poly(A) (Promega) was transformed into an *Ase*I restriction enzyme site by filling in *Eco*RI-digested pSP64 poly(A) with the Klenow fragment and then blunt-end ligating the vector. Restriction fragments containing the 3′-UTR of VEGF derived from clone 11.4 (12) were cloned into the multiple cloning site of this modified pSP64 vector. A series of deletions were made from the 3′ end of these sequences using unique restriction sites in the VEGF 3′-UTR. Digestion of these plasmids with *Ase*I-generated DNA templates containing a poly(dT) sequence that was transcribed into a 30-base long poly(A) tail at the 3′ end. Capped transcripts were synthesized from these templates with SP6 RNA polymerase using the MEGAscript *in vitro* transcription kit (Ambion, Austin, TX) according to the manufacturer's protocol with a 4:1 ratio of $m^7G5'pppG$ (cap analog) to GTP. Labeled RNA transcripts were produced by inclusion of [α-^{32}P]CTP (3000 Ci/mmol) in the reaction. 80,000 cpm were used for each degradation assay.

Degradation assays were performed by incubating the transcript (10^6 cpm) with 130 μg of cytoplasmic extract in a total volume of 39 μl in a master mix at room temperature. At each time point the reaction was stopped by transferring 3 μl from this master mix to a tube containing 15 μl of H_2O and 2 μl of 5 M NH_4OAc with 100 mM EDTA. The sample was extracted once with phenol:chloroform:isoamyl alcohol (25:24:1), and the supernatant was precipitated with 20 μl of isopropanol. The pellets were washed once with 80% ethanol and air-dried. Samples were then electrophoresed on a formaldehyde-agarose gel and transferred to GeneScreen (DuPont NEN). Quantitation of the remaining primary (undegraded) transcript at the different time points was performed with a Molecular Dynamics PhosphorImager. All time points were performed in triplicate.

Measurement of VEGF mRNA Half-life in PC12 Cells—PC12 cells were grown under normoxic or hypoxic conditions in DMEM with 1% fetal bovine serum for 24 h prior to the addition of actinomycin D in T 75-cm^2 flasks (Corning). For hypoxic cell cultures, cells were grown in flasks with a solid rubber stopper containing two 18-gauge needles allowing for gas inflow and outflow. All flasks were connected in a parallel using small bore, triple-leg extension tubing (Braun Medical Inc., Bethlehem, PA) to a defined gas mixture containing 1% O_2, 5% CO_2, and balance N_2. For hypoxic cultures actinomycin D (Sigma) was added to each flask through the 18-gauge outflow needle. This elaborate configuration allowed cells in each flask to be grown under hypoxic conditions for a defined period of time without any intervals of reoxygenation that would occur if all the flasks were kept in a common incubator or hypoxia apparatus. For the determination of VEGF mRNA half-life under hypoxic conditions the cells were grown under hypoxic conditions for 9 h prior to the addition of actinomycin D. For the determination of VEGF mRNA half-life under normoxic conditions, the cells were grown at 21% O_2 prior to the addition of the actinomycin D.

5 mg of actinomycin D were initially dissolved in 1 ml of Me_2SO and subsequently diluted with DMEM to a concentration of 50 μg/ml (10×) stock solution. Flasks were harvested for RNA at 0, 5, 10, 15, 30, 60, 120, 240, and 480 min after the addition of actinomycin D. Total RNA was prepared from the flasks using RNA STAT-60 (Tel-Test "B," Inc., Friendswood, TX) and isolated according to the manufacturer's protocol.

VEGF and 18 S rRNA were detected by RNase protection analysis of 10 μg of RNA isolated at the various time points. RNase protection assays were performed as described previously (8) to specifically detect the $VEGF_{165}$ isoform and 18 S rRNA. After electrophoresis on 6% polyacrylamide, 7 M urea gels, the protected fragments were quantitated using a PhosphorImager (Molecular Dynamics). The quantity of VEGF mRNA was normalized to the amount of 18 S rRNA (19) by calculating a VEGF/18 S ratio for each sample. All time points were performed in triplicate. The entire experiment was repeated three separate times. The half-life of VEGF mRNA was calculated by drawing the best fit linear curve on a log-linear plot of the VEGF/18 S ratio *versus* time. The time at half-maximal VEGF/18S ratio was taken to be the half-life.

RNA Electromobility Shift Assay (EMSA)—The bacteriophage T7 RNA polymerase promoter sequence was appended to the 5′ end of sense polymerase chain reaction (PCR) primers used to generate template DNA[2] (20, 21). For experiments involving the VEGF 3′-UTR *StuI-NsiI* fragment (used for mapping the constitutive RNA-binding protein) oligonucleotide PCR primers were 5′-ggatcc*TAATACGACTCACTATAGG*GAGGCCTGGTAATGGCTCCTCC-3′ (VEGF nucleotide 910–931, GenBank™ accession no. U22372) and 5′-GAGATGCATCCTCATAAATAG-3′ (VEGF nucleotide 1279–1259, GenBank™ accession no. U22372). For experiments involving the *NsiI*-transcription termination site fragment (used for mapping the hypoxia-induced RNA binding protein), oligonucleotide primers were 5′-cc*TAATACGACTCACTATAGGGAG*AATTTCAACTATTTATGAGGA-3′ (VEGF nucleotide 1251–1271, GenBank™ accession no. U22372) and 5′- TTTGAGATCAGAATTCAATTCTTTAATAGAAAATGCC-3′ (VEGF nucleotide 1877–1841, GenBank™ accession no. U22372). PCR products were gel-purified and [^{32}P]CTP-labeled RNA transcripts were generated with T7 polymerase using Maxiscript (Ambion) according to the manufacturer's protocol. Nonradioactive transcripts used in competition experiments were similarly generated with Maxiscript. A 162-bp fragment of the tyrosine hydroxylase gene (nucleotide 1521–1682, GenBank™ accession no. M10244) (16) was generated by PCR, cloned into the psp73 (Promega) vector, and used to generate tyrosine hydroxylase RNA transcripts. A template used to generate an iron response element (IRE) transcript was kindly supplied by Dr. Beric R. Henderson (22).

A series of overlapping oligonucleotides was used to prepare templates for the generation of short transcripts containing the putative constitutive RNA-protein binding site. Competitor WT_1 (VEGF nucleotide 1050–1080, GenBank™ accession no. U22372) was generated by overlapping oligonucleotides T7A (5′-gcggatcc*TAATACGACTCACTATAGGGAG*GTGTGTGAGTGGCTTACCCTTCCCCATTTTC-3′) (VEGF nucleotide 1050–1080, GenBank™ accession no. U22372) and B (5′-ccgattcGAAAATGGGGAAGGGTAAGCCACTCACACA-3′)(VEGF nucleotide 1080–1051, GenBank™ accession no. U22372). Competitor WT_2 (VEGF nucleotide 1050–1091, GenBank™ accession no. U22372) was generated by overlapping oligonucleotides T7A and C (5′-cCCTTGGGAAGGGAAAATGGGGAAGGGTAAGCCACTCACACA-3′) (VEGF nucleotide 1091–1051, GenBank™ accession no. U22372). Competitor M (VEGF nucleotide 1050–1080 containing a 3-bp change in the VEGF sequence, GenBank™ accession no. U22372) was generated by overlapping oligonucleotides T7A and D (5′- ccgattcGAAAATGGGGA<u>CTT</u>GTAAGCCACTCACACA-3′) (VEGF nucleotide 1080–1051, GenBank™ accession no. U22372). Equimolar amounts of each of the oligonucleotides was annealed with its partner and then treated with Klenow fragment to fill in the overhang. These oligonucleotide generated templates then were used to make RNA transcripts with T7 RNA polymerase according to the manufacturer's protocol for short transcripts (Ambion).

Radiolabeled RNA transcripts (100,000 cpm/reaction) with or without nonradioactive competitor were incubated with 20 μg of S100 cytoplasmic extract for 15 min at room temperature. 25 units of ribonuclease T1 were then added followed 10 min later by heparin to a final concentration of 5 mg/ml. Electrophoresis of RNA-protein complexes was carried out on 7% native polyacrylamide gel (acrylamide/methylene bisacrylamide ratio, 30:1) with 0.5 × TBE (30 mM Tris, 30 mM boric acid, 0.06 mM EDTA, pH 7.3 at 20 °C) at 4 °C. The gels were preelectrophoresed for 1 h at 35 A followed by electrophoresis of RNA-protein complexes for 1.5 h at 30 A. Gels were dried and exposed to x-ray film (Kodak). The RNA-protein bands were quantitated by PhosphorImager analysis (Molecular Dynamics).

Statistical Analysis—Where indicated, data are presented as the mean ± the standard error of the mean (23). Student's unpaired *t* test was employed to assess differences between two groups. Regression

[2] Sequences for oligonucleotides described under "Materials and Methods" are denoted as follows: VEGF, upper case letters; bacteriophage T7 RNA polymerase promoter core, italicized, upper case letters; appended sequence for PCR, lower case letters; mutated VEGF sequence, underlined letters.

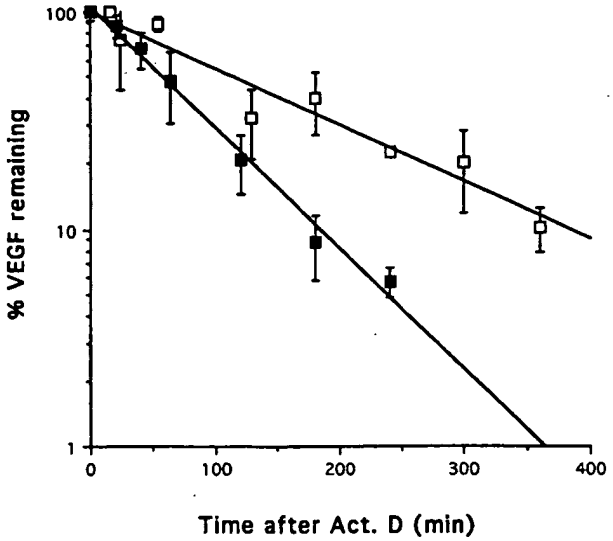

FIG. 1. **VEGF mRNA levels following treatment with actinomycin D.** The time course, RNA harvest, and analysis was performed as described under "Materials and Methods." Data are shown from a representative experiment with each time point performed in triplicate. VEGF RNA is normalized to 18 S rRNA. The experiment was performed three times. □, hypoxia; ■, normoxia.

lines for determination of mRNA half lives were drawn using the Cricket Graph program (Cricket Software, Malverna, PA).

RESULTS

Determination of VEGF mRNA Transcription Termination Site—32 cDNA clones for rat VEGF were isolated that hybridized to two contiguous fragments from the VEGF 3'-UTR as described under "Materials and Methods." Sequencing of six independent inserts verified a single transcription termination site determined by identification of a poly(A) tail preceded by sequence that was identical to the genomic DNA sequence for the VEGF gene previously reported (12). In all cases the transcription termination site was mapped to nucleotides 1875–1877 (GenBank™ accession no. U22372). The transcription termination site maps approximately 20 bp 3' to a consensus polyadenylation site (24) and is consistent with the site we previously described by Northern blot analysis (12). This polyadenylation site would generate a mRNA of 3.7 kb which is the size of the most abundant species seen by Northern blot.

Stabilization of VEGF mRNA by Hypoxia following Treatment with Actinomycin D—Quantitation of the half-life of the $VEGF_{165}$ isoform was determined as described under "Materials and Methods." The half-life was determined to be 43 ± 6 min (n = 3) under normoxic conditions and 106 ± 9 min (n = 3) under hypoxic conditions (Fig. 1) for a mean increase of 2.5 ± 0.4. Similar results were obtained when the VEGF RNA was normalized to β-actin or to 18 S rRNA.

Mapping Instability Elements in the VEGF mRNA 3'-UTR in a Cell-free System under Normoxic Conditions—[^{32}P]CTP-labeled, capped, and polyadenylated transcripts containing the entire VEGF 3'-UTR or deletions from the 3' end of the UTR (Fig. 2*A*) were synthesized and degradation assessed *in vitro* (Fig. 2, *A–C*) as described under "Materials and Methods." The half-life of each transcript was determined, and results were normalized to the half-life of the full-length transcript containing the entire 3'-UTR (Fig. 2*A*). Deletion of specific sequences in the 3'-UTR resulted in a marked stabilization of the transcripts in this *in vitro* assay. Specifically, deletion of the *NsiI-XbaI* fragment and the *StuI-NsiI* fragment each resulted in an approximately 2-fold increase in transcript stability (Fig. 2, *B* and *C*). Deletion of sequences 5' to the *StuI* site or 3' to the *XbaI* site had no significant effect on transcript stability. This would suggest the presence of two independent instability sequences in the VEGF 3'-UTR. Each of these instability regions co-localizes with one of the two nonameric consensus instability sequences (UUAUUUA(U/A)(U/A)) (25, 26) (Fig. 2*A*).

Mapping Elements Which Mediate the Hypoxic Stabilization of the VEGF 3' mRNA UTR in Vitro—S100 cytoplasmic extracts from hypoxic cells were prepared in an identical fashion to those from normoxic cells. *In vitro* RNA degradation assays (Fig. 3, *A–C*) were performed as described under "Materials and Methods" and demonstrated that VEGF 3'-UTR transcripts had a significantly longer half-life *in vitro* when incubated with hypoxic *versus* normoxic extracts (ratio 1.5 ± 0.1 n = 12) (Fig. 3*A*). Progressive 3' deletion analysis of the VEGF 3'-UTR demonstrated that this preferential stabilization by hypoxia was lost upon deletion of the *NsiI-XbaI* fragment. Similar results were obtained with both PC12 and H9c2 cells.

RNA EMSA—RNA transcripts of different regions of the VEGF 3'-UTR incubated with S100 extract allowed for the identification by EMSA of both constitutive and hypoxia-induced VEGF mRNA binding proteins. The constitutive protein complex was found to map between the *NsiI* and *StuI* restriction enzyme sites (Fig. 4*A*). This complex could be completely inhibited by competition with excess unlabeled transcript from this region, but was not competed out with 500-fold excess β-actin or IRE transcripts (Fig. 4*B*). Proteinase K treatment of the extracts completely inhibited formation of the complex. Interestingly, 100-fold excess of a 162-base RNA transcript of the tyrosine hydroxylase 3'-UTR, corresponding to the region previously demonstrated to bind a hypoxia-inducible protein (16), completely inhibited formation of this complex. A region of the VEGF *StuI-NsiI* fragment was identified which is highly homologous to a region within a 28-base fragment specifically protected by the tyrosine hydroxylase RNA-binding protein (16) and to a region within the Epo 3'-UTR demonstrated to be the site for an RNA-binding protein (15) (Fig. 4*C*). Oligonucleotides were constructed from this region as described under "Materials and Methods" to define the binding site by competition studies. RNA derived from template WT_1 or WT_2 was capable of specifically competing with the protein complex binding to *StuI-NsiI* RNA transcripts, whereas template M, which contains a 3-nucleotide substitution in this region of homology, did not efficiently compete with the complex.

A hypoxia-inducible protein complex was mapped by EMSA between the *NsiI* site and the transcription termination site (Fig. 4*A*) using a template generated by a strategy described under "Materials and Methods." The RNA-protein complex was induced 2.2 ± 0.2-fold (n = 12) by EMSA using hypoxic *versus* normoxic S100 extracts (Fig. 4*D*). This complex could be inhibited by excess unlabeled transcript from this region, but was not displaced by a 500-fold excess of IRE transcript (Fig. 4*D*) or Epo transcripts. Proteinase K treatment of the extracts completely inhibited formation of the complex. 3' truncated forms of this template were generated using restriction endonucleases *XbaI*, *EcoRI*, *HinfI*, and *MseI* (Fig. 4*A*). RNA transcripts from these truncated templates allowed the binding site for this hypoxia-inducible species to be further defined within a *MseI-XbaI* fragment (nucleotide 1412–1754, GenBank™ accession no. U22372) (Fig. 4*D*).

Genistein Blocks Hypoxic Stabilization of VEGF 3'-UTR Transcripts in Vitro—PC12 or H9c2 cells were incubated with 500 μM genistein, a tyrosine kinase inhibitor, for 30 min prior to their placement in the hypoxia chamber. Cells were exposed to hypoxia or normoxia for 4 h. Hypoxic and normoxic S100 extracts were then prepared in parallel from cells exposed to genistein and cells that were not exposed to genistein. As demonstrated in Fig. 5, *A* and *B*, genistein inhibited the pref-

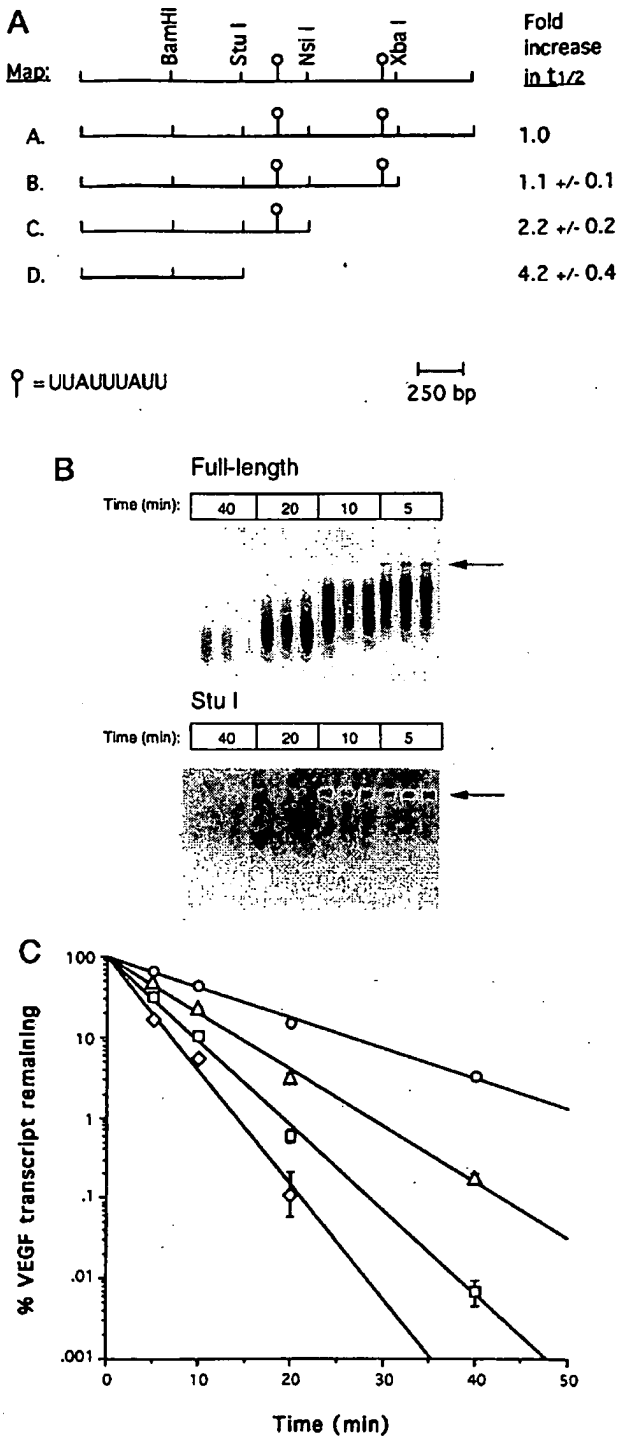

FIG. 2. **Mapping instability elements in the VEGF 3'-UTR under normoxic conditions.** [^{32}P]CTP-labeled, capped, and polyadenylated transcripts were generated *in vitro* as described under "Materials and Methods." *A*, restriction map of constructs in pSP64A (*Asel*). Linear fragments (*A–D*) were cloned in the pSP64A (*Asel*) vector and used to generate sense 3'-UTR transcripts *in vitro*. Deletions from the 3' end of the UTR were produced with the designated restriction enzymes. *Construct A* (full-length) (nucleotide 1–2201, GenBank™ accession no. U22372) contains the entire 3'-UTR and yields a RNA of 2.2 kb. *Construct B* (*XbaI*) (nucleotide 1–1754, GenBank™ accession no. U22372) is derived by deletion of the *XbaI* from construct A and yields a RNA of 1.7 kb. *Construct C* (*NsiI*) (nucleotide 1–1255, GenBank™ accession no. U22372) is derived by deletion of the *NsiI-XbaI* fragment from construct B and yields a RNA of 1.2 kb. *Construct D* (*StuI*) (nucleotide 1–913, GenBank™ accession no. U22372) is derived by deletion of the *StuI-XbaI* fragment from construct B and yields a RNA of 900 bases. The locations of the nonameric instability consensus signals are depicted by *lines* with *open circles*. The half-life in minutes obtained for each construct was expressed relative to the half-life of construct A for each individual experiment. Results are expressed as the mean ± S.E. of four different experiments. In the experimental conditions described under "Materials and Methods" with S100 extract from normoxic cells, the half-life of construct A was approximately 3 min. *B*, representative autoradiograph of products from a cell-free degradation assay of constructs A (*Full-length*) and D (*StuI*) as described under "Materials and Methods." Time refers to the time after the addition of normoxic cytoplasmic extract to the RNA. The *arrow* points to the undegraded transcript. *C*, log-linear regression lines of VEGF RNA degradation quantitated by PhosphorImager analysis. The half-life of each construct was calculated from the regression line extrapolated to time 0. In the representative experiment shown, the half-life of construct A (full-length, □) was 2.6 min, B (*XbaI*, ◇) was 2.0 min, C (*NsiI*,) was 4.0 min, and D (*StuI*, ○) was 8.0 min.

erential stabilization of hypoxic *versus* normoxic extracts in the *in vitro* RNA degradation assay. The change in the ratio of the half-life of the VEGF 3'-UTR transcript with hypoxic *versus* normoxic extracts in the presence of genistein (1.4 in the absence of genistein *versus* 0.5 in its presence) was equivalent to that seen when deletional analysis was performed on the VEGF 3'-UTR (Fig. 3*A*). No significant change was seen in the hypoxic induction of a previously described (12) VEGF promoter-driven luciferase construct in transient transfection assays in cells treated with genistein (data not shown). In addition, S100 extracts prepared from genistein-treated cells failed to demonstrate the hypoxia-induced increase in the electromobility shift of the *NsiI* transcription termination RNA fragment described above (Fig. 5*C*).

DISCUSSION

Hypoxia exerts its control on VEGF gene expression by increasing VEGF steady-state mRNA levels. Previous work has strongly suggested that an increase in transcription rate of the VEGF gene cannot account for all of the observed increase in the steady-state VEGF mRNA levels induced by hypoxia (12). These studies provide further evidence for a post-transcriptional mechanism contributing to VEGF mRNA induction by hypoxia. Several cis-acting elements that may mediate the turnover of VEGF mRNA under normoxic and hypoxic conditions are identified.

The half-life of the VEGF mRNA, determined using actinomycin D, is increased 2.5 ± 0.4-fold by hypoxia. Steady-state kinetics (27) would predict that the increase in steady-state mRNA with hypoxia would be the product of the increase in the transcription rate and the increase in the mRNA half-life. These data therefore provide an adequate explanation for the discrepancy between the increase in the steady-state mRNA (12.0 ± 0.6) and the increase in the transcription rate (3.1 ± 0.6) in PC12 cells.

We have demonstrated using an *in vitro* RNA degradation assay that there are two distinct cis-acting instability elements in the VEGF 3'-UTR. The VEGF 3'-UTR contains two consensus nonameric sequences 5'-UUAUUUA(U/A)(U/A)-3' (25, 26) that have been demonstrated to mediate the rapid turnover of multiple cytokine mRNAs. These nonameric consensus sequences fall within the fragments shown to significantly affect transcript stability in the *in vitro* degradation assays. We cannot rule out however that other sequences contained within these fragments are responsible for or contribute to the RNA instability.

The increased stability of VEGF 3'-UTR transcripts *in vitro* in the presence of hypoxic *versus* normoxic extracts has allowed us to map an element that when deleted from the UTR abrogates this increased stability with hypoxic extracts. From these studies one may hypothesize that a trans-acting factor that mediates stability binds to this region or, alternatively, the region is necessary for formation of a RNA secondary structure that mediates the change in RNA stability.

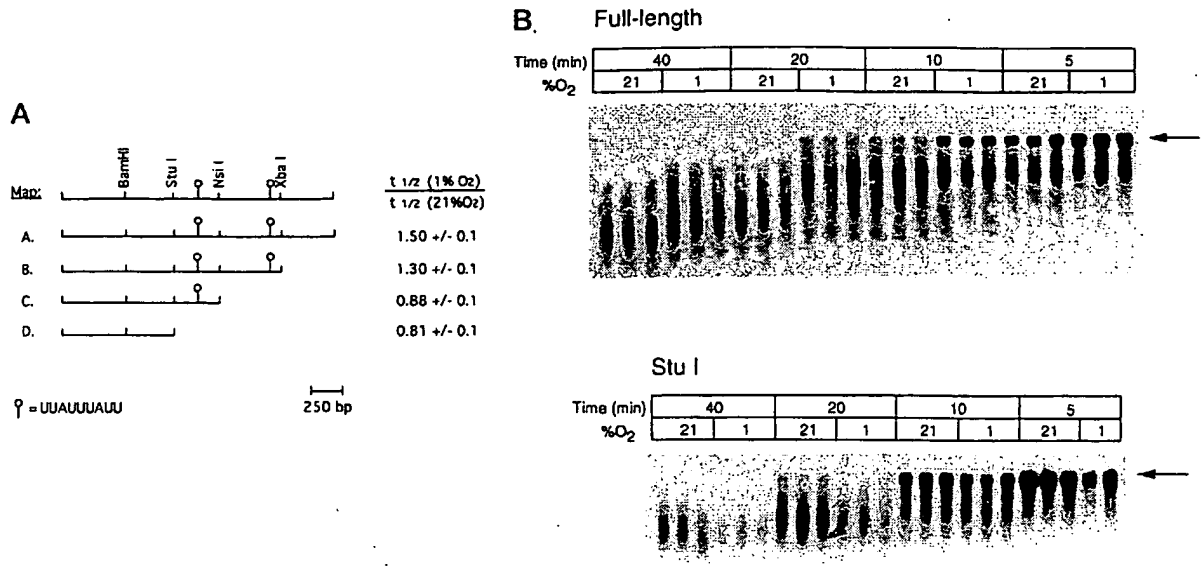

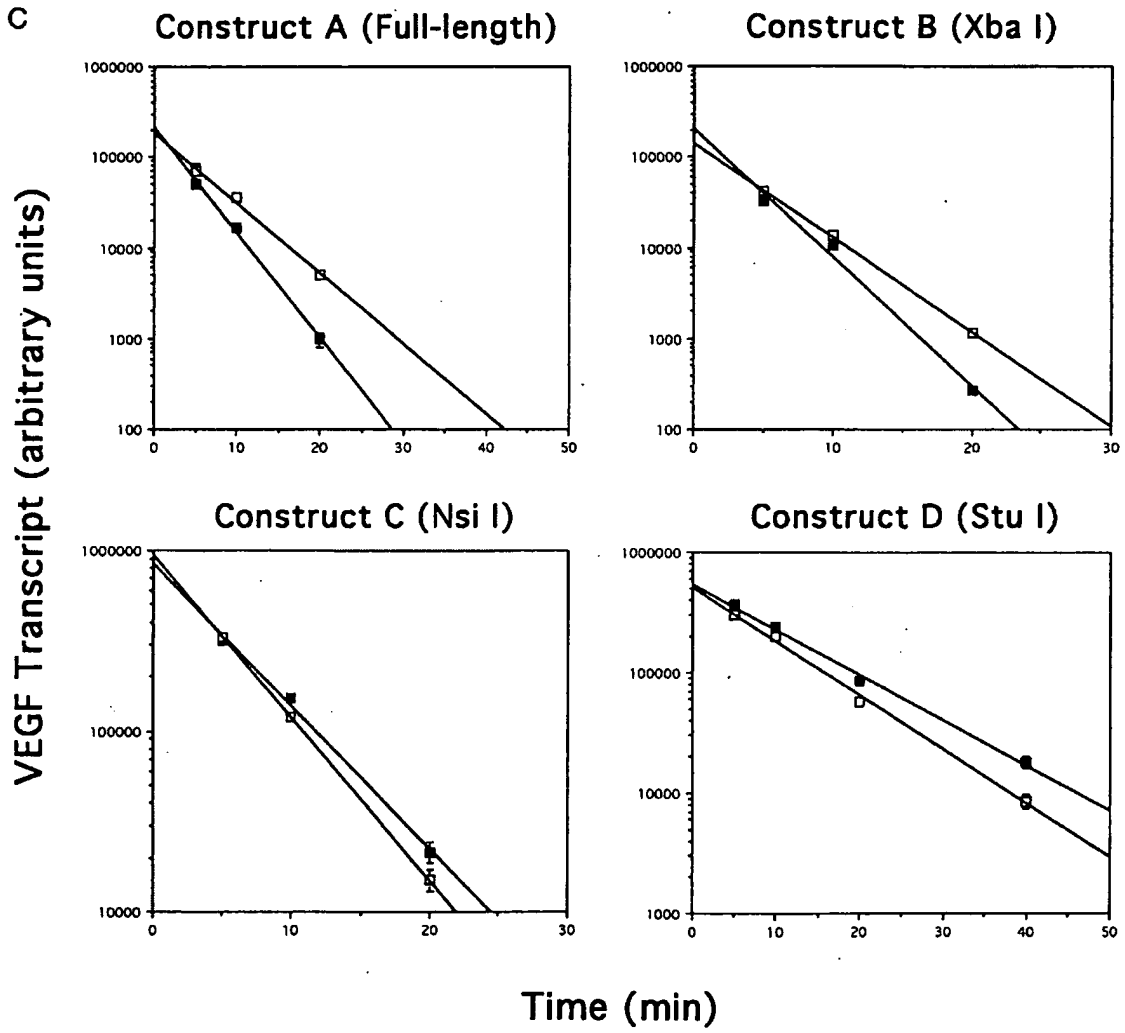

FIG. 3. **Mapping an element in the VEGF 3'-UTR that mediates stabilization by hypoxia.** [^{32}P]CTP-labeled, capped, and polyadenylated transcripts were generated *in vitro* as described under "Materials and Methods." *A*, restriction map of constructs *A–D* in pSP64A (*AseI*) as described in the legend to Fig. 2*A*. A half-life for each construct was determined with normoxic and hypoxic extracts using the identically labeled transcript. The results are expressed as a ratio of the transcript half-life using hypoxic to normoxic extracts. All of the time points were performed in triplicate. Each transcript was assayed three different times with different extracts. *B*, representative autoradiograph of products from the degradation assay of constructs A (*Full-length*) and D (*StuI*). Time refers to time after the addition of the normoxic or hypoxic extract to the labeled transcript. The *arrow* points to the undegraded transcript. One of the RNA pellets in the triplicate 5 min 1% O_2 time point for the *StuI* RNA fragment was lost in processing, and the data from this sample are not included. *C*, log-linear regression lines of VEGF RNA degradation quantitated by PhosphorImager analysis. The half-life of each construct was calculated from these regression lines using normoxic (■) and hypoxic (□) extracts. This is a representative experiment of the data summarized from three independent experiments in Fig. 3*A*. Each time point was performed in triplicate.

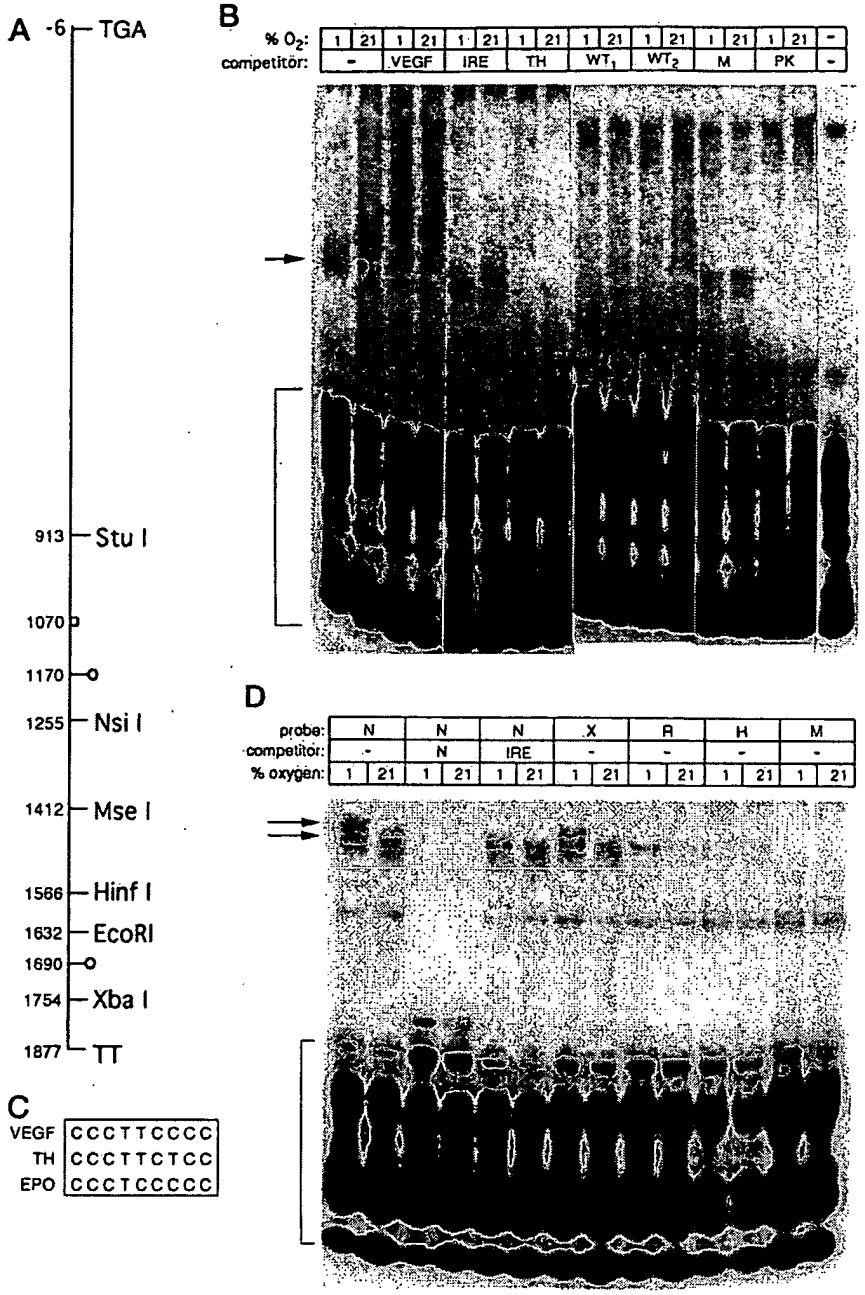

FIG. 4. **Identification of constitutive and hypoxia inducible RNA-protein complexes by EMSA.** *A*, map of the VEGF mRNA 3'-UTR demonstrating location of templates used for generation of riboprobes for EMSA and to map the cis-elements with which the RNA binding proteins interact. A T7 promoter was appended to the sense primer for generation of templates as described under "Materials and Methods." The *StuI-NsiI* template corresponds to nucleotide 909-1279 of the VEGF 3'-UTR, GenBank™ accession no. U22372. The *NsiI* transcription termination (*TT*) site template includes nucleotide 1251–1877 of the VEGF 3'-UTR, GenBank™ accession no. U22372. Restriction endonuclease *MseI*, *HinfI*, *EcoRI*, and *XbaI* sites in the *NsiI*-TT site template are located at nucleotides 1412, 1566, 1632, and 1754, respectively, of the VEGF mRNA 3'-UTR, GenBank™ accession no. U22372. TGA is the translation termination codon of VEGF and is located 6 bp 5' to nucleotide 1 in GenBank™ accession no. U22372. TT is the transcription termination site of VEGF mRNA. The nonameric instability consensus signals are depicted by *lines* with *open circles*. The small open box at nucleotide 1070 is the proposed site to which the constitutive protein complex binds. *B*, EMSA of the constitutive RNA-protein complex. RNA EMSA using the *NsiI-StuI* fragment as template was performed as described under "Materials and Methods." Unlabeled RNA transcripts for competition studies were generated from the following templates: *NsiI-StuI* (*VEGF*); IRE (22); tyrosine hydroxylase (*TH*) 162-bp fragment (16); oligonucleotides WT_1, WT_2, and M as described under "Materials and Methods." Proteinase K (*PK*) indicates extracts were first treated with proteinase K before adding the probe. The *arrow* points to the constitutive RNA-protein complex. The *bracket* encompasses free and degraded probe. *C*, sequence homology. Region of homology between the rat VEGF 3'-UTR, rat tyrosine hydroxylase 3'-UTR, and human Epo 3'-UTR. This region of the *NsiI-StuI* fragment of the VEGF 3'-UTR (nucleotide 1066–1075) was demonstrated to bind a protein(s) in S100 cytoplasmic extracts. The tyrosine hydroxylase sequence is within a 28-bp sequence of the tyrosine hydroxylase 3'-UTR (nucleotide 1552–1579) (32) that is protected by a hypoxia-inducible protein (16). The Epo sequence (nucleotide 2831–2841) (33) is within a 120 bp sequence of the Epo 3' UTR shown to bind a Epo mRNA binding protein that is up-regulated by hypoxia in brain and spleen (15). Nucleotide sequence for rat VEGF, rat tyrosine hydroxylase, and human Epo refer to GenBank™ accession nos. U22372, M10244, and M11319, respectively. *D*, EMSA of the hypoxia-inducible complex. RNA EMSA using the *NsiI*-transcription termination fragment generated by PCR or agarose gel-purified restriction endonuclease digested subfragments of this fragment as templates for the generation of probe (labeled RNA transcript). [^{32}P]CTP labeled RNA transcripts were *NsiI*-transcription termination (*N*), *NsiI-XbaI* (*X*), *NsiI-EcoRI* (*R*), *NsiI-HinfI* (*H*), or *NsiI-MseI* (*M*). Unlabeled competitors were the *NsiI*-transcription termination transcript (*N*) or IRE transcripts (22) present in 100 × molar excess to the labeled probe. Similar results were obtained with four different preparations of S100 extract. The *arrows* point to the hypoxia-inducible complex. The *bracket* encompasses the free and degraded probe.

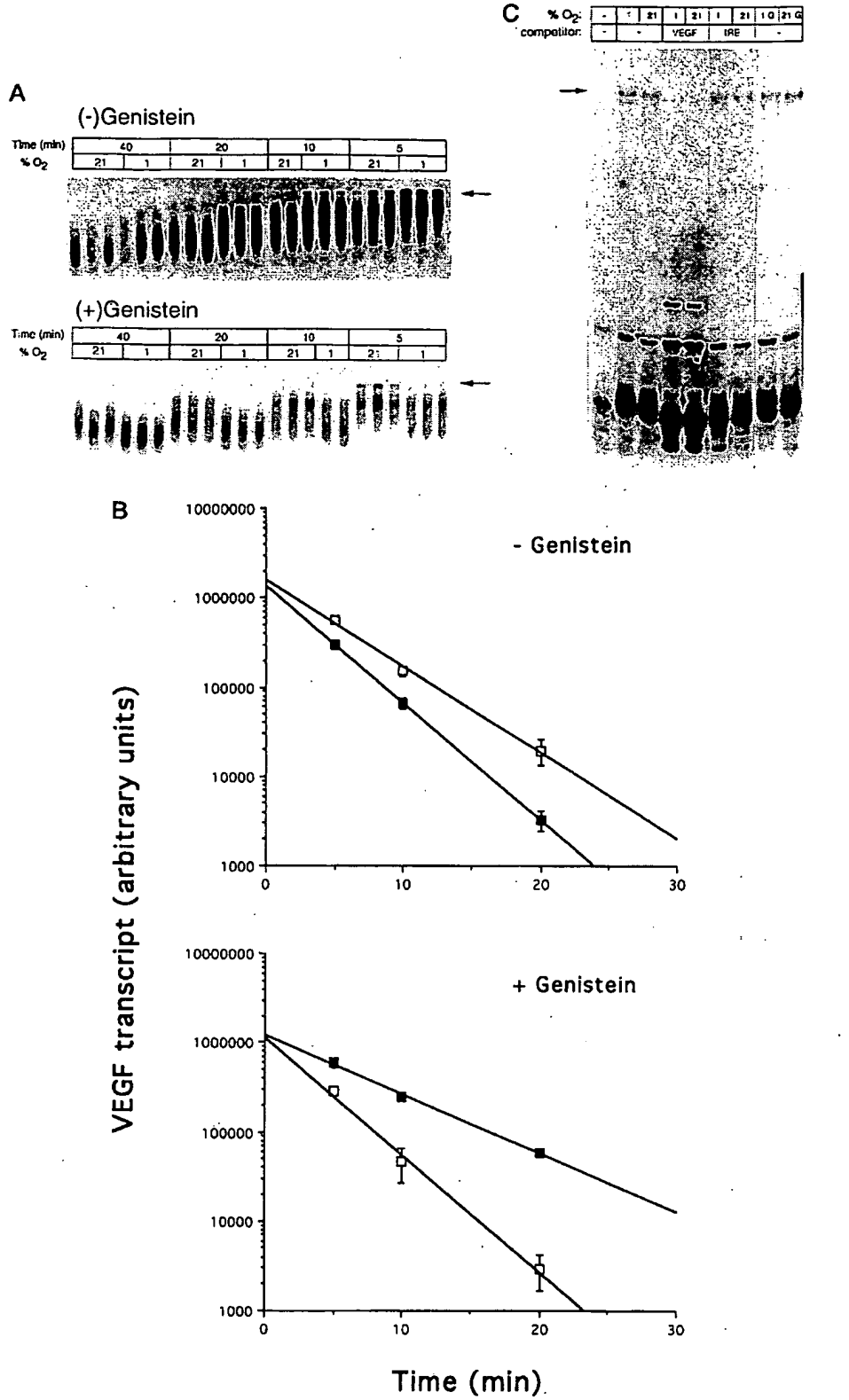

FIG. 5. **Genistein inhibits hypoxic stabilization of VEGF 3′-UTR transcripts *in vitro*.** Cells were pretreated with 500 uM genistein, an inhibitor of the hypoxic induction of VEGF mRNA (32), for 30 min prior to beginning the hypoxic exposure. After 4 h extracts were prepared from normoxic and hypoxic cells. Degradation of full-length VEGF 3′-UTR transcript (construct A, Fig. 2*A*) was assessed as described under "Materials and Methods." *A*, representative autoradiograph of decay kinetics of the VEGF 3′-UTR with genistein treated or control cells using hypoxic and normoxic extracts. The *arrow* points to undegraded transcript. One of the RNA pellets in the triplicate 10 min 1% O_2 time point for genistein treated cells and one of the RNA pellets in the triplicate 10 min 21% O_2 time point for control cells were lost in processing and the data from these samples are not included. *B*, regression analysis of *A* demonstrating an inhibition in the stabilization of VEGF 3′-UTR transcripts in extracts prepared from genistein-treated cells. The experiment was performed three times with different preparations of extract. In the representative experiment shown, the ratio of the half-lives in hypoxia (□) to normoxia (■) of the VEGF 3′-UTR transcript is decreased from 1.4 in control cells to 0.5 in genistein-treated cells. *C*, genistein inhibited formation of the hypoxia-inducible RNA-protein complex on EMSA. The *Nsi*I-transcription termination template was used for EMSA analysis as described under "Materials and Methods." The competitor was an RNA transcript derived from the *Nsi*I-transcription termination template (*VEGF*) or the IRE element (22). *1 G* or *21 G* indicates that the S100 extract was made under hypoxic or normoxic conditions, respectively, from cells treated with genistein. The *arrow* points to the hypoxia-inducible species.

In EMSA studies, the region of the VEGF mRNA 3′-UTR to which the hypoxia-induced protein complex bound correlated with the RNA degradation assays and points toward an important role for this complex in mediating the increased stabilization of VEGF mRNA by hypoxia. The hypoxia-inducible complex is occasionally seen to migrate as a doublet using the entire *Nsi*I transcription termination site riboprobe (Fig. 4*D*). This has not been observed with truncated forms of the template (*Nsi*I-*Eco*RI), although hypoxia-inducible binding is still seen. In addition, further truncation of this fragment (*Nsi*I-*Hin*fI) still results in binding of a protein by EMSA, but the complex is no longer hypoxia-inducible.

Genistein, a tyrosine kinase inhibitor, was recently shown to inhibit the hypoxic induction of VEGF mRNA (28) through its action on Src. A signal transduction cascade leading to the hypoxic induction of VEGF through Raf was demonstrated using the dominant inhibitory Raf-1 mutant Raf(301) (28, 29). In other systems this cascade has been shown to proceed through mitogen-activated protein kinase and ultimately to modulate transcription of specific genes and phosphorylation of specific gene products (30, 31). We have shown here that genistein interferes with the post-transcriptional induction of VEGF by hypoxia. 500 uM genistein had no effect on the hypoxic induction of 5′ promoter reporter constructs but inhibited the preferential stabilization of VEGF 3′-UTR transcripts *in vitro* by hypoxic *versus* normoxic extracts and inhibited formation of a hypoxia-inducible protein-RNA complex by EMSA. One possibility is that the signal cascade through *src/raf* and possibly mitogen-activated protein kinase has as its terminal event a protein that binds to the VEGF mRNA 3′-UTR and mediates its hypoxic stabilization.

An understanding of the molecular basis of the regulation of VEGF by hypoxia forms the essential groundwork for the rational design of pharmacological agents to modulate VEGF expression and thereby augment or inhibit neovascularization. The *in vitro* degradation assays and EMSA described here should allow for the rapid and economic assessment of multiple agents that may affect VEGF mRNA stability.

Acknowledgment—We thank Dr. H. Franklin Bunn for critical review of this manuscript.

REFERENCES

1. Sabri, M. N., DiSciascio, G., Cowley, M. J., Alpert, D., and Vetrovec, G. W. (1991) *Am. Heart J.* **121**, 876–880
2. Shweiki, D., Itin, A., Soffer, D., and Keshet, E. (1992) *Nature* **359**, 843–845
3. Aiello, L. P., Avery, R. L., Arrigg, P. G., Keyt, B. A., Jampel, H. D., Shah, S. T., Pasquale, L. R., Thieme, H., Iwamoto, M. A., Park, J. F., Nguyen, H. V., Aiello, L. M., Ferrara, N., and King, G. (1994) *N. Engl. J. Med.* **331**, 1480–1487
4. Leung, D. W., Cachianes, G., Kuang, W. J., Goeddel, D. V., and Ferrara, N. (1989) *Science* **246**, 1306–1309
5. Levy, A. P., Tamargo, R., Brem, H., and Nathans, D. (1989) *Growth Factors* **2**, 9–19
6. Senger, D., Ven De Water, L., Brown, L., Nagy, J., Yeo, K.-T., Yeo, T.-K., Berse, B., Jackman, R., Dvorak, A., and Dvorak, H. (1993) *Cancer Metastasis Rev.* **12**, 303–324
7. Goldberg, M. A., and Schneider, T. (1994) *J. Biol. Chem.* **269**, 4355–4359
8. Levy, A. P., Levy, N. S., Loscalzo, J., Calderone, A., Takahashi, N., Yeo, K.-T., Koren, G., Colucci, W., and Goldberg, M. (1995) *Circ. Res.* **76**, 758–766
9. Sharma, H., Sassen, L., Verdouw, P., and Schaper, W. (1992) *J. Mol. Cell. Cardiol.* **24**, Suppl. V, S.10 (abstr.)
10. Sharma, H. S., Wunsch, M., Schmidt, M., Schott, R. J., Kandolf, R., and Schaper, W. (1992) *Exper. Suppl.* **61**, 255–260
11. Sharma, H. S., Wunsch, M., Brand, T., Verdouw, P. D. and Schaper, W. (1992) *J. Cardiovasc. Pharmacol.* **20**, S23–S31
12. Levy, A. P., Levy, N. S., Wegner, S., and Goldberg, M. A. (1995) *J. Biol. Chem.* **270**, 13333–13340
13. Goldberg, M. A., Gaut, C. C., and Bunn, H. F. (1991) *Blood* **77**, 271–277
14. Ho, V., Acquaviva, A., Duh, E., and Bunn, H. F. (1995) *J. Biol. Chem.* **270**, 10084–10090
15. Rondon, I. J., MacMillan, L. A., Beckman, B. S., Goldberg, M. A., Schneider, T., Bunn, H. F., and Malter, J. S. (1991) *J. Biol. Chem.* **266**, 16594–16598
16. Czyzyk-Krzeska, M. F., Dominski, Z., Kole, R., and Millhorn, D. E. (1994) *J. Biol. Chem.* **269**, 9940–9945
17. Wang, X., Kiledjian, M., Weiss, I. M., and Liebhaber, S. A. (1995) *Mol. Cell. Biol.* **15**, 1769–1777
18. Gorospe, M., and Baglioni, C. (1994) *J. Biol. Chem.* **269**, 11845–11851
19. Khalili, K., and Weinmann, R. (1984) *J. Mol. Biol.* **180**, 1007–1021
20. Mullis, K. B., and Faloona, F. (1987) *Methods Enzymol.* **155**, 335–350
21. Stoflet, E. S., Koeberl, G., Sarkar, G., and Sommer, S. S. (1988) *Science* **239**, 491–494
22. Mullner, E. W., Neupert, B., and Kuhn, L. C. (1989) *Cell* **58**, 373–382
23. Skoog, D. A., and West, D. M. (1980) *Analytical Chemistry*, 3rd Ed., W. B. Saunders, Philadelphia
24. Sheets, M. D., Ogg, S. C., and Wickens, M. P. (1990) *Nucleic Acids Res.* **18**, 5799–5805
25. Lagnado, C. A., Brown, C. Y., and Goodall, G. J. (1994) *Mol. Cell. Biol.* **14**, 7984–7995
26. Zubiaga, A. M., Belasco, J. G., and Greenberg, M. E. (1995) *Mol. Cell. Biol.* **15**, 2219–2230
27. Rodgers, J. R., Johnson, M. L., and Rosen, J. M. (1985) *Methods Enzymol.* **109**, 572–592
28. Mukhopadhyay, D., Tsiokas, L., Zhou, X.-M., Foster, D., Brugge, J. S., and Sukhatme, V. P. (1995) *Nature* **375**, 577–581
29. Kolch, W., Heidecker, G., Lloyd, P., and Rapp, U. R. (1991) *Nature* **349**, 426–428
30. Auruch, J., Zhang, X. F., and Kyriakis, J. M. (1994) *Trends Biochem. Sci.* **19**, 279–283
31. Daum, G., Eisenman-Tappe, I., Fries, H. W., Troppmair, J., and Rapp, U. R. (1994) *Trends Biochem. Sci.* **19**, 474–480
32. Grima, B., Lamouroux, A., Blanot, F., Biguet, N. F., and Mallet, J. (1985) *Proc. Natl. Acad. Sci. U. S. A.* **82**, 617–621
33. Lin, F. K., Suggs, S., Lin, C. H., Browne, J. K., Smalling, R., Egrie, J. C., Chen, K. K., Fox, G. M., Martin, F., Stabinsky, Z., Badrawi, S. M., Lai, P. H., and Goldwasser, E. (1985) *Proc. Natl. Acad. Sci. U. S. A.* **82**, 7580–7584

Journal of Neurochemistry
Lippincott Williams & Wilkins, Inc., Philadelphia

Growth Factor-Mediated Stabilization of Amyloid Precursor Protein mRNA Is Mediated by a Conserved 29-Nucleotide Sequence in the 3′-Untranslated Region

Lakshman E. Rajagopalan and James S. Malter

Department of Pathology and Laboratory Medicine, University of Wisconsin Medical School, Madison, Wisconsin, U.S.A.

Abstract: Using a cell-free translation system, we previously demonstrated that the turnover and translation of amyloid precursor protein (APP) mRNA was regulated by a 29-nucleotide instability element, located 200 nucleotides downstream from the stop codon. Here we have examined the regulatory role of this element in primary human capillary endothelial cells under different nutritional conditions. Optimal proliferation required a growth medium (endothelial cell growth medium) supplemented with epidermal, basic fibroblast, insulin-like, and vascular endothelial growth factors. In vitro transcribed mRNAs with the 5′-untranslated region (UTR) and coding region of β-globin and the entire 3′-UTR of APP 751 were transfected into cells cultured in endothelial cell growth medium. Wild-type globin-APP mRNA containing an intact APP 3′-UTR and mutant globin-APP mRNA containing a mutated 29-nucleotide element decayed with identical half-lives ($t_{1/2}$ = 60 min). Removal of all supplemental growth factors from the culture medium significantly accelerated the decay of transfected wild-type mRNA ($t_{1/2}$ = 10 min), but caused only a moderate decrease in the half-life of transfected mutant mRNA ($t_{1/2}$ = 40 min). We therefore conclude that the 29-nucleotide 3′-UTR element is an mRNA destabilizer whose function can be inhibited by inclusion of the aforementioned mixture of growth factors in the culture medium. **Key Words:** Amyloid protein precursor—3′-Untranslated region—mRNA decay—Growth factor—Capillary endothelial cells.
J. Neurochem. **74,** 52–59 (2000).

The deposition of β-amyloid peptide (βA4), around the cerebral vasculature and neurons, is a pathological hallmark of Alzheimer's disease (AD), hereditary cerebral hemorrhage with amyloidosis, Dutch type (HCHWA-D), and Down's syndrome (DS) (Selkoe, 1993; Castano et al., 1996). This 39–42 amino acid peptide is derived from the aberrant processing (Citron et al., 1992) of a larger, membrane-associated glycoprotein, the β-amyloid precursor protein (βAPP). All mutations that cause the inherited forms of AD, HCHWA-D, and DS act by a common mechanism of increasing βA4 deposition.

In the vast majority of AD cases that are late-onset and sporadic, the etiology of the disease remains poorly understood. Overexpression of different isoforms of βAPP in transfected cells or transgenic animals alters its normal processing, resulting in the deposition of amyloidogenic fragments (Fukuchi et al., 1992; Yoshikawa et al., 1992). In postmortem AD brain, increases in the proportions of different APP mRNA isoforms have been reported. Neuronal cells showed moderate, but significant, disease-associated increases in the proportion of Kunitz-type protease inhibitor (KPI)-containing APP 751 and APP 770 mRNA isoforms (Johnson et al., 1990; Johnston et al., 1996). In skin fibroblasts from DS patients, the proportions of KPI-containing isoforms were elevated significantly at a very young age (mean age, 5 years), but not so in the aged DS group (Urakami et al., 1996). Thus, in sporadic AD and in DS, the early overexpression of specific APP isoforms could initiate and/or propagate pathological cascades.

Overexpression of APP and βA4 deposition can be accelerated by growth factors and proinflammatory cytokines. The coexpression of transforming growth factor-β1 (TGF-β1) in transgenic mice expressing human βAPP accelerated the overexpression of APP and βA4 deposition in cerebral blood vessels and meninges (Wyss-Coray et al., 1997). βA4 also induced production and secretion of interferon-γ and interleukin-1β (IL-1β) in human vascular endothelial cells (Suo et al., 1998).

Received July 29, 1999; revised manuscript received September 16, 1999; accepted September 16, 1999.

Address correspondence and reprint requests to Dr. J. S. Malter at Department of Pathology and Laboratory Medicine, University of Wisconsin Medical School, Madison, WI 53792, U.S.A. E-mail: js.malter@hosp.wisc.edu

Abbreviations used: βA4, β-amyloid peptide; AD, Alzheimer's disease; APP, amyloid precursor protein; bFGF, basic fibroblast growth factor; DS, Down's syndrome; EBM, endothelial cell basal medium; EGF, epidermal growth factor; EGM, endothelial cell growth medium; FBS, fetal bovine serum; GAP-43, growth-associated protein-43; Gl-APP, globin-APP; Gl-APPmut, mutated globin-APP; Gl-APPwt, wild-type globin-APP; HCHWA-D, hereditary cerebral hemorrhage with amyloidosis, Dutch type; HUVEC, human umbilical vein endothelial cells; IGF-1, insulin-like growth factor-1; IL-1, interleukin-1; KPI, Kunitz-type protease inhibitor; TGF-β, transforming growth factor-β; UTR, untranslated region; VEGF, vascular endothelial growth factor.

Thus, βA4 acting in concert with proinflammatory cytokines could trigger a self-propagating cycle of chronic βAPP overexpression and deposition of βA4, with neurodegenerative consequences. Factors that control both APP expression and processing are therefore of critical significance in AD pathogenesis.

Previous work from our laboratory identified a conserved 29-nucleotide sequence, ~200 nucleotides downstream from the APP stop codon that functioned as an APP mRNA-destabilizing element in a rabbit reticulocyte lysate cell-free translation system (Rajagopalan et al., 1998). We hypothesized that this instability element could similarly regulate APP mRNA decay in intact cells. Preliminary studies with the widely used rat pheochromocytoma (PC12) and human neuroblastoma (SH-SY5Y) cell lines revealed that endogenous APP mRNA was constitutively stable ($t_{1/2}$ > 12 h; unpublished observations). This likely reflects dysregulated mRNA decay, as is often seen in tumor lines (Ross et al., 1991). For example, labile mRNAs coding for cytokines, growth factors, and protooncogenes that typically decayed with half-lives of 15–30 min, were six- to 10-fold more stable ($t_{1/2}$ > 3 h) in transformed cell lines (Ross et al., 1991).

Human umbilical vein endothelial cells (HUVEC) have the advantage of being primary cells that transcribe KPI-containing APP 751 and APP 770 mRNA isoforms (Haass et al., 1992) that are elevated in AD and DS (Johnson et al., 1990; Johnston et al., 1996; Urakami et al., 1996). Further, the lysosomal processing of βAPP in these cells has been shown to generate potentially amyloidogenic, β-peptide-bearing fragments (Haass et al., 1992). Goldgaber et al. (1989) demonstrated that in HUVEC, growth factors could up-regulate the APP promoter and thereby increase steady-state APP mRNA levels. However, the short half-life (4 h) of the APP transcript in the absence of growth factors (Goldgaber et al., 1989) suggested that regulation may also occur posttranscriptionally at the level of APP mRNA decay. HUVEC therefore provided a good vascular endothelial cell model to examine the regulation of APP expression and its processing.

In this study, we have examined the decay of endogenous APP mRNA and the role of the 29-nucleotide instability element in regulating the decay of transfected, chimeric, globin-APP (Gl-APP) mRNAs. Chimeric mRNAs consisted of the globin 5′-untranslated region (5′-UTR) and coding regions fused to full-length APP 751 3′-UTR containing either a wild-type (Gl-APPwt) or mutated (Gl-APPmut) 29-nucleotide instability element. Our data demonstrate that in rapidly dividing cells cultured in endothelial cell growth medium (EGM; see Experimental Procedures), APP mRNAs (wild-type and mutated) were equally stable. When all supplemental growth factors were removed, but proliferation maintained, APP mRNAs containing an intact 29-nucleotide, 3′-UTR element were rapidly destabilized. These data demonstrate for the first time that APP mRNA decay is *cis*-sequence-specific and can be modulated by the extracellular environment.

EXPERIMENTAL PROCEDURES

Cell culture

HUVEC (obtained from Clonetics, San Diego, CA, U.S.A.) were cultured on BIOCOAT Collagen I-coated six- or 12-well plates (Becton–Dickinson, Franklin Lakes, NJ, U.S.A.). In accordance with the manufacturer's protocol for optimal growth, cells were cultured in a growth medium (EGM-2) containing epidermal growth factor (EGF), basic fibroblast growth factor (bFGF), insulin-like growth factor 1 (IGF-1), vascular endothelial growth factor (VEGF), and 5% fetal bovine serum (FBS). To transfer to a growth factor-lacking medium, cells were first washed two or three times in endothelial cell basal medium (EBM-2) before being cultured in EBM-2 supplemented with 1, 2.5, or 5% FBS. Where indicated, cells were trypsinized by strictly following the manufacturer's protocol. Fifth-passage HUVEC were used in all experiments.

Plasmid construction

The construction of plasmids pT7APP751wtT90 and pT7APP751mutT90 has been described previously (Rajagopalan et al., 1998). The 5′-UTR and coding region of β-globin were PCR-amplified from the plasmid pSP6β-globinT90 (Rajagopalan et al., 1998). Primers were designed to create a *Not*I restriction site at the 5′ end and a *Bgl*II site at the 3′ end. The PCR product was then digested with *Not*I and *Bgl*II and ligated into *Not*I/*Bgl*II-digested pT7APP751wtT90 to produce pT7Globin-APP-I.

Full-length APP wild-type and mutated 3′-UTRs were PCR-amplified from pT7APP751wtT90 and pT7APP751mutT90, respectively. Primers were designed to create a *Bgl*II site at the 5′ end and an *Sph*I site at the 3′ end. Each PCR product was then digested with *Bgl*II and *Sph*I and ligated into *Bgl*II/*Sph*I-digested pT7Globin-APP-I to produce pT7Globin-APP3′UTRwtT90 and pT7Globin-APP3′UTRmutT90, respectively (see Fig. 3). Linearization of the plasmids with *Hin*dIII and transcription with T7 polymerase yielded polyadenylated (A_{90}) chimeric RNAs with the 5′-UTR and coding region of β-globin, followed by the 3′-UTR of APP containing either an intact (wild-type) or mutated 29-nucleotide 3′-UTR element.

mRNA synthesis and transfection

Capped, polyadenylated mRNAs were synthesized in vitro, purified, and evaluated for their integrity as previously described (Rajagopalan et al., 1998). Particle-mediated transfer of mRNAs into adherent HUVEC was performed using the Accell gene gun (Rajagopalan and Malter, 1996).

Northern analysis

As stated previously, HUVEC were seeded at identical densities and cultured in either six- or 12-well collagen-coated plates. Each well represented either a distinct culture condition or an individual time point. In experiments examining either the steady-state levels or decay rates of endogenous APP mRNA, cells were lysed by addition of 1 ml of TRI reagent (Molecular Research Center Inc., Cincinnati, OH, U.S.A.) to each well. The entire content of each well was then transferred to a 1.5-ml Eppendorf tube and snap-frozen in an ethanol bath at −80°C. After completion of an individual experiment, total RNA was quantitatively isolated from all conditions and analyzed by northern blotting and phosphorimaging as previously described (Rajagopalan and Malter, 1994). APP-specific signals were normalized to those of actin before being graphed.

RNA dot blots

At the indicated time points, transfected cells were trypsinized and washed twice with HEPES-buffered saline solution before being lysed in 1 ml of TRI reagent. Total RNA pellets from each time point were dissolved and denatured (70°C water bath, 15 min) in 3 μl of sample buffer (30 μl of deionized formamide, 2.4 μl of 25× MOPS, 10.8 μl of 37% formaldehyde, 16.8 μl of diethyl pyrocarbonate-treated water), before being dotted onto a MAGNA nylon transfer membrane (Micron Separations Inc., Westborough, MA, U.S.A.). Samples were allowed to air-dry and then were briefly immersed in 10× saline–sodium citrate buffer and auto UV-cross-linked in a Stratalinker (Stratagene, La Jolla, CA, U.S.A.). Transfected, chimeric Gl-APP mRNAs were detected by hybridization to random-primed globin cDNA probes (Rajagopalan and Malter, 1994). Gl-APP-specific signals were then normalized to those of actin and plotted versus time.

RESULTS

Modulation of APP mRNA steady-state levels by growth factors and serum

Previous studies have shown that the steady-state level of endogenous APP mRNA could be up-regulated in HUVEC by IL-1 (α and β), phorbol 12-myristate 13-acetate, or bFGF (Goldgaber et al., 1989). However, the underlying mechanism for these effects was not determined. We therefore investigated if APP mRNA decay could be altered by culture conditions.

Fifth-passage HUVEC were cultured on collagen I-coated six-well plates in EGM-2 (see Experimental Procedures) containing 5% FBS. At 70% confluence, one set of cells (four wells) was maintained in EGM-2 plus 5% FBS (condition I, Fig. 1), whereas the other sets of cells were washed and transferred to EBM-2 containing 5% (condition II), 2.5% (condition III), or 1% (condition IV) FBS. EGM-2 and EBM-2 were identical except for the absence of supplemental growth factors in the latter. After 5 h, cells were lysed, and total RNA was isolated and northern blotted (see Experimental Procedures). APP-specific signals were normalized to those of actin and plotted for each condition (Fig. 1). To assess growth rates, separate sets of cells were trypsinized and counted at the start and at the end of the 5-h incubations (Table 1). Removal of all supplemental growth factors (condition I versus II) caused a significant decrease of ~30% in steady-state APP mRNA levels. Cells cultured in conditions I and II had identical growth rates (Table 1). Thus, changes in APP mRNA levels were not a result of alterations in the rates of cell proliferation. APP mRNA continued to decline as serum content of the medium was decreased further to 2.5 and 1% (Fig. 1, conditions III and IV). However, growth rates of cells cultured under conditions III and IV were inhibited considerably (Table 1). Cells remained differentiated and morphologically indistinguishable under all culture conditions.

Effects of medium growth factor and serum content on APP mRNA half-life

The medium-dependent alterations in APP mRNA steady-state levels could be the result of either changes in gene transcription (Goldgaber et al., 1989), mRNA turnover (Zaidi and Malter, 1994), or both. We therefore measured APP mRNA decay after blocking transcription with actinomycin D. The experiment described in Fig. 1 was repeated, and actinomycin D (5 μg/ml) was added following 5-h incubations in different culture conditions (I, II, III, or IV; see Table 1). Cells were lysed either immediately (0 time) or at 2, 4.5, and 7 h after actinomycin D addition. Total RNA was isolated from each sample and northern blotted (Fig. 2A). APP mRNA showed no perceptible decay ($t_{1/2}$ > 12 h) in growth factor-supplemented medium with 5% FBS (EGM-2, condition I). However, when cells were cultured for 5 h in a growth factor-lacking medium (EBM-2) supplemented with 5% FBS (condition II), a 35–50% decline in APP mRNA steady-state level (compare 0 times, condition I versus II) was accompanied by a greater than threefold decrease in APP mRNA half-life ($t_{1/2}$ = 4 h; Fig. 2B). The decline in APP mRNA steady state was therefore largely the result of accelerated decay. Varying the FBS content of EGM-2 from 2 to 10% did not alter APP mRNA steady-state level or half-life (>12 h; data not shown), thereby linking accelerated decay to the absence of supplemental growth factors. As the amount of serum in EBM-2 was lowered to 2.5 and 1%, APP mRNA steady-state levels continued to decrease (0 time, conditions III and IV, Fig. 2A). However, these de-

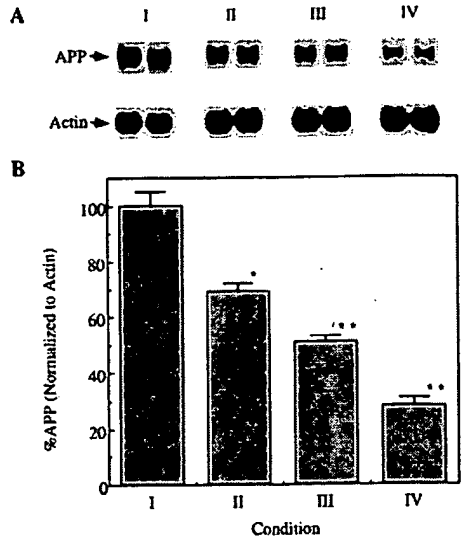

FIG. 1. Culture conditions modulate steady-state levels of endogenous APP mRNA in HUVEC. Fifth-passage HUVEC were cultured on collagen-coated plates to 70% confluence under condition I (Table 1). At this point, one set of cells was maintained in condition I. Other sets of cells were switched to either condition II, III, or IV (Table 1) and cultured for 5 h, after which cells were lysed and total RNA isolated for northern analysis. **A:** Northern blots were hybridized sequentially with cDNA probes for APP and actin. Each condition in this figure is represented by duplicate samples. **B:** Signals were quantified by phosphorimaging, and APP-specific signals were normalized to those for actin and plotted for the different culture conditions. Data points represent the means ± SD of five separate determinations (*$p < 0.01$; **$p < 0.001$).

TABLE 1. *Culture conditions and growth of HUVEC*

	Supplemental growth factors[a]	% FBS	Cell count ($\times 10^{-4}$) (70% confluence) 0 h	5 h
Condition I (EGM)	Yes	5	7.12 ± 0.12	8.6 ± 0.05
Condition II (EBM)	No	5	7.06 ± 0.16	8.7 ± 0.12
Condition III (EBM)	No	2.5	6.91 ± 0.16	7.5 ± 0.21
Condition IV (EBM)	No	1	7.09 ± 0.12	7.3 ± 0.18

[a] EGF, bFGF, IGF-1, and VEGF.

creases were due mostly to transcriptional down-regulation, because APP mRNA remained very stable ($t_{1/2}$ > 12 h) under these conditions. Culture conditions can therefore induce dramatic changes in the amount of APP mRNA via both transcriptional and posttranscriptional events.

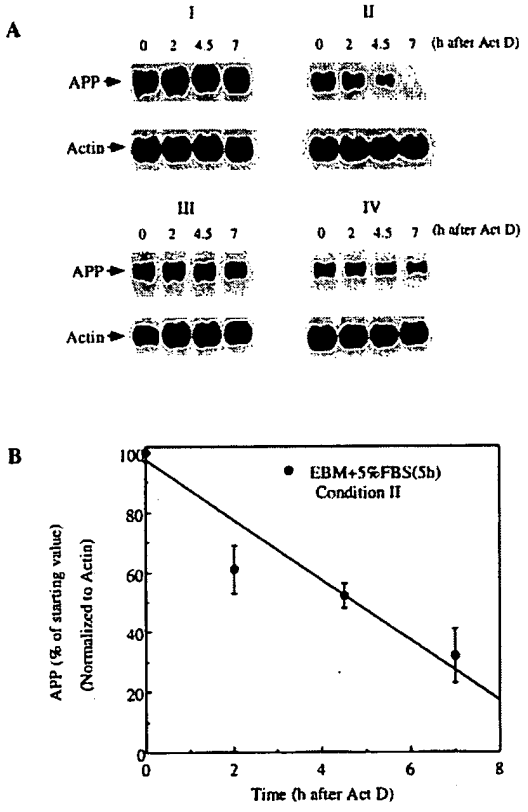

FIG. 2. Decay rates of endogenous APP mRNA in HUVEC are altered by growth factors and serum. Cells were cultured as indicated in Fig. 1. Following the 5-h incubation, transcription was blocked with actinomycin D (Act D; 5 μg/ml), and cells were lysed either immediately or 2, 4.5, or 7 h after actinomycin D addition. **A:** Total RNA was isolated and analyzed as indicated in Fig. 1. **B:** APP signals were normalized to those of actin and plotted versus time for condition II. Each time point is the mean ± SD of three determinations.

APP 3′-UTR-mediated decay of transfected mRNA: influence of growth factors

Using a rabbit reticulocyte lysate cell-free translation system, previous work from our laboratory had established a 29-nucleotide sequence in the 3′-UTR as necessary and sufficient for regulated APP mRNA decay (Rajagopalan et al., 1998). We therefore wanted to determine whether changes in APP mRNA half-life in HUVEC (Fig. 2, condition I versus II) were mediated by the same 29-nucleotide sequence. To do this, we constructed plasmids (see Experimental Procedures and Fig. 3) from which we transcribed chimeric Gl-APP mRNAs containing the entire 5′-UTR and coding region of globin fused to the 3′-UTR of APP. Gl-APPwt mRNA contained an intact 29-nucleotide element, whereas Gl-APPmut mRNA had a scrambled 29-nucleotide element. All mRNAs were capped at their 5′ ends and contained a 90-nucleotide poly(A) tail at the 3′ end. Chimeric RNAs were used to distinguish transfected mRNAs from endogenous APP mRNA and to permit identification of essential *cis*-elements that controlled decay.

In initial studies, we transfected Gl-APPwt mRNA into HUVEC at 70% confluence (see Experimental Procedures), cultured for 5 h in either EGM-2 plus 5% FBS (condition I) or EBM-2 plus 5% FBS (condition II) as described in Fig. 1. At the indicated time points after

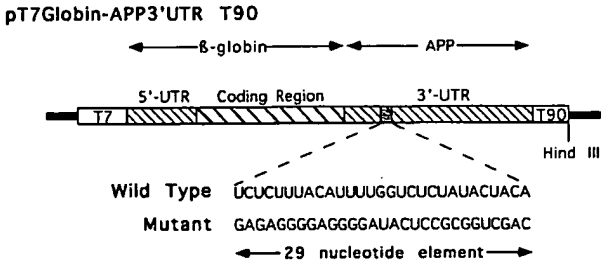

FIG. 3. T7Globin-APP3′UTR T90 in vitro transcription vectors. Chimeric cDNA was constructed containing the 5′-UTR and coding sequence of globin followed by the entire 3′-UTR of APP with either a wild-type (Gl-APPwt) or mutated (Gl-APPmut) 29-nucleotide element (see Experimental Procedures). The chimeric constructs were cloned into transcription vectors, downstream from a T7 RNA polymerase site and upstream from a 90-nucleotide oligo(dT) tract. Linearization of the transcription vectors at the unique *Hin*dIII site permitted the synthesis of mRNAs containing 90-nucleotide poly(A) tails.

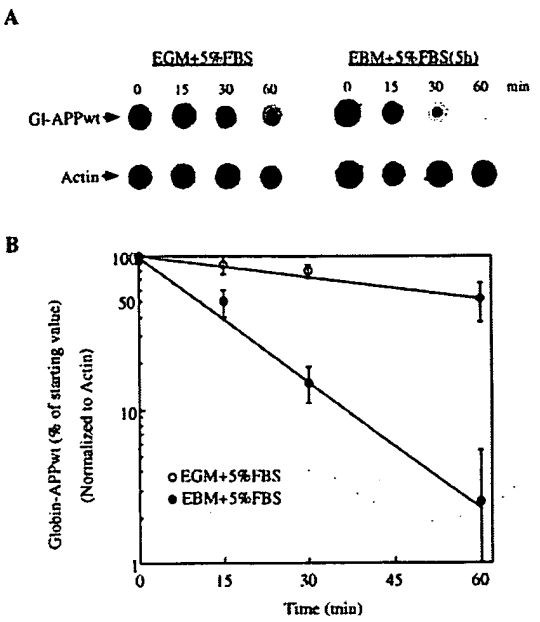

FIG. 4. Growth factors stabilize transfected Gl-APPwt mRNA. HUVEC were cultured for 5 h in either condition I or condition II, as described in Fig. 1. Capped, polyadenylated, in vitro transcribed Gl-APPwt mRNAs were delivered into cells via the particle-mediated gene transfer technology. At the indicated time points following transfection, cells were trypsinized, washed twice in HEPES buffer, and then lysed. **A:** Total RNA was isolated from each sample and dot blotted. Blots were then sequentially hybridized with cDNA probes for globin and actin. **B:** Gl-APP-specific signals were normalized to those of actin and plotted versus time. Each time point is the mean ± SD of six determinations.

transfection (Fig. 4), cells were trypsinized and washed twice in HEPES-buffered saline before lysis and isolation of total RNA. This procedure eliminated any mRNA bound to the collagen matrix or to the plasma membrane. Transfected intracellular mRNA was then detected by dot blot hybridization with radiolabeled globin cDNA probes (Fig. 4A). Nontransfected HUVEC showed no detectable endogenous globin mRNA (data not shown). Gl-APP-specific signals were normalized to those of endogenous actin to control for variations in cells harvested, and plotted versus time (Fig. 4B). Each time point is the mean ± SD of four to eight separate transfections.

In cells cultured in condition I, transfected Gl-APPwt mRNA decayed with a half-life of 60 min (Fig. 4B). With cells cultured in the absence of all supplemental growth factors (condition II), decay of transfected Gl-APPwt mRNA was accelerated sixfold ($t_{1/2}$ = 10 min; Fig. 4B). The relative change in decay of transfected Gl-APPwt mRNA upon removal of growth factors was therefore similar to that observed with endogenous APP mRNA. However, the absolute decay rate of transfected Gl-APPwt mRNAs was considerably faster than that of endogenous APP mRNA after transcription was blocked with actinomycin D (compare Figs. 2B and 4B). We have observed previously a similar phenomenon in peripheral blood mononuclear cells with transfected versus endogenous GM-CSF (granulocyte-macrophage colony-stimulating factor) mRNAs (Rajagopalan and Malter, 1996).

APP mRNA decay in HUVEC is mediated by the 29-nucleotide 3′-UTR element

To examine whether the 29-nucleotide APP 3′-UTR element was necessary for rapid APP mRNA decay in the absence of supplemental growth factors, we transfected cells with chimeric Gl-APP mRNA in which the 29-nucleotide sequence had been mutated (Gl-APPmut; Fig. 3). Experiments were performed under identical cell culture conditions as described in Fig. 4. In the presence of growth factors (condition I), the decay of Gl-APPmut mRNA was identical ($t_{1/2}$ = 60 min; Fig. 5) to that of Gl-APPwt mRNA. Whereas removal of all supplemental growth factors accelerated the decay of transfected Gl-APPwt mRNA sixfold (Fig. 4), it produced only a modest decline in the half-life of transfected Gl-APPmut mRNA ($t_{1/2}$ = 40 min; Fig. 5). Thus, modification of the 29-nucleotide element was sufficient to confer near constitutive stability to Gl-APP mRNA. The 29-nucleotide element therefore functions to destabilize APP mRNA in the absence of the complete mixture of supplemental growth factors. Conversely, the functionality of the element can be masked by the inclusion of EGF, bFGF, IGF-1, and VEGF in the culture medium. We are currently examining the individual and synergistic contributions to APP mRNA decay of these as well as other growth factors, such as tumor necrosis factor-α, IL-1 (α and β), and TGF-β, that are also elevated in AD.

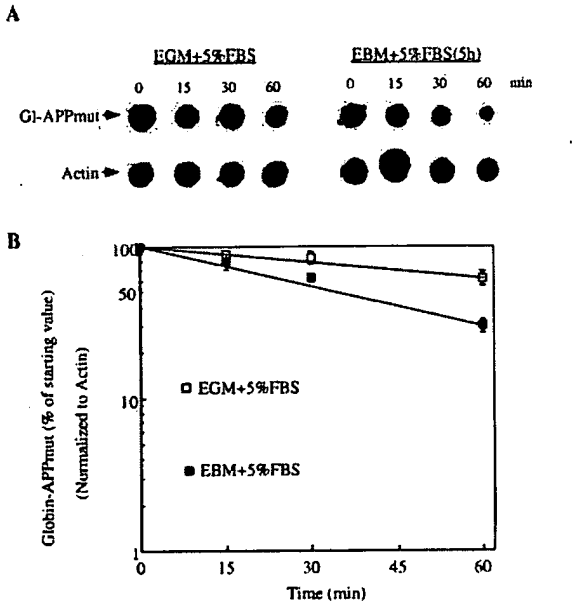

FIG. 5. Decay and growth factor-mediated stabilization of Gl-APP mRNA are sequence-specific. This experiment was performed as in Fig. 4, except that cells were transfected with Gl-APPmut mRNAs. Each time point is the mean ± SD of six determinations.

DISCUSSION

Growth factor-mediated stabilization of APP mRNA could play a crucial role in APP overexpression and accelerated βA4 deposition. This observation is particularly relevant in AD brain, where a growing list of inflammatory cytokines and growth factors, such as IL-1α (Griffin et al., 1989), bFGF (Stopa et al., 1990), TGF-β (van der Wal et al., 1993), IGF-1 (Connor et al., 1997), and VEGF (Kalaria et al., 1998) are chronically elevated. Epidemiological studies have shown that anti-inflammatory drugs can significantly delay the clinical expression of AD (McGeer et al., 1996). Further, after traumatic head injury, a strong risk factor for AD (Mayeux et al., 1993; Nicoll et al., 1995), proliferating microglia and reactive astrocytes synthesize and secrete high levels of tumor necrosis factor-α and TGF-β (Mattson et al., 1997). Thus, inflammatory mediators likely participate in the initiation and maintenance of the pathological cascade resulting in βA4 deposition.

An understanding of the cellular and molecular mechanisms connecting inflammatory cytokines to APP gene regulation, however, is limited. Studies with primary human vascular endothelial cells (HUVEC; Goldgaber et al., 1989) and neuronal cells (Ringheim et al., 1997; Yang et al., 1998) have shown that bFGF and IL-1 (α and β) increased APP mRNA and protein levels. This was partly attributable to an up-regulation of APP promoter activity. The APP gene promoter has multiple regulatory sequences that are conserved across species (Adroer et al., 1997). Of these, the AP-1 (transcription factor) consensus binding sequence was essential for growth factor-mediated up-regulation of APP production and secretion. More recently, enhanced translation was shown to be solely responsible for IL-1 (α and β)-mediated increases in astrocyte APP expression (Rogers et al., 1999). The regulatory sequence mapped to the 5′-UTR of APP mRNA and was homologous to translational control elements in the 5′-UTRs of ferritin mRNAs (Rogers et al., 1999).

The half-life of APP mRNA, however, varied greatly among the different cell-types, ranging from as little as 4.5 h in unstimulated HUVEC (Goldgaber et al., 1989) to >12 h in cell lines such as PC12 and SH-SY5Y (L. E. Rojagopalan and J. S. Malter, unpublished observations). We therefore reasoned that posttranscriptional changes in APP mRNA half-life could also contribute to expression. Here we have used a primary human vascular endothelial cell model to examine this important aspect of regulation. HUVEC were cultured to 70% confluence, in accordance with the manufacturer's protocol for optimal growth, in an EGM (see Experimental Procedures) containing EGF, bFGF, IGF-1, VEGF, and 5% FBS (condition I). Under these conditions, endogenous APP mRNA was very stable ($t_{1/2}$ > 12 h). Upon shifting to a basal medium also containing 5% FBS (EBM, condition II) for 5 h, APP mRNA was rapidly destabilized ($t_{1/2}$ = 4.5 h). Cell proliferation rates were indistinguishable between these two conditions, eliminating cell-cycle effects as a possible cause. Changing the serum content of the growth medium (EGM) from 2 to 10% had no effect on APP mRNA decay, thereby eliminating serum concentration as a contributing factor. These data suggest that the supplemented growth factors (EGF, bFGF, IGF-1, and VEGF) together mediate enhanced APP mRNA stability, presumably through cell-surface receptor signaling. Previously, we have shown that stabilized APP mRNAs accumulate and serve as coding templates for proportionally greater protein synthesis (Rajagopalan et al., 1998). This results from reuse of APP mRNAs by the protein synthetic machinery.

In this study, steady-state APP mRNA levels were also altered by cell (HUVEC) proliferation rates. In cells arrested by low FBS and EBM-2 media, we observed a significant stabilization of APP mRNA ($t_{1/2}$ > 12 h). mRNA stabilization due to serum deprivation and cell-growth arrest has been reported for a number of other eukaryotic mRNAs, such as those encoding lysyl oxidase (Gacheru et al., 1997), insulin-like growth factor II (Scheper et al., 1996), and collagen (Kindy et al., 1988). However, in our studies, APP mRNA steady-state levels declined substantially despite stabilization, probably due to simultaneous down-regulation of the APP promoter (Goldgaber et al., 1989). Thus, growth factors and rates of cell proliferation can influence APP expression through transcriptional, as well as posttranscriptional, events.

Our earlier observations in a cell-free system identified a conserved 29-nucleotide destabilizing element ~200 nucleotides downstream from the APP mRNA stop codon (Zaidi and Malter, 1994; Rajagopalan et al., 1998). Mutation of this element resulted in substantial stabilization of APP mRNA and a two- to fourfold increase in APP synthesis (Rajagopalan et al., 1998). We were therefore interested in determining (a) whether this sequence functioned as a destabilizing element in intact, proliferating cells, and (b) whether it mediated APP mRNA decay in response to extracellular stimuli, such as growth factors. To accomplish this, we transfected cells with in vitro synthesized chimeric Gl-APP mRNAs containing either an intact (Gl-APPwt) or mutated (Gl-APPmut) 29-nucleotide element (Fig. 3). This enabled us to distinguish transfected mRNAs from full-length, endogenous APP mRNA and to examine mRNA decay rates in the absence of global transcription blockade. Although the use of transcriptional poisons, such as actinomycin D, has permitted measurements of relative mRNA decay rates, there is growing evidence that such drugs have profound effects on mRNA turnover. Sequences that normally destabilize c-*fos* (Shyu et al., 1989), c-*myc* (Wisdom and Lee, 1991), or erythropoietin (Goldberg et al., 1991) mRNAs are nonfunctional in the presence of actinomycin D. In addition, actinomycin D specifically and rapidly stabilized transfected GM-CSF mRNAs, suggesting direct inhibition of mRNA decay pathways (Rajagopalan and Malter, 1996).

mRNAs were delivered into HUVEC via particle-mediated gene transfer (Rajagopalan and Malter, 1996).

By this method, cells can be transfected rapidly with little damage (10–15% cell death) and transfected mRNAs are quickly mobilized onto polysomes for translation (Rajagopalan and Malter, 1996). When cells were cultured briefly in basal medium (EBM-2), transfected Gl-APPwt mRNA decayed very rapidly with a half-life of 10 min. Mutation of the 29-nucleotide sequence (Gl-APPmut) stabilized the mRNA ($t_{1/2}$ = 40 min), thereby establishing this sequence as a functional destabilizing element in primary human cells. Inclusion of EGF, bFGF, IGF-1, and VEGF in the culture medium stabilized Gl-APP mRNA in a sequence-specific manner. The half-life of Gl-APPwt mRNA increased sixfold from 10 to 60 min, whereas that of Gl-APPmut mRNA showed only a modest increase from 40 to 60 min. Decay rates of transfected mRNAs are generally very rapid and are likely a truer representation of actual decay rates (Rajagopalan and Malter, 1996). Decay measurements made on endogenous mRNAs after transcription is blocked with actinomycin D probably overestimate true half-lives. The turnover of labile cellular components, essential for rapid decay (Brewer and Ross, 1989; Altus and Nagamine, 1991), as well as a direct inhibitory effect on turnover, by actinomycin D (Rajagopalan and Malter, 1996), are probable reasons. However, the relative rates of decay are preserved under both situations. We therefore have shown for the first time that a *cis*-element can specifically target APP mRNA for rapid decay in cells. When present together in the culture medium, EGF, bFGF, IGF-1, and VEGF, growth factors that are elevated in AD brain, mask this instability element, thereby stabilizing APP mRNA.

Signal transduction pathways that link cell-surface events to mRNA decay are poorly understood. Recently, the c-*jun* amino-terminal kinase pathway was implicated in the regulation of IL-2 (Chen et al., 1998) and IL-3 mRNA (Ming et al., 1998) turnover, mediated by specific *cis* sequences in the 5′-UTR, coding region, and 3′-UTR of these mRNAs. Thus, defined *cis*-acting sequences can mediate mRNA turnover through distinct signaling pathways. We are currently examining the role of growth factor-mediated signaling in modulating APP mRNA decay. Further, as both the soluble form of βAPP and the insoluble βA4 can independently activate mitogen-activated protein kinase pathways (Greenberg et al., 1994; McDonald et al., 1998), it is interesting to postulate that synergy may exist with growth factors in regulating APP mRNA turnover.

The APP destabilizing sequence described here is rich in uridine and cytidine residues. A very similar 26-nucleotide mRNA-destabilizing sequence has been identified in the 3′-UTR of the growth-associated protein-43 (GAP-43) mRNA (Chung et al., 1997). GAP-43 is a phosphoprotein expressed at high concentrations in neuronal growth cones during development and axonal regeneration. In AD, as well as in Parkinson's disease and DS, the neuronal expression of GAP-43 mRNA and protein are considerably reduced, whereas astrocyte expression is up-regulated (de la Monte et al., 1995). Thus, posttranscriptional events regulating the expression of key neuronal, glial, and vascular endothelial proteins could have considerable significance on the onset of neurodegenerative cascades.

The posttranscriptional regulation of APP gene expression is therefore complex and likely has significant implications regarding the production of APP and βA4 and the development of AD. We have a valid and versatile system with which to examine the individual and synergistic contributions to APP gene regulation of key cytokines and growth factors that are elevated in AD brain. Our data suggest that dysregulation of APP mRNA decay may play a role in APP overproduction.

Acknowledgment: We would like to thank members of the laboratory for their thoughtful comments. This work was supported by National Institutes of Health grant AG 10675 (to J.S.M.).

REFERENCES

Adroer R., Lopez-Acedo C., and Oliva R. (1997) Conserved elements in the 5′ regulatory region of the amyloid precursor protein gene in primates. *Neurosci. Lett.* **226**, 203–206.

Altus M. S. and Nagamine Y. (1991) Protein synthesis inhibition stabilizes urokinase-type plasminogen activator mRNA. Studies in vivo and in cell-free decay reactions. *J. Biol. Chem.* **266**, 21190–21196.

Brewer G. and Ross J. (1989) Regulation of c-*myc* mRNA stability in vitro by a labile destabilizer with an essential nucleic acid component. *Mol. Cell. Biol.* **9**, 1996–2006.

Castano E. M., Prelli F., Soto C., Beavis R., Matsubara E., Shoji M., and Frangione B. (1996) The length of amyloid-beta in hereditary cerebral hemorrhage with amyloidosis, Dutch type. Implications for the role of amyloid-beta 1–42 in Alzheimer's disease. *J. Biol. Chem.* **271**, 32185–32191.

Chen C. Y., Del Gatto-Konczak F., Wu Z., and Karin M. (1998) Stabilization of interleukin-2 mRNA by the c-*jun* NH_2-terminal kinase pathway. *Science* **280**, 1945–1949.

Chung S., Eckrich M., Perrone-Bizzozero N., Kohn D. T., and Furneaux H. (1997) The elav-like proteins bind to a conserved regulatory element in the 3′-untranslated region of GAP-43 mRNA. *J. Biol. Chem.* **272**, 6593–6598.

Citron M., Oltersdorf T., Haass C., McConlogue L., Hung A. Y., Seubert P., Vigo-Pelfrey C., Lieberburg I., and Selkoe D. J. (1992) Mutation of the beta-amyloid precursor protein in familial Alzheimer's disease increases beta-protein production. *Nature* **360**, 672–674.

Connor B., Beilharz E. J., Williams C., Synek B., Gluckman P. D., Faull R. L., and Dragunow M. (1997) Insulin-like growth factor-1 (IGF-1) immunoreactivity in the Alzheimer's disease temporal cortex and hippocampus. *Brain Res. Mol. Brain Res.* **49**, 283–290.

de la Monte S. M., Ng S. C., and Hsu D. W. (1995) Aberrant GAP-43 gene expression in Alzheimer's disease. *Am. J. Pathol.* **147**, 934–946.

Fukuchi K., Kamino K., Deeb S. S., Smith A. C., Dang T., and Martin G. M. (1992) Overexpression of amyloid precursor protein alters its normal processing and is associated with neurotoxicity. *Biochem. Biophys. Res. Commun.* **182**, 165–173.

Gacheru S. N., Thomas K. M., Murray S. A., Csiszar K., Smith-Mungo L. I., and Kagan H. M. (1997) Transcriptional and posttranscriptional control of lysyl oxidase expression in vascular smooth muscle cells: effects of TGF-beta 1 and serum deprivation. *J. Cell. Biochem.* **65**, 395–407.

Goldberg M. A., Gaut C. C., and Bunn H. F. (1991) Erythropoietin mRNA levels are governed by both the rate of gene transcription and posttranscriptional events. *Blood* **77**, 271–277.

Goldgaber D., Harris H. W., Hla T., Maciag T., Donnelly R. J., Jacobsen J. S., Vitek M. P., and Gajdusek D. C. (1989) Interleukin 1 regulates synthesis of amyloid β-protein precursor mRNA in human endothelial cells. *Proc. Natl. Acad. Sci. USA* **86**, 7606–7610.

Greenberg S. M., Koo E. H., Selkoe D. J., Qiu W. Q., and Kosik K. S. (1994) Secreted beta-amyloid precursor protein stimulates mitogen-activated protein kinase and enhances tau phosphorylation. *Proc. Natl. Acad. Sci. USA* **91**, 7104–7108.

Griffin W. S., Stanley L. C., Ling C., White L., MacLeod V., Perrot L. J., White C. L., and Araoz C. (1989) Brain interleukin 1 and S-100 immunoreactivity are elevated in Down syndrome and Alzheimer disease. *Proc. Natl. Acad. Sci. USA* **86**, 7611–7615.

Haass C., Koo E. H., Mellon A., Hung A. Y., and Selkoe D. J. (1992) Targeting of cell-surface β-amyloid precursor protein to lysosomes: alternative processing into amyloid-bearing fragments. *Nature* **357**, 500–503.

Holtzman D. M., Bayney R. M., Li Y. W., Khosravi H., Berger C. N., Epstein C. J., and Mobley W. C. (1992) Dysregulation of gene expression in mouse trisomy 16, an animal model of Down's syndrome. *EMBO J.* **11**, 619–627.

Johnson S. A., McNeill T., Cordell B., and Finch C. E. (1990) Relation of neuronal APP-751/APP-695 ratio and neuritic plaque density in Alzheimer's disease. *Science* **248**, 854–857.

Johnston J. A., Norgren S., Ravid R., Wasco W., Winblad B., Lannfelt L., and Cowburn R. F. (1996) Quantification of APP and APLP2 mRNA in APOE genotyped Alzheimer's disease brains. *Brain Res. Mol. Brain Res.* **43**, 85–95.

Kalaria R. N., Cohen D. L., Premkumar D. R., Nag S., LaManna J. C., and Lust W. D. (1998) Vascular endothelial growth factor in Alzheimer's disease and experimental cerebral ischemia. *Brain Res. Mol. Brain Res.* **62**, 101–105.

Kindy M. S., Chang C. J., and Sonenshein G. E. (1988) Serum deprivation of vascular smooth muscle cells enhances collagen gene expression. *J. Biol. Chem.* **263**, 11426–11430.

Mattson M. P., Barger S. W., Furukawa K., Bruce A. J., Wyss-Coray T., Mark R. J., and Mucke L. (1997) Cellular signalling roles of TGF beta, TNF alpha and beta APP in brain injury responses and Alzheimer's disease. *Brain Res. Brain Res. Rev.* **23**, 47–61.

Mayeux R., Ottman R., Tang M. X., Noboa-Bauza L., Marder K., Gurland B., and Stern Y. (1993) Genetic susceptibility and head injury as risk factors for Alzheimer's disease among community-dwelling elderly persons and their first-degree relatives. *Ann. Neurol.* **33**, 494–501.

McDonald D. R., Bamberger M. E., Combs C. K., and Landreth G. E. (1998) Beta-amyloid fibrils activate mitogen-activated protein kinase pathways in microglia and THP1 monocytes. *J. Neurosci.* **18**, 4451–4460.

McGeer P. L., Schulzer M., and McGeer E. G. (1996) Arthritis and antiinflammatory agents as possible protective factors for Alzheimer's disease: a review of 17 epidemiologic studies. *Neurology* **47**, 425–432.

Mills J. and Reiner P. B. (1999) Regulation of amyloid precursor protein cleavage. *J. Neurochem.* **72**, 443–460.

Ming X. F., Kaiser M., and Moroni C. (1998) c-*jun* N-terminal kinase is involved in AUUUA-mediated interleukin-3 mRNA turnover in mast cells. *EMBO J.* **17**, 6039–6048.

Nicoll J. A. R., Roberts G. W., and Graham D. I. (1995) Apolipoprotein E4 allele is associated with deposition of amyloid β-protein following head injury. *Nat. Med.* **1**, 135–137.

Premkumar D. R. and Kalaria R. N. (1996) Altered expression of amyloid beta precursor mRNAs in cerebral vessels, meninges, and choroid plexus in Alzheimer's disease. *Ann. NY Acad. Sci.* **777**, 288–292.

Rajagopalan L. E. and Malter J. S. (1994) Modulation of granulocyte-macrophage colony-stimulating factor mRNA stability in vitro by the adenosine-uridine binding factor. *J. Biol. Chem.* **269**, 23882–23888.

Rajagopalan L. E. and Malter J. S. (1996) Turnover and translation of in vitro synthesized messenger RNAs in transfected, normal cells. *J. Biol. Chem.* **271**, 19871–19876.

Rajagopalan L. E., Westmark C. J., Jarzembowski J. A., and Malter J. S. (1998) hnRNP C increases amyloid precursor protein (APP) production by stabilizing APP mRNA. *Nucleic Acids Res.* **26**, 3418–3423.

Ringheim G. E., Aschmies S., and Petko W. (1997) Additive effects of basic fibroblast growth factor and phorbol ester on beta-amyloid precursor protein expression and secretion. *Neurochem. Int.* **30**, 475–481.

Rogers J. T., Leiter L. M., McPhee J., Cahill C. M., Zhan S.-S., Potter H., and Nilsson L. N. G. (1999) Translation of the Alzheimer amyloid precursor protein mRNA is up-regulated by interleukin-1 through 5′-untranslated region sequences. *J. Biol. Chem.* **274**, 6421–6431.

Ross H. J., Sato N., Ueyama Y., and Koeffler H. P. (1991) Cytokine messenger RNA stability is enhanced in tumor cells. *Blood* **77**, 1787–1795.

Scheper W., Holthuizen P. E., and Sussenbach J. S. (1996) Growth-condition-dependent regulation of insulin-like growth factor II mRNA stability. *Biochem. J.* **318**, 195–201.

Selkoe D. J. (1993) Physiological production of the beta-amyloid protein and the mechanism of Alzheimer's disease. *Trends Neurosci.* **16**, 403–409.

Shyu A. B., Greenberg M. E., and Belasco J. G. (1989) The c-*fos* transcript is targeted for rapid decay by two distinct mRNA degradation pathways. *Genes Dev.* **3**, 60–72.

Stopa E. G., Gonzalez A. M., Chorsky R., Corona R. J., Alvarez J., Bird E. D., and Baird A. (1990) Basic fibroblast growth factor in Alzheimer's disease. *Biochem. Biophys. Res. Commun.* **171**, 690–696.

Suo Z., Tan J., Placzek A., Crawford F., Fang C., and Mullan M. (1998) Alzheimer's beta amyloid peptides induce inflammatory cascade in human vascular cells: the roles of cytokines and CD40. *Brain Res.* **807**, 110–117.

Urakami K., Kataoka J., Okada A., Isoe K., Wakutani Y., Ji Y., Adachi Y., Ohno K., and Takahashi K. (1996) Analysis of amyloid precursor protein mRNAs in skin fibroblasts in Down's syndrome. *Dementia* **7**, 82–85.

van der Wal E. A., Gomez-Pinilla F., and Cotman C. W. (1993) Transforming growth factor-beta 1 is in plaques in Alzheimer and Down pathologies. *Neuroreport* **4**, 69–72.

Wisdom R. and Lee W. (1991) The protein-coding region of c-*myc* mRNA contains a sequence that specifies rapid mRNA turnover and induction by protein synthesis inhibitors. *Genes Dev.* **5**, 232–243.

Wyss-Coray T., Masliah E., Mallory M., McConlogue L., Johnson-Wood K., Lin C., and Mucke L. (1997) Amyloidogenic role of cytokine TGF-β1 in transgenic mice and in Alzheimer's disease. *Nature* **389**, 603–606.

Yang Y., Quitschke W. W., and Brewer G. J. (1998) Upregulation of amyloid precursor protein gene promoter in rat primary hippocampal neurons by phorbol ester, IL-1 and retinoic acid, but not by reactive oxygen species. *Brain Res. Mol. Brain Res.* **60**, 40–49.

Yoshikawa K., Aizawa T., and Hayashi Y. (1992) Degeneration in vitro of post-mitotic neurons overexpressing the Alzheimer amyloid protein precursor. *Nature* **359**, 64–67.

Zaidi S. H. E. and Malter J. S. (1994) Amyloid precursor protein mRNA stability is controlled by a 29-base element in the 3′-untranslated region. *J. Biol. Chem.* **269**, 24007–24013.

Oncogene (1996) 13, 105-115

A *bcl-2*/IgH antisense transcript deregulates *bcl-2* gene expression in human follicular lymphoma t(14;18) cell lines

S Capaccioli[1], A Quattrone[1], N Schiavone[1], A Calastretti[2], E Copreni[2], A Bevilacqua[2], G Canti[2], L Gong[2], S Morelli[2] and A Nicolin[2]

[1]*Institute of General Pathology, University of Florence, 50134 Florence;* [2]*Department of Pharmacology, University of Milan, 20129 Milan, Italy*

The 14;18 chromosome translocation, characteristic of most human follicular B-cell lymphomas, juxtaposes the *bcl-2* gene with the IgH locus, creating a *bcl-2*/IgH hybrid gene. By mechanisms that are still under investigation, this event increases the cellular levels of the *bcl-2* mRNA and thereby induces an overproduction of the antiapoptotic BCL-2 protein which is likely responsible for neoplastic transformation. In an effort to identify potential upregulators of *bcl-2* activity in t(14;18) cells, we found, by strand-specific RT-PCR, a *bcl-2* antisense transcript that is present in the t(14;18) DOHH2 and SU-DHL-4 but not in the t(14;18)-negative Raji and Jurkat lymphoid cell lines, and thus appears to be dependent on the *bcl-2*/IgH fusion. This antisense transcript is a hybrid *bcl-2*/IgH RNA, that originates in the IgH locus, encompasses the t(14;18) fusion site and spans at least the complete 3' UTR region of the *bcl-2* mRNA. To achieve some insight into its biological function, we treated the t(14;18) DOHH2 cell line with oligonucleotides (ODNs) by specifically targeting the *bcl-2*/IgH antisense strand. These ODNs lowered *bcl-2* gene expression, inhibited neoplastic cell growth by inducing apoptosis. We would like to propose the hypothesis that the *bcl-2*/IgH antisense transcript may contribute, by an unknown mechanism, to upregulation of *bcl-2* gene expression in t(14;18) cells. The possibility has been considered that the hybrid antisense transcript mask AU-rich motifs present in the 3' UTR of the *bcl-2* mRNA characterized in other genes as mRNA destabilizing elements.

Keywords: antisense RNA; hybrid RNA; synthetic oligonucleotides; apoptosis; *bcl-2* regulation

Introduction

The prevailing karyotypic abnormalities related to hematological malignancies are chromosomal translocations (Dalla Favera *et al.*, 1982; Tsujimoto *et al.*, 1984; Cory, 1986; Rowley, 1990; Stanbridge and Nowell, 1990; Gu *et al.*, 1992), which give rise to hybrid genes either endowed with deregulated expression (Chen-Levy *et al.*, 1989; Polack *et al.*, 1993) or producing hybrid proteins (Konopka *et al.*, 1984; De The *et al.*, 1991). The t(14;18)(q32;q21), the most common chromosomal translocation, is consistently associated with the majority of follicular and some diffuse B-cell lymphomas. While breaks in the chromosome 14 generally occur in one of the six J_H elements in the IgH locus, about 60% of breakpoints in the chromosome 18 are clustered in the 3' UTR of the *bcl-2* gene, within the 150 base pair of the mbr (Tsujimoto *et al.*, 1984; Cleary *et al.*, 1986; Kneba *et al.*, 1991). By juxtaposing the truncated chromosomes a hybrid *bcl-2*/IgH fusion gene originates that does not imply a disruption of the *bcl-2* open reading frame nor production of a hybrid protein (Cleary *et al.*, 1986). Instead, higher levels of a *bcl-2*/IgH hybrid mRNA and a normal BCL-2 protein are present in the t(14:18) B-cells compared to the t(14;18)-negative counterparts (Cleary *et al.*, 1986; Nunez *et al.*, 1990; Graninger *et al.*, 1987). It is commonly accepted that in t(14;18) B-cell lymphomas the *bcl-2* expression is transcriptionally upregulated by the flanking IgH locus, where a potent enhancer, the Eμ enhancer, has been identified in the intronic region between the J_6 element and the μ-switch region (Tsujimoto *et al.*, 1984; Cleary *et al.*, 1986; Nowell and Croce, 1987; Reed *et al.*, 1989), but direct evidence of such phenomenon does not exist, and the mechanism of *bcl-2* upregulation in t(14;18) cells is still under investigation. The BCL-2 protein has been shown to prevent programmed cell death, providing a cell survival advantage (Vaux *et al.*, 1988; Nunez *et al.*, 1990; Hockenberry *et al.*, 1993; Jacobson *et al.*, 1993) that appears to be implicated in neoplastic transformation (Korsmeyer *et al.*, 1990; Adams and Cory, 1991).

On the basis of previous reports about the involvement of antisense transcription in gene expression control (for a review see Nellen and Lichtenstein, 1993), we tackled the problem of *bcl-2* deregulation in t(14;18) B cells by considering the possible existence of an antisense transcript. Our results demonstrate that an antisense transcript is present in t(14;18) cell lines, originating in the IgH locus and spanning the *bcl-2*/IgH fusion point, for a minimal length of about 2–2.4 kb. Experiments carried out with oligonucleotides targeting the hybrid antisense RNA showed the lowering of the cellular levels of *bcl-2* gene mRNA and protein, activating programmed death in the t(14;18)-treated cells. We might suggest for this antisense *bcl-2*/IgH transcript a role in the deregulation of *bcl-2* expression in t(14;18) cells, that could represent a new mechanism of neoplastic transformation.

Correspondence: A Nicolin, at Department of Pharmacology, School of Medicine Via Vanvitelli 32, 20129 Milan, Italy
Received 15 December 1995; revised 28 March 1996; accepted 28 March 1996

Results

Strand specific RT-PCR identifies an antisense transcript in t(14;18) bcl-2/IgH cell lines

We have noted that an adenine and uridine rich region is present in the 3' UTR of *bcl-2* mRNA and is conserved in all the t(14;18)-derived hybrid genes involving the major breakpoint region on chromosome 18 (Figure 1). These regions are known to function in some genes as *cis*-acting mRNA destabilizing elements (Asson-Batres *et al.*, 1994). Speculating on possible post-transcriptional deregulative mechanisms of *bcl-2* expression present in t(14;18) cells, we hypothesized that the production of an antisense transcript could be responsible for overlapping these AU-rich elements (AUREs), thus stabilizing the hybrid *bcl-2*/IgH mRNA. In order to verify this possibility, i.e. to detect the putative *bcl-2*/IgH antisense transcript, a study was conducted in t(14;18) DOHH2 and SU-DHL-4 cell lines or in t(14;18)-negative Raji and Jurkat cell lines. Northern and ribonuclease protection analyses gave ambiguous results, perhaps being inadequate to detect low expressing RNAs as antisense transcripts might be for their rapid degradation (Nellen and Lichtenstein, 1993). The highly sensitive strand-specific RT-PCR assay was therefore employed using the primers shown in Figure 2. Total RNA was extracted, deprived of contaminating genomic DNA by DNAse treatment and subjected to separate strand-specific reverse transcriptions by using either primer 1 or primer 2. The two strand-specific cDNAs were detected by amplifying with primer pair 1 and 2 a region of 271 bp in the *bcl-2* 3' UTR portion shared by all cell lines. Reverse transcription of the putative antisense RNA – by extension of primer 1 – gave an amplification product of the expected size only in the t(14;18) cell lines, while reverse transcription of the mRNA – by extension of primer 2 – gave a signal in all four cell lines tested (Figure 3A). In order to be sure that the antisense and sense signals were not due to contaminating genomic DNA, an aliquot of each RNA preparation was subjected to RNAse treatment before reverse transcription, and in no case were amplification products obtained with primer 1 and 2. Southern hybridization with a *bcl-2* probe (Figure 3B) and sequencing confirmed the identity of the antisense derived amplification products observed in the two translocated cell lines. The absence of the antisense transcript-derived signal in Raji and Jurkat cells indicates that the existence of this transcript is dependent on the (14;18) translocation.

Table 1 Sequence, position and orientation of the ODNs used for *bcl-2*/IgH sense and antisense RNA targeting

ODN orientation	*ODN code*	*Target*	*Sequence*
Sense	S_b	*bcl-2*	5'-GTGAGCAAAGGTGATCGT-3'
Antisense	As_b	*bcl-2*	5'-ACGATCACCTTTGCTCAC-3'
Inverted	I_b	*bcl-2*	5'-CGAACCGGGATGGACTTC-3'
Scrambled	Sc_b		5'-AGCGATGGTCGTGTGAAA-3'
Sense	S_h	IgH	5'-ACCATGTTCCGAGGGGAC-3'
Antisense	As_h	IgH	5'-GTCCCCTCGGAACATGGT-3'
Inverted	I_h	IgH	5'-TGCTAGTGGAAACGAGTG-3'
Scrambled	Sc_h		5'-CAGGGGAGCCTTGTACCA-3'

b: *bcl-2* gene h: IgH locus

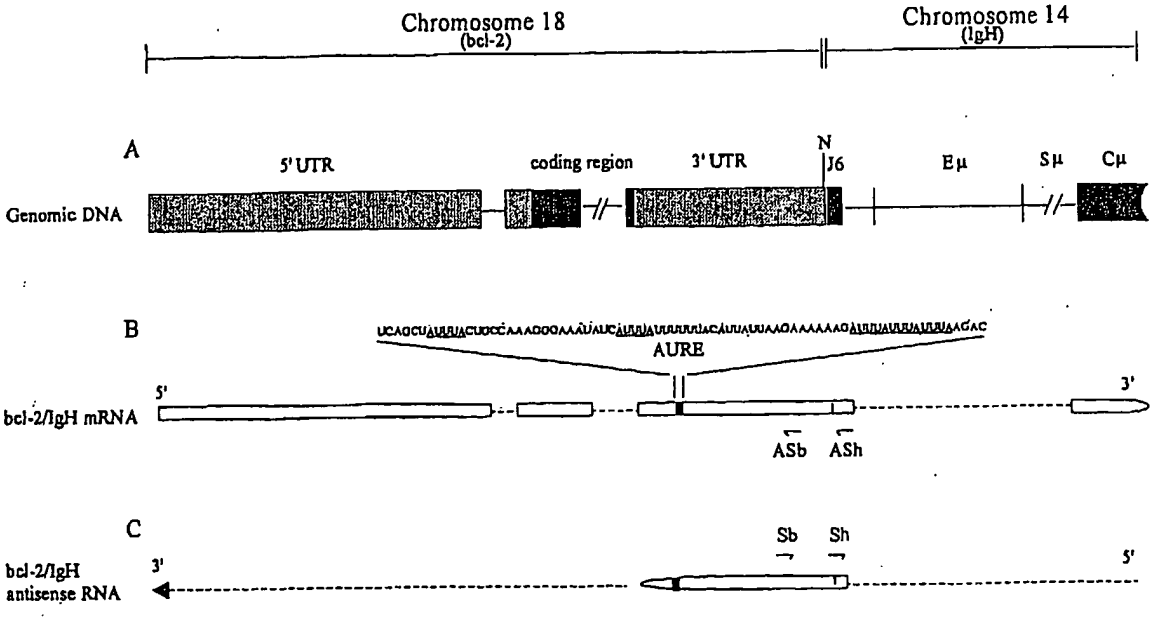

Figure 1 Schematic structure of t(14;18) chromosome translocation. Single stretches are reported in scale. (A) The *bcl-2*/IgH hybrid gene is partially represented, showing both the 5' and 3' untranslated regions (UTR) of the *bcl-2* portion (grey hatched) – enframing the *bcl-2* coding region (black hatched) – and the coding regions of IgH portion (black hatched). Intronic sequences are reported as lines. (B) The relevant portion *bcl-2*/IgH hybrid mRNA, where the AU-rich region is located and the conserved sequence reported. (C) The antisense hybrid transcript, showing the extension of the portion revealed by strand-specific RT-PCR and the mRNA AU-rich region overlapping stretch. Positions of ODNs used for the antisense strategy are also reported. The N region (N), i.e. the random inserted nucleotides in the translocation site, and the enhancer (Eμ), the switch (Sμ) and the constant (Cμ) μ regions of the IgH portion are reported

The antisense transcript is a hybrid transcript starting from the IgH portion and spanning the 3' UTR of the bcl-2 *gene mRNA*

The possibility was evaluated that the translocation-dependence of the antisense transcript was due to localization of the start site of antisense transcription on the IgH portion of the hybrid gene. Antisense strand specific RT-PCR was therefore performed in the region encompassing the *bcl-2*/IgH junction site of both DOHH2-primers 4 and 5-and SU-DHL-4-primers 3 and 5-cell lines (see Figure 2) using the same negative controls as in Figure 3A. PCR products of the expected size were generated (312 bp and 198 bp for DOHH2 and SU-DHL-4 cells respectively), demonstrating that the antisense transcript is a hybrid transcript originating in the IgH locus (Figure 4). Similarly, a third antisense strand specific PCR-with primers 6 and 7-gave an amplification product of 410 bp in the *bcl-2* side immediately downstream from

Panel A

ODN code	Gene	Sequence	Position	Orientation
Strand-specific RT-PCR				
Primer 1	*bcl-2*	5'-AGAATCAGCCTTGAAACATTGATGG3'	2426-2450 (Cleary *et al.* 1986)	Antisense
Primer 2	*bcl-2*	5'-TCACCTTCTCAGAATGCTTTTGAAG- 3	2672-2696 (Cleary *et al.* 1986)	Sense
Primer 3	*bcl-2*	5'-CGAAAGCTGCTTTAAAAAAATACATGCATCTCAGCG-3'	2544-2580 (Cleary *et al.* 1986)	Antisense
Primer 4	*bcl-2*	5'-GCAATTCCGCATTTAATTCATGGTATTCAGGAT-3'	2868-2899 (Cleary *et al.* 1986)	Antisense
Primer 5	IgH	5'-GGTGACCAGGGTCCCTTGGCCCCAG-3'	2973-2998 (Ravetch *et al.* 1981)	Sense
Primer 6	*bcl-2*	5'-AGTCAACATGCCTGC-3'	752 -766 (Ravetch *et al.* 1981)	Antisense
Primer 7	*bcl-2*	5'-GGTGATCCGGCCAACAAC-5'	1130-1147 (Ravetch *et al.* 1981)	Sense

Panel B

Quantitative RT-PCR

Primer A	*bcl-2*	5'-GGACAACATCGCCCTGTG-3'	551-568 (Cleary *et al.* 1986)	Sense
Primer B	*bcl-2*	5'-AGTCTTCAGAGACAGCCAGGA-3'	668-688 (Cleary *et al.* 1986)	Antisense
Primer C	ß-actin	5'-GCGGGAAATCGTGCGTGACATT-3'	2104-2125 (Miyashita *et al.* 1994)	Sense
Primer D	ß-actin	5'-GATGGAGTTGAAGGTAGTTTCGTG-3'	2409-2432 (Miyashita *et al.* 1994)	Antisense
Primer E	$ß_2$-m	5'-ACCCCCACTGAAAAAGATGA-3'	1544-1563 (Ng *et al.* 1985)	Sense
Primer F	$ß_2$-m	5'-ATCTTCAAACCTCCATGATG-3'	3508-3517 (Ng *et al.* 1985)	Antisense

Panel C

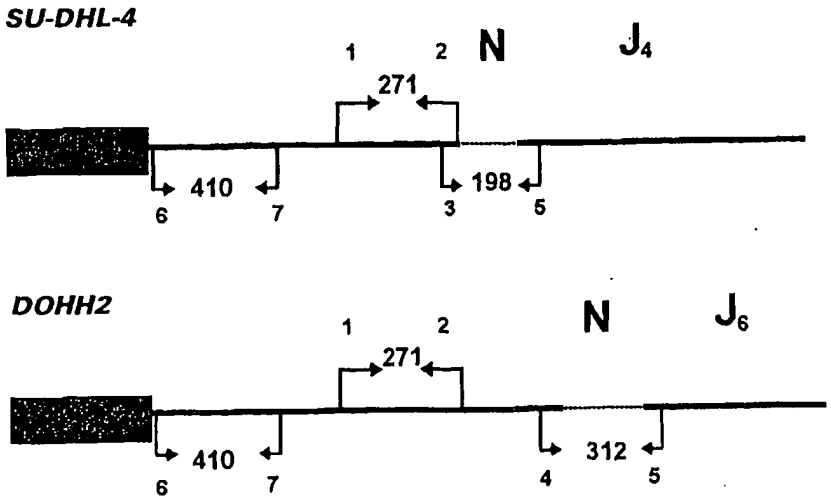

Figure 2 Panel A. Sequence and orientation of primers used in the strand-specific RT-PCR assay. Panel B. Sequence and orientation of primers used in the quantitative RT-PCR assay. Panel C. Primer position and expected product sizes of strand-specific RT-PCR

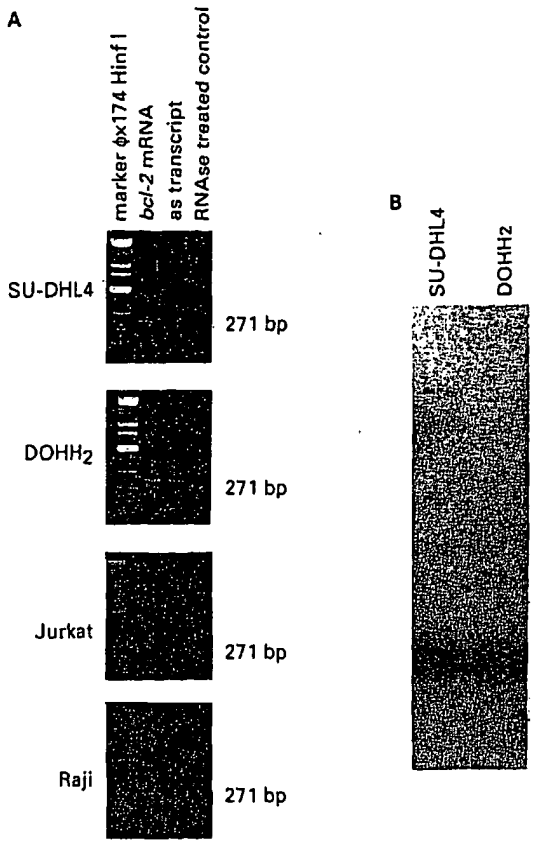

Figure 3 Detection of *bcl-2* antisense transcripts by strand-specific RT-PCR in t(14;18) cell lines. (A) PCR amplification of reverse transcribed bcl-2/IgH mRNA (extension primer 2) and antisense transcript (extension primer 1) of a region upstream of the bcl-2 3' UTR breakpoint in the t(14;18) DOHH2 and SU-DHL-4 cell lines. DNA-free total RNA was reverse transcribed and subjected to 30 cycles and 45 cycles of PCR for sense and antisense detection, respectively, as described in Materials and methods. Using primers 1 and 2 all cell lines gave products of the expected size of 271 bp (as determined by comparison to the DNA marker) when amplifying the mRNA-derived cDNA, while only the DOHH2 and SU-DHL-4 cell lines gave the same products when amplifying the antisense RNA-derived cDNA. No PCR products were obtained when using RNAse treated extracts for reverse transcription, excluding any possible false positive due to contaminating genomic DNA. (B) Southern hybridization with a 1.9 kb *bcl-2* probe covering the 3' UTR region amplified by PCR confirms the identity of the antisense transcripts. The antisense RNA-derived amplification products were transferred to a Hybond N membrane and hybridized with with ^{32}P internally labelled probe, as described in Materials and methods

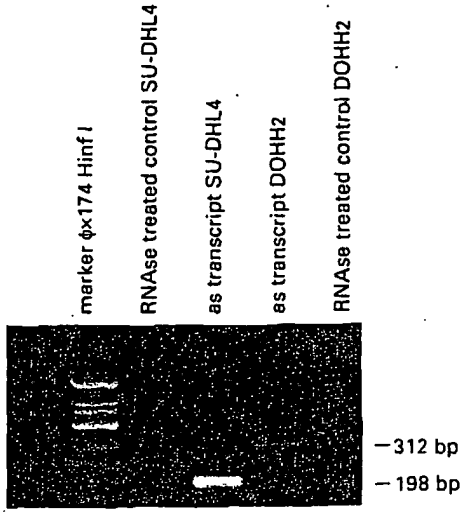

Figure 4 The *bcl-2* antisense transcript is a hybrid transcript. DNA-free total RNA extracted from DOHH2 and SU-DHL-4 cells was reverse transcribed with the antisense specific primer 5, consensus for the J_H region of the IgH gene, and PCR amplified using the same primer opposite to primers 3 (for the SU-DHL-4 cells) and 4 (for the DOHH2 cells), located in the *bcl-2* 3' UTR upstream to the translocation point. Amplification conditions were as detailed in Materials and methods. As compared to the DNA marker, PCR gave the expected product sizes of 198 bp for SU-DHL-4 and 312 bp for DOHH2 cells (see also Table 1), demonstrating the IgH origin of the antisense transcript. RNAse-treated controls were negative, excluding genomic DNA contamination

the translation stop codon (Figure 5). Thus, in the two cell lines tested, the antisense transcripts appear to overlap the entire untranslated region of the *bcl-2* gene, from the breakpoint to the 5' end of the 3' UTR, for a minimal length of about 2 (SU-DHL-4) and 2.4 (DOHH2) kb.

Sense oligonucleotides targeted to different regions of the hybrid antisense transcript induce apoptosis

The antisense oligonucleotide strategy offers the opportunity to selectively target an RNA for degradation, usually with the aim of modulating the cellular level of a specific protein (Wagner, 1994). In order to assess the role of the antisense transcript in *bcl-2* upregulation in t(14;18) cells, we designed ODNs complementary to upstream and downstream regions with respect to the DOHH2 fusion point. ODNs targeting the *bcl-2* 3' UTR were designed either in the sense (S_b) or the antisense (AS_b) orientation. ODNs targeting the IgH locus were in the J_6 element also in either orientations (S_h and AS_h). ODN administration was maintained in all cases for 3 days at 10 μM concentration. The two antisense ODNs, AS_b and AS_h, targeting the *bcl-2* and IgH portions of the hybrid mRNA, did not induce significant growth perturbations compared to untreated controls, or scrambled ODN (Sc_b and Sc_h) and inverted ODN (I_b and I_h) treated controls. On the contrary, the sense S_b and S_h ODNs, targeting the antisense transcript, were able to significantly reduce the cell number compared to controls (Table 2). Thus, the cell number was decreased by sense-orientated ODNs only. Very similar effects have been obtained with the S_b and S_h ODNs in the SU-DHL-4 cells, while as expected, sense ODNs targeting the DOHH2 specific fusion point were ineffective in SU-DHL-4 cells (not shown). Furthermore, since no reduced cell number was observed by treating t(14;18)-negative human lymphoma cells with S_b and S_h, the sense ODN apoptotic effect appears to be restricted to cells bearing the *bcl-2*/IgH translocation. In order to ascertain if this apoptotic effect could be attributed to a cell survival disadvantage consequent to a lowering of *bcl-2* gene expression, a preliminary microscopic examination of the sense-treated cells was carried out. A high number of cells with the characteristic features of apoptosis compared to controls was observed. Apoptotic death of DOHH2 cells was then quantified by flow cytometry determination of DNA breaks labelled with FITC-dUPT. A

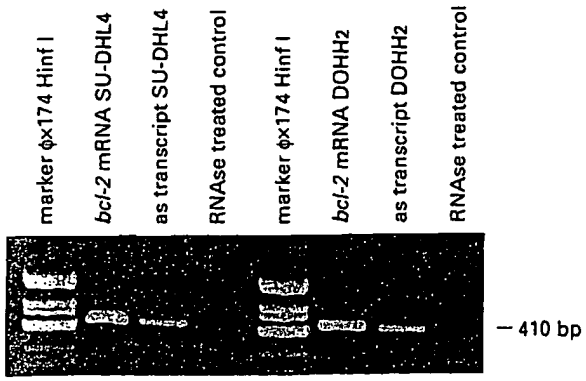

Figure 5 The *bcl-2*/IgH antisense transcript covers at least the complete 3' UTR of the *bcl-2* gene portion. The antisense transcript region immediately downstream from the stop codon of *bcl-2* mRNA was reversely transcribed with the antisense specific primer 6 and the cDNA was amplified with primer 6 and 7 as described in Materials and methods. The expected amplification products of 410 bp were obtained both in DOHH2 and in SU-DHL-4 cell lines and identified by sequence analysis. DNA contamination was excluded by negative controls as described in Figures 2 and 3

Table 2 Effect of a 3-day treatment with 10 μM ODNs targeting both the *bcl-2* and the IgH portions of the *bcl-2*/IgH hybrid gene on DOHH2 cell growth

ODN code	*Cells* $\times 10^4$*/ml* ± *S.E.*	*MTT assay OD* ± *SE*
–	45 ± 12	1164 ± 10
S_b	18 ± 4*	561 ± 11*
As_b	58 ± 7	950 ± 10
SC_b	56 ± 1	967 ± 15
I_b	48 ± 5	993 ± 12
–	67 ± 2	1265 ± 20
S_h	30 ± 3*	380 ± 16*
AS_h	66 ± 6	1120 ± 19
SC_h	61 ± 4	980 ± 10
I_h	71 ± 7	1040 ± 12

ODN, 10 μM on day 0, 5 μm on days 1 and 2. Cell count and MMT assay were done on day 3. Assays were performed in triplicate and data were normalized from 5 experiments. ODN Sb corresponded to position 2625 – 2642 of the *bcl-2* gene in sense orientation, As_b was in the antisense orientation, Sc_b as scramble and I_b the inverted sequence, respectively (Kneba *et al.*, 1991). ODN S_h, position 3119 – 3136 of the J_6 gene in sense orientation (Kluin-Nelemans *et al.*, 1991), *$P \leq 0.05$

basal cell subpopulation with DNA breakages, i.e. undergoing apoptosis, was equally present in the control and AS_b-treated cells. This fraction (6–7%) increased to about 40% in the S_b treated cells (Figure 6). A corresponding increase of apoptotic cells was measured with S_h compared to AS_h-treated cells (not shown). The size histograms of sense ODN-treated cells showed a decrease in forward and an increase in light scattering, consistent with apoptotis (Carbonari *et al.*, 1994).

Sense oligonucleotide-induced apoptosis in DOHH2 cells are associated with a lowering of bcl-2 *gene mRNA and protein levels*

The possibility that the biological effects of sense ODNs in DOHH2 cells are due to a lowering of *bcl-2* gene expression, probably mediated by inactivation of the antisense transcript, has been tested. Cellular levels of *bcl-2* mRNA and BCL-2 protein following Sb-and S_h-ODN treatment were quantified. *bcl-2* mRNA levels were evaluated by a quantitative RT-PCR assay using β-actin as the internal standard gene. When compared to untreated or Sc_h ODN-treated controls, AS_b and AS_h ODNs induced a slight lowering of *bcl-2* mRNA level, which underwent a dramatic decrease following S_b and S_h ODN treatment (Figure 7). BCL-2 protein, coded for by the open reading frame in the 5' region of the hybrid mRNA about 2.4 kb upstream from the region targeted by the ODNs, was also quantified by flow cytometry with an anti-BCL-2 MoAb. As shown in Figure 8 and 9 the lowering of BCL-2 protein following ODN treatments is consistent with that of *bcl-2* mRNA: BCL-2 protein levels in AS_b-and AS_h-treated cells are very similar to those of controls, but appear to be sharply reduced in S_b and S_h treated cells.

Discussion

The regulation of *bcl-2* gene expression in t(14;18) cells, where *bcl-2* is fused with the IgH locus, is possibly altered by the presence of the Eμ enhancer, located in the intron between the last J element and the μ-switch region (Tsujimoto *et al.*, 1984). Although the mechanism of action of this enhancer is at present unknown, it has been suggested that Eμ enhancer transcriptionally upregulates *bcl-2* expression (Cleary *et al.*, 1986; Seto *et al.*, 1988; Nunez *et al.*, 1990). To date no direct proof of an IgH enhancer action on the *bcl-2* promoter has been provided. Moreover, the presence of an enormous intron (200–300 kb about in size) between exons II and III of the *bcl-2* gene (Seto *et al.*, 1988; McDonnell *et al.*, 1988) and a proposed post-transcriptional role of the Eμ enhancer in the *bcl-2* altered expression (Reed *et al.*, 1989) do not allow definite conclusions.

Here we provide evidence that in the t(14;18) DOHH2 and SU-DHL-4 cell lines the hybrid *bcl-2/IgH* gene is associated with ectopic transcription of an antisense RNA, arising in the IgH locus and overlapping at least the entire 3' UTR portion conserved in the translocated *bcl-2* allele. The antisense transcript has been detected by a strand specific RT-PCR assay (Zhou *et al.*, 1992; Noguchi *et al.*, 1994; Murphy and Knee, 1994) and identified by Southern blotting hybridization with a *bcl-2* probe. Unclear previous results obtained using Northern hybridization and RNAse protection can be explained, as recently reported (Noguchi *et al.*, 1994; Murphy and Knee, 1994), by the low steady state levels of antisense RNAs, making these techniques unsuitable for antisense detection.

cDNA for strand-specific RT-PCR is prepared using primers designed to reverse transcribe the hybrid mRNA or the supposed hybrid antisense transcript in the t(14;18) DOHH2 and SU-DHL-4 cell lines. t(14;18)-negative Raji or Jurkat cell lines are used as negative controls. While t(14;18) positive and negative cells reveal the presence of the *bcl-2* mRNA, PCR products corresponding to the antisense transcript are restricted to the two t(14;18) cell lines. RNA transcribed in the antisense orientation is detected with primers matching three *bcl-2*/IgH regions, i.e. the beginning of the *bcl-2* 3' UTR, a downstream region in the *bcl-2* 3' UTR, and the translocation-specific breakpoint region of either t(14;18) cell lines. Sequence

analysis of the amplification products of the fusion regions containing the clone specific N stretch further confirm the identity of the antisense transcript.

This antisense transcript is unambiguously dependent on the presence of the *bcl-2*/IgH fusion gene, since no *bcl-2* antisense transcripts are found in the t(14;18)-negative cell lines tested. The start site of the antisense transcript appears therefore to be located somewhere in the IgH gene. Furthermore, the hybrid antisense transcript is probably present in low copy number in the translocated cell lines tested, since neither Northern hybridization nor ribonuclease protection assays give reproducible results and a long lasting PCR is required to detect a clear antisense transcript signal.

We tried to obtain insights into the post-transcriptional regulative function, if any, of the *bcl-2*/IgH antisense transcript by targeting it with antisense ODNs, a class of molecules which are generally known to interfere with the specific RNA target by a RNAse H-mediated destabilizing action and a steric hindrance (Wagner, 1994). Previous works reported that antisense ODNs targeting the translation origin of *bcl-2* mRNA were able to inhibit *bcl-2* expression (Reed *et al.*, 1990; Cotter *et al.*, 1994) overcoming chemoresistance of lymphoma cells (Kitada *et al.*, 1993, 1994). In our model, antisense ODNs targeting the antisense hybrid transcript are obviously sense-orientated with respect to the *bcl-2*/IgH mRNA, as shown in Figure 1. The S_b ODN, designed to target the *bcl-2* 3' UTR of the hybrid antisense transcript upstream of the

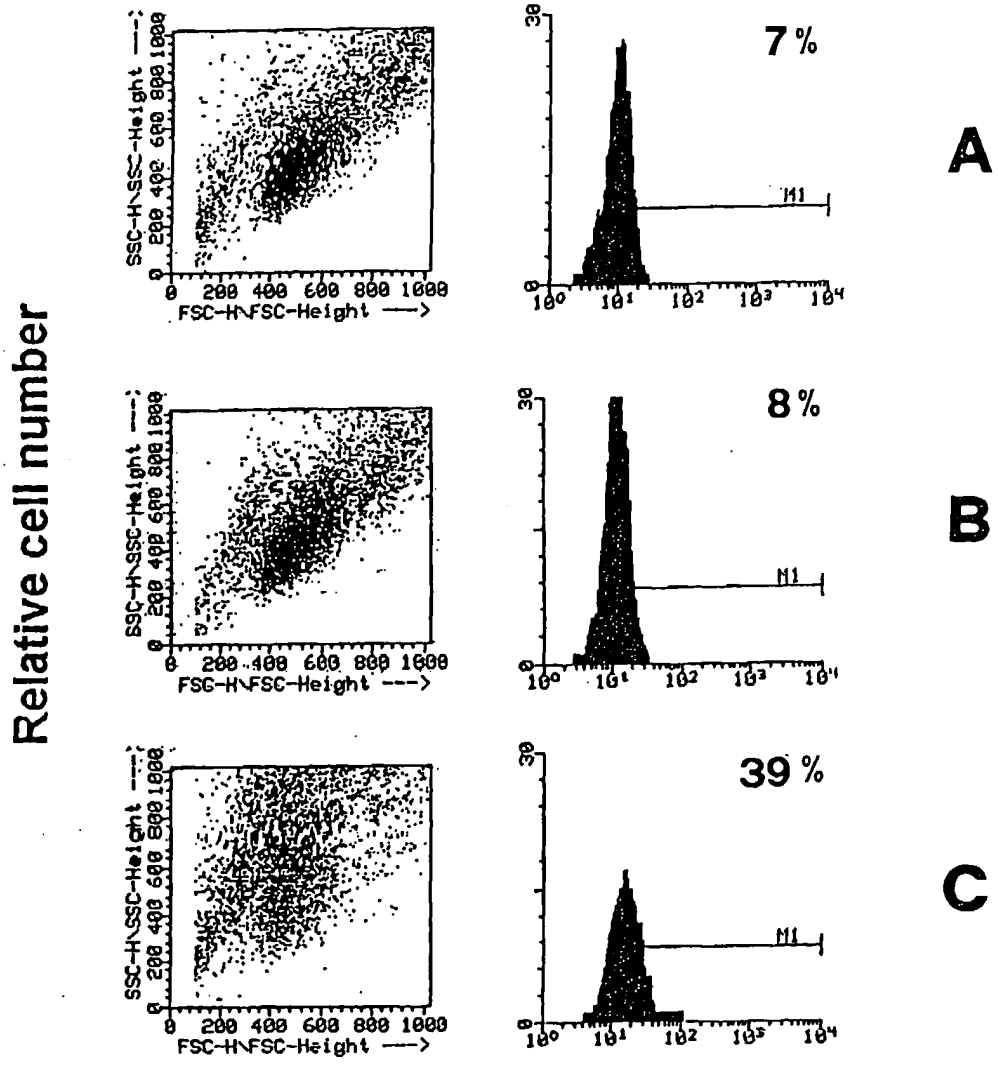

Figure 6 Sense ODN but not antisense ODN treatment increases the fraction of DOHH2 apoptotic cells. After ODN treatment as in Table 3, apoptosis-related DNA breaks were labelled at the 3' OH end by FITC-dUTP and measured by flow cytometry as described in Materials and methods. Results are presented as dot-plots and as histograms. (A) untreated cells; (B) AS_b-treated cells; (C) S_b-treated cells

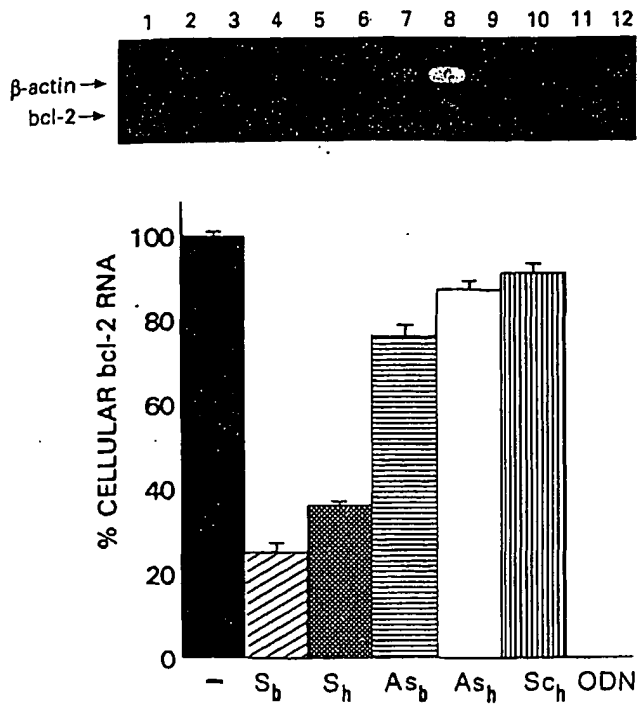

Figure 7 Quantitative RT-PCR determination of *bcl-2* mRNA. Cells 5×10^5/ml, in 25 ml flasks, were treated with ODNs at the modalities indicated in Table 2. Total RNA was extracted after 3 days of culture and the quantitative RT-PCR assay performed as described in Materials and methods. Top: agarose gel analysis of *bcl-2* and β-actin amplification products obtained from DOHH2 cells, untreated (lanes 1–4), or treated with S_b ODN (lanes 5–8) or S_h ODN (lanes 9–12) were quantified by densitometry. Lanes 1–4, 5–8 and 9–12, increasing aliquots of cDNA volumes used for PCR. Bottom: the amount of *bcl-2* mRNA relative to β-actin mRNA is expressed as percentage of the untreated controls

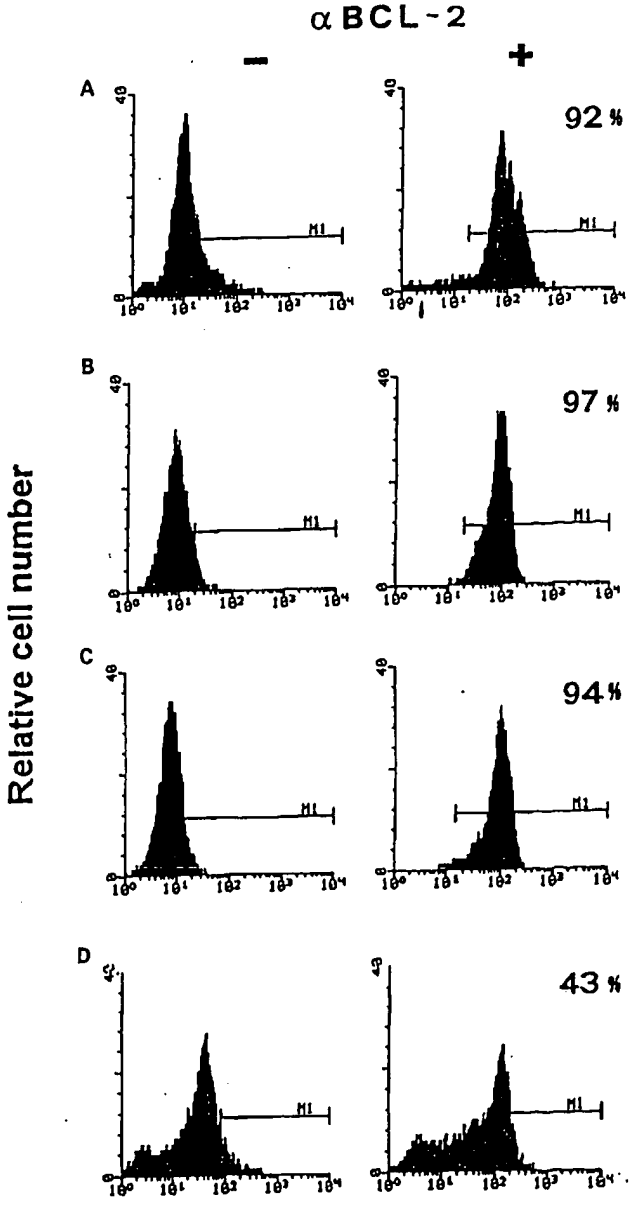

Figure 8 BCL-2 protein determination in S_b ODN-treated DOHH2 cells. Flow cytometry histograms of negative controls (–) and of BCL-2 MoAb (+) cells of untreated cells (A), ODN-Sc_b (B), ODN-As_b (C) and ODN-S_b (D) treated cells are reported. BCL-2 protein was quantified by indirect immunofluorescence after 3 days of culture as indicated in Table 2. In the cell samples exposed to sense oligonucleotides there is a sub-population of apoptotic cells (dot-plot of Figure 7) responsible for the non specific fluorescence as shown in panel 8D and 9D

mbr, and the S_h ODN, designed to target the J_6 element of the IgH locus, were both able to down-regulate *bcl-2* expression in the DOHH2 cell lines, lowering *bcl-2* mRNA and protein levels, and consequently inducing apoptosis. None of the ODNs used as controls, including the As_b ODN and the AS_h ODN, which are the antisense counterparts of the S_b ODN and the S_h ODN, respectively, were active. Assuming that ODNs might match only single stranded RNAs to form DNA-RNA heteroduplexes, the ineffectiveness of the antisense-orientated ODNs, compared to the sense-orientated ODNs, might eventually be explained by the higher steady-state levels of the hybrid mRNA with respect to the hybrid antisense transcript. Although substantial lack of data on this matter, it has been claimed that sub-stoichiometric amounts of antisense RNA can sometimes be very efficient (Nellen and Lichenstein, 1993). The effectiveness of sense ODNs targeting the fusion region of the DOHH2 cells used in some experiments (not shown) was, by virtue of the unique nucleotide sequence present in the fusion site, restricted to this cell line, while the ODNs targeting regions of the hybrid *bcl-2*/IgH RNA shared by most t(14;18) cells may virtually be effective in all follicular lymphoma cells.

Endogenous antisense transcripts have been frequently described in both prokaryotic and eukaryotic cells (Nellen and Lichtenstein, 1993; Taylor *et al*., 1991; Silverman *et al*., 1992; Shiang *et al*., 1993; Lerner *et al*., 1993; Peterson and Myers, 1993). In the latter, they have been found within genes relevant for cell proliferation, like C-and N-*myc* (Krystal *et al*., 1990; Celano *et al*., 1992; Spicer and Sonenshein, 1992), p53 (Khochbin *et al*., 1992), topoisomerase I (Shiang *et al*., 1993), IGF-II (Rivkin *et al*., 1993), and bFGF (Murphy and Knee, 1994; Volk *et al*., 1989; Kimelman and Kirschner, 1989; Borja *et al*., 1993). In particular, in a Burkitt lymphoma t(8;14) cell line where the μ-switch region of the IgH locus is fused to the coding

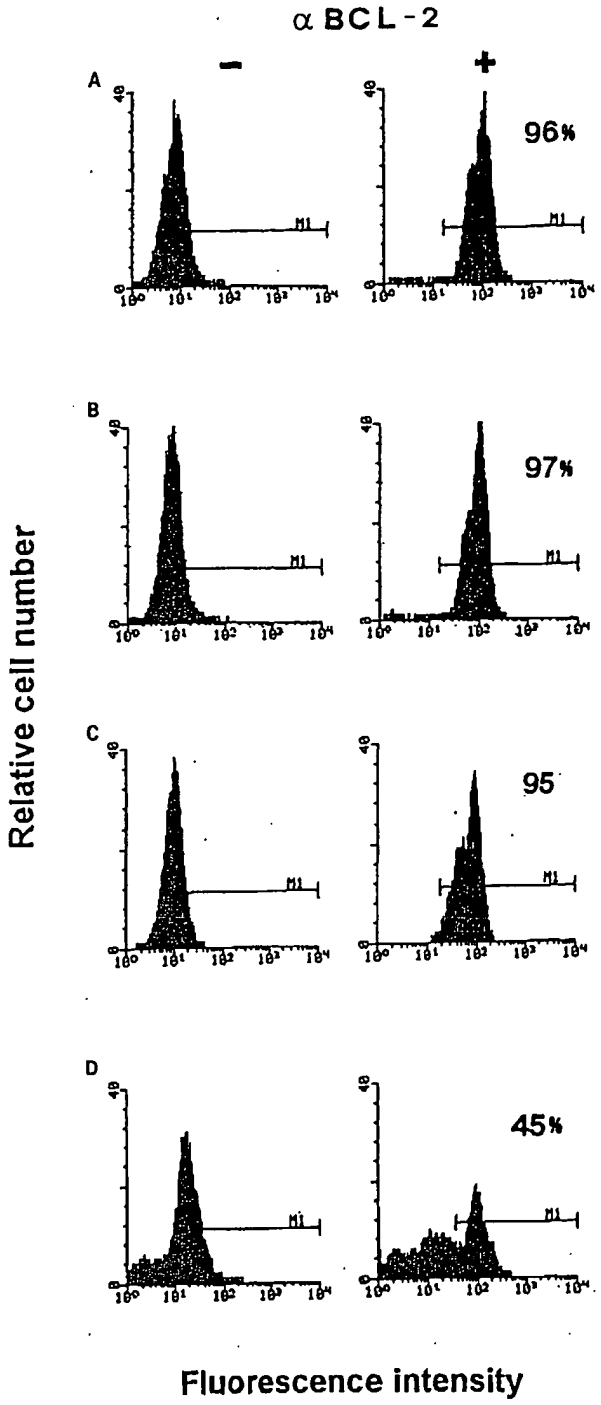

Figure 9 BCL-2 protein determination in S_h ODN-treated DOHH2 cells. Flow cytometry histograms of negative controls (−) and of BCL-2 MoAb (+) cells of untreated cells (A) or ODN-Sc_h (B), ODN-As_h (C) and ODN-S_h (D) treated cells are reported. BCL-2 protein was quantified as indicated in Figure 8

region of c-*myc* two antisense promoters affecting c-*myc* expression have been clearly identified starting from the μ-switch region (Apel *et al.*, 1992). The general relevance of antisense transcription as a possible mechanism modulating gene expression is so far unknown. The suggested activity of antisense transcripts is the specific down-regulation of protein levels by complexing the relevant RNA and thereby altering RNA functions with different mechanisms, including the activation of double-strand specific RNAses (Cornelissen, 1989; Nellen and Lichtenstein, 1993). Inhibition of gene expression obtained via artificial antisense constructs supports this possibility (Munir *et al.*, 1992). Although coding properties have been occasionally described for antisense transcripts (Kimelman and Kirschner, 1989), an unsuccessful search for potential open reading frames and its hybrid nature are against this possibility for the antisense *bcl-2*/IgH transcript. The two ODNs designed to inactivate the antisense transcript in the DOHH2 cells down-regulate *bcl-2* expression. This result might suggest that the *bcl-2*/IgH antisense transcript exerts the opposite effect of natural and transgenic antisense transcripts (Nellen and Lichtenstein, 1993). The hypothetical paradoxical behaviour of this *bcl-2*/IgH antisense transcript might be ascribed to the peculiar situation occurring in the t(14;18) cells, where the antisense transcript might mask a 5′ portion of the *bcl-2* 3′ UTR, that might behave as a consensus sequence for trans-regulating activities.

Moreover, specific sequences endowed with RNA destabilizing properties and characterized by reiterated and overlapping AUUUA motifs have been described for a number of mRNAs of human genes, like *fos* (Wilson and Treisman, 1988; Raymond *et al.*, 1989; Greenberg *et al.*, 1990; Roy *et al.*, 1992), *myc* (Schuler and Cole, 1988; Brewer and Ross, 1988), interferon β (Whittermore and Maniatis, 1990; Peppel *et al.*, 1991; Gessani *et al.*, 1993), TNF (Caput *et al.*, 1986; Jochum *et al.*, 1990; Jacob and Tashman, 1993) and GM-CSF (Schuler and Cole, 1988; Shaw and Kamen, 1986; Bickel *et al.*, 1992). Reiterated and overlapping AU-rich motifs with the same features as those found to negatively modulate the mRNA half-life have been found nested in a region (Figure 1) that is, surprisingly, highly conserved between human, mouse and chicken *bcl-2* 3′ UTR (our observation). The existence of putative regulatory elements in the 3′ UTR of *bcl-2* mRNA may also be argued on the basis of recent findings relative to endogenous *bcl-2* down-regulation by wild type p53 protein in the murine M1 leukaemia cell line (Selvakumaran *et al.*, 1994; Miyashita *et al.*, 1994b) and by mutated p53 protein in breast cancer cell lines (Haldar *et al.*, 1994), although a p53-responsive negative regulative element has been identified in a portion of the *bcl-2* gene corresponding to the mRNA 5′ UTR (Miyashita *et al.*, 1994a). In conclusion, a chimeric *bcl-2*/IgH antisense transcript has been found in the t(14;18) cell lines. The inhibition of *bcl-2* expression by synthetic ODNs designed to target the antisense RNA might suggest a novel molecular mechanism for neoplastic transformation in t(14;18) cells.

Materials and methods

Cell lines

The DOHH2 (Kluin-Nelemans *et al.*, 1991) and SU-DHL-4 (Cleary *et al.*, 1986) follicular lymphoma cell lines, carrying the 14;18 chromosomal translocation, and the t(14;18)-negative Raji B (Burkitt lymphoma) (Lenoir *et al.*, 1982) and Jurkat T (acute leukaemia) (Weiss and Stobo, 1984)

cell lines were used in this study. Cells were maintained under standard conditions in RPMI 1640 medium (Gibco, Gaithersburg, MD) supplemented with 10% fetal calf serum and controlled for mycoplasma. Viability was assessed by the trypan blue dye exclusion assay.

RNA extraction

Total cellular RNA was obtained from 10^7 cells using RNAzol B (Cynna Biotecx, Houston, USA) as extracting medium according to the manufacturer's instruction, treated with RQ1 RNase-free DNase (Promega, Madison, WI) in order to avoid possible DNA contamination, and purified by ethanol precipitation. RNA was then dissolved in 10 μl RNasin (1 U/μl), analysed on 1% agarose gel and quantitated spectrophotometrically.

Primers

The sequence, position and orientation of each primer used for the strand-specific or the quantitative RT-PCR (purchased from Genosys, Cambridge, England) analysis are shown in Figure 2.

Strand specific RT-PCR

Starting from the total RNA obtained as described, the sense or the putative antisense *bcl-2*/IgH RNA were reversely transcribed by strand-specific primers located either in the *bcl-2* or in the IgH locus, upstream of or downstream from the breakpoints of the DOHH2 and SU-DHL-4 cells. Total RNA from the t(14;18)-negative Raji and Jurkat cell lines was used as control. The reaction mixture (25 μl) contained about 2–3 μg of total RNA, 1 U/μl RNasin (Promega), 0.25 μg/μl BSA, 1 mM dNTPs, 50 mM Tris-HCl pH 8.3, 75 μM KCl, 3 mM $MgCl_2$, 10% glycerol and 12.5 pmol of each extension primer. After heating at 80°C for 5 min and rapidly cooling for primer annealing, the reaction was started by the addition of 500 U of Mo-MLV reverse transcriptase (Promega), protracted for 120 min at 37°C and blocked by heating at 95°C for 10 min. In order to have a control of the primer annealing specificity, a second reverse transcription was carried out for some experiments at 50°C. The strand-specific *bcl-2*/IgH cDNAs were treated with RNase ONE (Promega), purified by a double phenol:chloroform extraction, ethanol precipitated and detected following 30 (sense transcript) or 45 cycles (antisense transcript) of a standard hot-start PCR procedure with the primer pairs shown in Figure 2 at 1 μM final concentration. Primer pairs 1–2 and 6–7 targeted two *bcl-2* cDNA segments of the 3' UTR region shared by both cell lines, i.e. the first a segment upstream of the translocation point and the second a segment immediately downstream from the coding region. The *bcl-2*/IgH fusion region peculiar either of SU-DHL-4 (primer pair 3–5) or of DOHH2 (primer pair 4–5) were also targeted. Denaturation occurred for 1 min at 92°C, annealing for 1 min at 65°C (primer pairs 3–5 and 4–5) or at 56°C (primer pair 1–2) or at 60°C (primer pair 6–7), and extension for 1 min at 72°C. To detect any possible DNA contamination, negative controls were obtained by treating RNA extracts with RNase ONE before reverse transcription and were then tested in the same PCR assay.

Identification of PCR products

PCR products were routinely run on 2% agarose gel. Relevant bands were excised, purified by the GENE CLEAN II kit (Bio 101 Inc., La Jolla, CA) according to the manufacturer's instructions, and identified either by Southern blot assays, using as probe a 1.9 kb *bcl-2* cDNA fragment corresponding to the coding region and part of the 3' UTR of the *bcl-2* cDNA (Cleary *et al.*, 1986), and by sequencing, using the *fmol* sequencing kit (Promega).

Oligonucleotide treatment

HPLC-purified 18 mer phosphodiester ODNs used for cell treatments were purchased from Primm (Milan, Italy). Sequences were chosen to target either the sense or the putative antisense *bcl-2-IgH* transcript both upstream of and downstream from the DOHH2 junction region, from the 2625 to the 2642 residues of *bcl-2* cDNA (Cleary *et al.*, 1986) and from the 3119 to the 3136 residues of the J_H-consensus of the IgH locus (Ravatech *et al.*, 1981) respectively. Scrambled and inverted ODNs were used as negative controls. ODNs employed in cell treatments are reported in Table 1. ODNs were maintained for three days in the culture medium at concentrations ranging from 5 to 10 μM. In preliminary experiments carried out as previously reported (Capaccioli *et al.*, 1993) the ODN half-life in RPMI culture medium supplemented with 10% heat-inactivated (65°C) fetal calf serum was approximately 24 h. Therefore, ODNs were initially supplemented by the medium at 10 μM concentration, and at the halved concentration of 5 μM in the following 2 days of treatment. At the end of treatment cell growth inhibition, apoptosis rate, *bcl-2* mRNA and protein levels were quantified as described below.

Evaluation of cell growth inhbition

After the 3-day ODN treatments, cell growth was evaluated both by cell counting by two different operators, and by the MTT colorimetric assay (Denizot and Lang, 1986).

Evaluation of apoptosis rate

Cells undergoing programmed death were evaluated by quantifying in an EPICS-C cytofluorometer (Coulter Electronics, Hialeah, FL) equipped with an argon-ion laser (settings: 488 nm, 500 mw) the apoptotic DNA breaks after labelling their 3'-OH ends with fluoresceinated deoxyuridine (FITC-dUTP, Boehinger-Mannheim, Germany) by terminal deoxytransferase (TdT, Boehringer-Mannheim) (Delia *et al.*, 1993). Cells were fixed in 2% paraformaldehyde for 10 min, washed twice with 0.1 M Tris-buffered saline (pH 7.2), fixed for 1 min in acetone and washed with Tris-buffered saline. After incubation with 0.5 IU/μl TdT and 1.5 μM FITC-dUTP in 1 x TdT buffer for 1 h at 37°C, cells were again washed twice and analysed by flow cytometry.

Quantification of bcl-2 *mRNA by RT-PCR*

Cellular levels of *bcl-2* mRNA were determined by an internal standard-based semiquantitative RT-PCR method as previously described (Quattrone *et al.*, 1995; Aiello *et al.*, 1992), using either β_2 microglobulin or β-actin as internal standards. Total cellular RNA, extracted from about 10^6 cells, DNase treated and purified as described above, was reversely transcribed by using random hexamers in order to obtain a total cDNA preparation. Both the *bcl-2* and the internal standards, i.e. either β-2 microglobulin or β-actin, cDNA were amplified in separate reactions following a standard hot-start PCR procedure in the presence of [α^{32}P] dATP by using the quantitative RT-PCR primers shown in Table 1. PCR cycles were 30. Denaturation step was at 92°C for 1 min, extension at 72°C for 1 min and annealing at 56°C (primer pair A–B and C–D), or at 48°C (primer pair E–F) for 1 min. Amplification products were analysed on 2% agarose gel and identified as previously described. Quantification of

bcl-2 cDNA PCR products was carried out by radiometric counting of excised bands or by densitometric analysis: at least three values falling within the linear range of amplification referred to that of the standard gene PCR products were normalized for the relevant volumes in order to obtain the quantitative data.

Quantification of BCL-2 protein by flow cytometry

The cellular levels of BCL-2 protein were determined by a flow cytometry method as described (Aiello *et al.*, 1992). Briefly, 2×10^7 cells were pelletted, fixed in 2% paraformaldehyde/1% triton, resuspended in acetone, passed into cold absolute methanol and washed in phosphate buffer saline (PBS). Anti-BCL-2 MoAb (Pezzella *et al.*, 1990) and normal mouse serum were used in human AB serum-pretreated cells. Indirect immunofluorescence staining for BCL-2 was carried out in microtiter plates as published in detail (Aiello *et al.*, 1990). Following three washes, cells were analysed by the EPICS cytofluorometer equipped with an argon-ion laser (settings, 488 nm, 500 mw).

Abbreviations

mbr, major breaking region; RT-PCR, reverse transcriptase-polymerase chain reaction; UTR, untranslated region; J_H, heavy chain immunoglobulin joining region; AURE, adenine-uridine rich element.

Acknowledgements

We thank Dr Domenico Delia and Dr John Guardiola for invaluable suggestions, Dr Paola Ricciardi for assistance in cytofluorometric determinations, and Dr Francesco Pezzella for the αBCL-2 MoAb. This research was supported by Consiglio Nazionale delle Ricerche, CNR (P F ACRO), Rome, by Associazione Italiana per la Ricerca sul Cancro, AIRC, Milan, by Istituto Superiore di Sanità, Progetto AIDS, Rome and by Ministero dell'Università e della Ricerca Scientifica, MURST (40% and 60%). AQ was supported by a fellowship from AIRC, SM was supported by a fellowship from Consorzio Milano Ricerche.

References

Adams JM and Cory S. (1991). *Science*, **254**, 1161–1167.
Aiello A, Delia D, Fontanella E, Giardini R, Rilke F and Della Porta G. (1990). *Hematol. Oncol.*, **8**, 229–238.
Aiello A, Delia D, Borrello M, Biassoni D, Giardini R, Fontanella E, Pezzella F, Pulford K, Pierotti M and Della Porta G. (1992). *Cytometry*, **13**, 502–509.
Apel TW, Mautner J, Polack A, Bornkamm GW and Eick D. (1992). *Oncogene*, **7**, 1267–1271.
Asson-Batres MA, Spurgeon SL and Bagby Jr GC. (1994). *Ann. N.Y. Acad. Sci.*, **712**, 34–41.
Bickel M, Iwai Y, Pluznik DH and Cohen RB. (1992). *Proc. Natl. Acad. Sci. USA*, **89**, 10001–10005.
Borja AZ, Meijers C and Zeller R. (1993). *Dev. Biol.*, **157**, 110–118.
Brewer G and Ross J. (1988). *Mol. Cell Biol.*, **8**, 1697–1708.
Capaccioli S, Di Pasquale G, Mini E, Mazzei T and Quattrone A. (1993). *Biochem. Biophys. Res. Comm.*, **197**, 818–825.
Caput D, Beutler B, Hartog K, Thayer R, Brown-shimer S and Cerami A. (1986). *Proc. Natl. Acad. Sci. USA*, **83**, 1670–1674.
Carbonari M, Cibati M, Cherchi M, Sbarigia D, Pesce AM, Dell'Anna L, Modica A and Fiorilli M. (1994). *Blood*, **83**, 1268–1277.
Celano P, Berchtold CM, Kizer DL, Weeraratna A, Nelkin BD, Baylin SB and Casero RAJ. (1992). *J. Biol. Chem.*, **267**, 15092–15096.
Chen-Levy Z, Nourse J and Cleary ML. (1989). *Mol. Cell Biol.*, **9**, 701–710.
Cleary ML, Smith SD and Sklar J. (1986). *Cell*, **47**, 19–26.
Cornelissen M. (1989). *Nucleic Acids Res.*, **17**, 7203–7209.
Cory S. (1986). *Adv. Cancer Res.*, **47**, 189–234.
Cotter FE, Johnson P, Hall P, Pocock C, Al Mahdi, Cowell JK and Morgan G. (1994). *Oncogene*, **9**, 3049–3055.
Dalla Favera R, Bregni M, Erikson J, Patterson D, Gallo RC and Croce CM. (1982). *Proc. Natl. Acad. Sci. USA*, **79**, 7824–7827.
De The H, Lavau C, Marchio A, Chomienne C, Degos L and Dejean A. (1991). *Cell*, **66**, 675–684.
Delia D, Aiello A, Lombardo L, Pelicci PG, Grignani F, Formelli F, Menard S, Costa A, Veronesi U and Pierotti MA. (1993). *Cancer Res.*, **53**, 6036–6041.
Denizot F and Lang R. (1986). *J. Immunol. Meth.*, **89**, 271–277.
Gessani S, Dieffenbach CW, Conti L, Di Marzio P, Wilson KL and Belardelli F. (1993). *Virology*, **193**, 507–509.
Graninger WB, Seto M, Boutain B, Goldman P and Korsmeyer SJ. (1987). *J. Clin. Invest.*, **80**, 1512–1515.
Greenberg ME, Shyu AB and Belasco JG. (1990). *Enzyme*, **44**, 181–192.
Gu Y, Nakamura H, Alder H, Prasad R, Canaani O, Cimino G, Croce CM and Canaani E. (1992). *Cell*, **71**, 701–708.
Haldar S, Negrini M, Monne M, Sabbioni S and Croce CM. (1994). *Cancer Res.*, **54**, 2094–2097.
Hockenberry DM, Nunez G, Milliman C, Schreiber RD and Korsmeyer SJ. (1993). *Nature*, **348**, 334–336.
Jacob CO and Tashman NB. (1993). *Nucleic Acids Res.*, **21**, 2761–2766.
Jacobson MD, Burne JF, King MP, Miyashita T, Reed JC and Raff MC. (1993). *Nature*, **361**, 365–369.
Jochum C, Voth R, Rossol S, Meyer zum Buschenfelde KH, Hess G, Will H, Schroder HC, Steffen R and Muller WE. (1990). *J. Virol.*, **64**, 1956–1963.
Khochbin S, Brocard MP, Grunwald D and Lawrence JJ. (1992). *Ann. N.Y. Acad. Sci.*, **660**, 77–87.
Kimelman D and Kirschner MW. (1989). *Cell*, **59**, 687–696.
Kitada S, Miyashita T, Tanaka S and Reed JC. (1993). *Antisense Res. Dev.*, **3**, 157–169.
Kitada S, Takayama S, De Riel K, Tanaka S and Reed JC. (1994). *Antisense Res. Dev.*, **4**, 71–79.
Kluin-Nelemans HC, Limpens J, Meerabux J, Beverstock GC, Jansen JH, de Jong D and Kluin PM. (1991). *Leukemia*, **5**, 221–224.
Kneba M, Eick M, Herbst H, Willigeroth S, Pott C, Bolz M, Bergholz M, Neumann C, Stein H and Krieger G. (1991). *Cancer Res.*, **51**, 3243–3250.
Konopka JB, Watanabe SM and Witte ON. (1984). *Cell*, **37**, 1035–1042.
Korsmeyer SJ, McDonnell TJ, Nunez G, Hockenberry DM and Young R. (1990). *Microbiol. Immunol.*, **166**, 203–207.
Krystal GW, Armstrong BC and Battey JF. (1990). *Mol. Cell Biol.*, **10**, 4180–4191.
Lenoir GM, Preud'homme JL, Bernheim A and Berger RC. (1982). *Nature*, **298**, 474–476.
Lerner A, D'Adamio L, Diener AC, Clayton LK and Reinherz EL. (1993). *J. Immunol.*, **151**, 3152–3162.

McDonnell TJN, Deane N, Platt FM, Nunez G, Jaeger U, McKearn JP and Korsmeyer SJ. (1988). *Cell*, 57, 79–88.
Miyashita T, Harigai M, Hanada M and Reed JC. (1994a). *Cancer Res.*, 54, 3131–3135.
Miyashita T, Krajewski S, Krajewska M, Wang HG, Lin HK, Liebermann D, Hoffman B and Reed JC. (1994b). *Oncogene*, 9, 1799–1805.
Munir MI, Rossiter BJF and Caskey C. (1992). *Antisense RNA production in mammalian fibroblast and transgenic mice, in antisense RNA and DNA*. Murray JAH (ed). Wiley-Liss: New York.
Murphy PR and Knee RS. (1994). *Mol. Endocrinol.*, 8, 852–859.
Nellen W and Lichtenstein C. (1993). *TIBS*, 18, 419–423.
Ng SY, Gunning P, Eddy R, Ponte P, Leavitt J, Shows T and Kedes L. (1985). *Mol. Cell Biol.*, 5, 2720–2732.
Noguchi M, Miyamoto S, Silverman TA and Safer B. (1994). *J. Biol. Chem.*, 269, 29161–29167.
Nowell PC and Croce CM. (1987). *Development and recognition of the transformed cell*. Greene MI and Hamaoka T (eds). Plenum Publishing Corporation: New York.
Nunez G, London L, Hockenberry DM, Alexander M, McKearn JP and Korsmeyer SJ. (1990). *J. Immunol.*, 144, 3602–3610.
Peppel K, Vinci JM and Baglioni C. (1991). *J. Exp. Med.*, 173, 349–355.
Peterson JA and Myers AM. (1993). *Nucleic Acids Res.*, 21, 5500–5508.
Pezzella F, Tse AG, Cordell JL, Pulford K, Gatter KC and Mason DY. (1990). *Am. J. Pathol.*, 137, 225–232.
Polack A, Feederle R, Klobeck G and Hortnagel K. (1993). *EMBO J.*, 12, 3313–3320.
Quattrone A, Fibbi G, Pucci M, Anichini E, Capaccioli S and Del Rosso M. (1995). *Cancer Res.*, 55, 90–95.
Ravatech JV, Siebenlist U, Korsmeyer SJ, Waldman T and Leder P. (1981). *Cell*, 27, 583–591.
Raymond V, Atwater JA and Verma IM. (1989). *Oncogene Res.*, 5, 1–12.
Reed JC, Tsujimoto Y, Epstein SF, Cuddy M, Slabiak T, Nowell PC and Croce CM. (1989). *Oncogene Res.*, 4, 271–282.
Reed JC, Stein CA, Subasinghe C, Haldar S, Croce CM, Yum S and Cohen JJ. (1990). *Cancer Res.*, 50, 6565–6570.
Rivkin M, Rosen KM and Villa Komaroff L. (1993). *Mol. Reprod. Dev.*, 35, 394–397.
Rowley JD. (1990). *Cancer Res.*, 50, 3816–3821.
Roy N, Laflamme G and Raymond V. (1992). *Nucleic Acids Res.*, 20, 5753–5762.
Schuler GD and Cole MD. (1988). *Cell*, 55, 1115–1122.
Selvakumaran M, Lin HK, Miyashita T, Wang HG, Krajewski S, Reed JC, Hoffman B and Liebermann D. (1994). *Oncogene*, 9, 1791–1798.
Seto M, Jaeger U, Hockett RD, Graninger WB, Bennett S, Goldman P and Korsmeyer SJ. (1988). *EMBO J.*, 7, 123–131.
Shaw G and Kamen R. (1986). *Cell*, 46, 659–667.
Shiang R, Lidral AC, Ardinger HH, Buetow KH, Romitti PA, Munger RG and Murray JC. (1993). *Am. J. Hum. Genet.*, 53, 836–843.
Silverman TA, Noguchi M and Safer B. (1992). *J. Biol. Chem.*, 267, 9738–9742.
Spicer DB and Sonenshein GE. (1992). *Mol. Cell Biol.*, 12, 1324–1329.
Stanbridge EJ and Nowell PC. (1990). *Cell*, 63, 867–874.
Taylor ER, Seleiro EA and Brickell PM. (1991). *J. Mol. Endocrinol.*, 7, 145–154.
Tsujimoto Y, Finger LR, Yunis JJ, Nowell PC and Croce CM. (1984). *Science*, 226, 1097–1099.
Vaux DL, Cory S and Adams JM. (1988). *Nature*, 335, 440–442.
Volk R, Koster M, Poting A, Hartmann L and Knoche W. (1989). *EMBO J.*, 8, 2983–2988.
Wagner RW. (1994). *Nature*, 372, 333–335.
Weiss A and Stobo JD. (1984). *J. Exp. Med.*, 160, 1284–1299.
Whittermore LA and Maniatis T. (1990). *Proc. Natl. Acad. Sci. USA*, 87, 7799–7803.
Wilson T and Treisman R. (1988). *Nature*, 336, 396–399.
Zhou BS, Beidler DR and Cheng YC. (1992). *Cancer Res.*, 52, 4280–4285.

MOLECULAR AND CELLULAR BIOLOGY, July 1996, p. 3511–3522
0270-7306/96/$04.00+0

Vol. 16, No. 7

Identification of Sequences in c-*myc* mRNA That Regulate Its Steady-State Levels

NEWMAN M. YEILDING, MUHAMMAD T. REHMAN, AND WILLIAM M. F. LEE*

Department of Medicine and Cancer Center, University of Pennsylvania, Philadelphia, Pennsylvania

Received 13 February 1996/Returned for modification 1 April 1996/Accepted 17 April 1996

The level of cellular *myc* proto-oncogene expression is rapidly regulated in response to environmental signals and influences cell proliferation and differentiation. Regulation is dependent on the fast turnover of c-*myc* mRNA, which enables cells to rapidly alter c-*myc* mRNA levels. Efforts to identify elements in *myc* mRNA responsible for its instability have used a variety of approaches, all of which require manipulations that perturb normal cell metabolism. These various approaches have implicated different regions of the mRNA and have led to a lack of consensus over which regions actually dictate rapid turnover and low steady-state levels of c-*myc* mRNA. To identify these regions by an approach that does not perturb cell metabolism acutely and that directly assesses the effect of a c-*myc* mRNA region on the steady-state levels of c-*myc* mRNA, we developed an assay using reverse transcription and PCR to compare the steady-state levels of human *myc* mRNAs transcribed from two similarly constructed *myc* genes transiently cotransfected into proliferating C2C12 myoblasts. Deletion mutations were introduced into *myc* genes, and the levels of their mRNAs were compared with that of a near-normal, reference *myc* mRNA. Deletion of most of the *myc* 3′ untranslated region (UTR) raised *myc* mRNA levels, while deletion of sequences in the *myc* 5′ UTR (most of exon 1), exon 2, or the protein-coding region of exon 3 did not, thus demonstrating that the 3′ UTR is responsible for keeping *myc* mRNA levels low. Using a similar reverse transcription-PCR assay for comparing the steady-state levels of two β-globin–*myc* fusion mRNAs, we showed that fusion of the *myc* 3′ UTR lowers globin mRNA levels by destabilizing β-globin mRNA. Surprisingly, fusion of the protein-coding region of *myc* exon 3 also lowered globin mRNA steady-state levels. Investigating the possibility that exon 3 coding sequences may play some other role in regulating c-*myc* mRNA turnover, we demonstrated that these sequences, but not *myc* 3′ UTR sequences, are necessary for the normal posttranscriptional downregulation of c-*myc* mRNA during myoblast differentiation. We conclude that, while two elements within c-*myc* mRNA can act as instability determinants in a heterologous context, only the instability element in the 3′ UTR regulates its steady-state levels in proliferating C2C12 cells.

Regulated expression of the c-*myc* gene is important for normal cell growth and differentiation, and the short half-life of its mRNA (12, 24) enables cells to rapidly regulate expression levels by either transcriptional (4, 14, 17, 19, 20, 26, 31, 34, 36, 44) or posttranscriptional mechanisms (6, 13, 15, 25, 50). Attempts to identify the *cis*-acting element(s) responsible for the rapid decay of c-*myc* mRNA have implicated several instability determinants. 5′ truncated *myc* mRNAs resulting from chromosomal translocations in B-cell lymphomas were found to be unusually stable (18, 38, 40), leading to speculation that this region contains destabilizing sequences. However, fusion of c-*myc* exon 1 sequences to more stable mRNAs does not confer instability (24, 37), suggesting that exon 1 destabilizes only in particular mRNA contexts or that the 5′ truncated *myc* mRNAs are stabilized because of unusual sequences in the 5′ leader (24, 37). The 3′ untranslated region (UTR) of c-*myc* mRNA was implicated as an instability determinant by the presence of AU-rich regions and AUUUA motifs also found in the 3′ UTRs of many other labile mRNAs, including granulocyte-macrophage colony-stimulating factor and c-*fos* mRNAs (10, 27, 42, 43). This was confirmed by studies of mRNA decay after inhibition of transcription with actinomycin D, which indicated that *myc* 3′ UTR sequences are important for its rapid turnover (1, 23, 24). Finally, protein-coding sequences in *myc* exon 3 have been imputed to be determinants of instability through studies of the decay of chimeric *myc* mRNAs after actinomycin D treatment (21), in vitro assays of *myc* mRNA decay (5); studies of *myc* mRNA induction following translation inhibition (32, 50), and studies of the decay of *myc* mRNAs transcribed from a serum-inducible promoter (50). Thus, by using inhibitors of transcription or translation and serum-inducible promoters, different elements within *myc* mRNA have been implicated as being instability determinants.

The methodologies used to identify *myc* mRNA instability elements acutely perturb the cell, so their effects on *myc* mRNA metabolism may not be restricted to the intended effect. For example, actinomycin D globally inhibits transcription and has been shown to artifactually prolong the half-lives of certain mRNAs (35, 43, 50); cycloheximide globally inhibits translation, and only mRNA instability elements whose function is translation dependent can be revealed by cycloheximide induction studies (50); and use of inducible promoters raises the issue of whether measurements made under conditions necessary for promoter induction are generally applicable (50). These factors and concerns may explain why different approaches have implicated different regions of *myc* mRNA as instability determinants and why determinants implicated by one approach frequently have not been confirmed by another. mRNA turnover can be determined without grossly perturbing cell metabolism and introducing potential artifacts by using radiolabeled uridine, but pulse-chase or chase-in experiments (37, 39) are cumbersome to perform and unsuited for studying short-lived, low abundance mRNAs, and they cannot be used

* Corresponding author. Mailing address: 663 CRB, 415 Curie Blvd. University of Pennsylvania, Philadelphia, PA 19104. Phone: (215) 898-0258 or 898-0259. Fax: (215) 573-2028.

to study mRNAs from transfected genes when mRNA from the endogenous homolog is present.

The limitations of conventional means for analyzing *myc* mRNA turnover have led us to develop an assay that can identify instability determinants that regulate steady-state levels of c-*myc* mRNA with a minimum of cell perturbation. Our approach is to compare the steady-state levels of mRNAs from two cotransfected genes, one that produces a near-normal *myc* mRNA and one that produces a mutant *myc* mRNA. When transcription and processing of the two mRNAs are similar, their relative turnover rates are reflected in their comparative steady-state levels, and if the half-life of one is known, the half-life of the other can be deduced. By its nature, this assay detects mRNA elements that regulate steady-state levels and are physiologically significant. We present the results of studies identifying sequences in *myc* mRNA that determine its steady-state levels.

MATERIALS AND METHODS

Cell culture and DNA transfection. All experiments were performed with C2C12 myoblasts (7) obtained from the American Type Culture Collection (Rockville, Md.) and maintained in Dulbecco's minimum essential medium (DMEM) supplemented with 10% fetal calf serum, 5% CO_2, penicillin, and streptomycin. Plasmids containing test genes were stably cotransfected into C2C12 cells with a plasmid containing a Neo^r gene by using the calcium phosphate method. After selection in 400 μg of G418 (Gibco) per ml, pools of 20 to 50 surviving colonies were expanded for study. C2C12 cells were also transiently transfected with calcium phosphate and glycerol shock, and their cytoplasmic RNAs were extracted for analysis 2 or 3 days later. When two plasmids were transiently cotransfected, a plasmid transfection mixture was created by pooling equal numbers of bacteria (determined by optical density at 600 nm) containing the two plasmids prior to purification by cesium chloride gradient centrifugation; this assures, as much as possible, that the two plasmids will be comparable in terms of quality and transfectability.

Plasmid constructions. Salient features of the plasmids used in this study are diagrammed in Fig. 1. The normal human c-*myc* gene contains three exons, and CM19 is a pUC-based plasmid that contains all of human c-*myc* from the *Xho*I site (between the P1 and P2 promoters) to the *Eco*RI site (3′ to exon 3) under the transcriptional control of the Moloney murine leukemia virus long terminal repeat (MLV LTR); it is identical to the pM21 (45) except that the *Cla*I site 5′ to the LTR has been deleted. A tagged CM19 gene, CM19m1409, was created by introducing an A-to-C mutation at *myc* codon 281 by site-directed mutagenesis. This generated a *Bam*HI site and allows CM19m1409 to be distinguished from CM19 while preserving the correct reading frame and encoded amino acid (serine).

The following *myc* deletion mutants were created for our studies. *myc*(X/N) was made by using the *Hin*cII-*Bam*HI segment of the simian virus 40 (SV40) T antigen gene containing the polyadenylation signal (SVpA), after passage through a shuttle vector to generate suitable restriction sites, to replace the *Nsi*I-*Eco*RI segment of CM19; all but the first 75 bases of the *myc* 3′ UTR were deleted in *myc*(X/N). *myc*(X/N)m1409 was created similarly by replacing the *Nsi*I-*Eco*RI site of CM19m1409 with the SVpA and is identical to *myc*(X/N) except for the A-to-C mutation at *myc* codon 281. *myc*(P/R) was created by ligating the MLV LTR to the *Pvu*II site in *myc* exon 1, resulting in deletion of all but the last 41 nucleotides (nt) of *myc* exon 1. *myc*(P/N) was created by substituting the SVpA for the *Nsi*I-*Eco*RI segment of *myc*(P/R). The construction of plasmids *myc*(Δ265-433), *myc*(Δ371-433), *myc*(Δ312-433), and *myc*(Δ41-178) in which *myc* codons 265 to 433, 371 to 433, 312 to 433, and 41 to 178 were deleted, respectively, was previously described (45). *myc*(Δ312-433)SVpA was created by substituting the SVpA for the *Nsi*I-*Eco*RI segment of *myc*(Δ312-433). To create *myc*(Δ6-203)(Δ371-433)SVpA, the 5′ half (*Hin*dIII-*Bgl*II fragment) of a *myc* deletion mutant in which codons 6 to 203 were removed from *myc* exon 2 (45) was used to replace the equivalent portion of *myc*(Δ371-433), and the SVpA was substituted for the *Nsi*I-*Eco*RI segment; *myc*(Δ6-203)(Δ371-433)SVpA has most of *myc* exon 2, a substantial portion of exon 3, and most of the *myc* 3′ UTR deleted. CM19pA1 was created by PCR amplification of sequences from the first *myc* AATAAA polyadenylation signal to the downstream *Eco*RI site of CM19 by using oligonucleotide primers introducing a 5′ *Nsi*I site and ligated into the *Nsi*I-*Eco*RI site of CM19; CM19pA1 is identical to CM19 except that sequences between the *Nsi*I site and 1 nt 5′ to the first *myc* AATAAA are deleted. CM19pA2 was created in an similar manner, and differs from CM19 in that sequences between the *Nsi*I site and 5 nt 5′ to the second *myc* AATAAA are deleted.

To construct human β-globin–*myc* fusion genes, a C-to-A mutation was first introduced by site-directed mutagenesis at codon 141 of a pGEM2-based human β-globin gene to create an *Nco*I site. β-globin–*myc* fusion genes were created by using a duplex polylinker with a 5′ *Nco*I overhang and a 3′ *Xho*I overhang to connect *myc* sequences 3′ to the *Xho*I site in *myc* *Xho*I-linker insertion or deletion mutants (45) to β-globin sequences 5′ to the newly created *Nco*I site. These chimeric genes are fused to preserve the authentic *myc* reading frame and are under the transcriptional control of the MLV LTR. They are named to indicate both the first *myc* codon fused in frame to human β-globin sequences and the polyadenylation signal used. For example, βGm263SVpA contains the first 140 codons of MLV β-globin fused in frame to a *myc* segment from codon 263 to the *Nsi*I site 75 nt 3′ to the *myc* translation termination codon and uses the SVpA. With the exception of βGm(40-263)SVpA (see below), plasmids contain all *myc* codons from the named codon through the *Nsi*I site. To create tagged β-globin–*myc* fusion genes, a C-to-T mutation was introduced into β-globin codon 122, which destroys an *Eco*RI site but preserves the encoded amino acid (phenylalanine). Tagged genes are designated with a RI$^-$ suffix. βGm(40-263)SVpARI$^-$ was created by ligating the *Xho*I-*Bst*EII fragment of In40 (45) to the *Bst*EII-*Cla*I fragment of pSP65*myc*IIA (45) and inserting this fragment into the *Xho*I site of βGm434SVpARI$^-$ by using a short polylinker with a 5′ *Cla*I and a 3′ *Xho*I overhang, which frameshifts *myc* codons 434 to 439 to the +1 reading frame. It has β-globin codons 1 to 140 followed in frame by *myc* codons 40 to 263 followed by 11 irrelevant codons and uses the SVpA.

To create βG-rpL32, cDNA sequences containing the first 133 codons (out of a total of 135) of ribosomal protein L32 (rpL32) (16) (gift from Xinkang Wang) were PCR amplified with oligonucleotide primers introducing a 5′ *Xho*I site and a 3′ *Hin*cII site and inserted in frame between the *Xho*I-*Hin*cII sites of βGm434SVpARI$^-$. βG-CAT fuses the last 181 codons (out of a total of 219) of the bacterial gene encoding chloramphenicol acetyltransferase (CAT) and SVpA to globin and was created by inserting the *Xho*I-*Bam*HI fragment of MLV-CAT-SVpA (49) into βGm434SVpARI$^-$.

RT-PCR+1 assay of comparative mRNA abundance. Total cytoplasmic RNA was extracted from transiently transfected C2C12 myoblasts by a reduced-scale modification of the method of Laski et al. (29). Oligo(dT) primed reverse transcription of cytoplasmic RNA was performed with MLV reverse transcriptase (Gibco BRL) according to the manufacturer's instructions. PCR amplification of cDNA was performed with *Taq* polymerase (Promega) in 50 mM Tris-HCl (pH 9.0), 20 mM $(NH_4)_2SO_4$, 1.5 mM $MgCl_2$, 200 mM deoxynucleoside triphosphates, and 1 mM oligonucleotide primers on a PTC-100 thermal cycler (MJ Research, Cambridge, Mass.). From cells transiently cotransfected with recombinant human *myc* genes, a 248-bp sequence of human *myc* cDNA was amplified with oligonucleotide primers HMF1182 and HMR1430 (see below and Fig. 2) for 30 cycles of 92°C for 30 s, 60°C for 30 s, and 72°C for 30 s. Following completion of PCR, a ^{32}P-end-labeled, nested primer, HMF1269, was added to each PCR mixture for one additional cycle (the +1 cycle) of amplification. *myc* reverse transcription (RT)-PCR+1 products were restricted with *Bam*HI, heat denatured, and resolved on a 6% polyacrylamide Sequagel (National Diagnostics). From cells transiently cotransfected with β-globin–*myc* fusion genes, a 214-bp sequence of β-globin cDNA was amplified with oligonucleotide primers βGF2 and βG3′Rev (see below) for 30 cycles of 92°C for 30 s, 62°C for 15 s, and 72°C for 15 s. A +1 cycle was conducted with a ^{32}P-end-labeled nested primer, βGF1, and the products were restricted with *Eco*RI and resolved by electrophoresis. RT-PCR+1 products were quantitated on a Molecular Dynamics PhosphorImager (Sunnyvale, Calif.) with ImageQuant software. The relative abundance of the RT-PCR+1 products (and, hence, of the mRNAs) from two cotransfected genes is normalized for the molar ratio of the cotransfected plasmids determined by Southern analysis (see below).

To create a radiolabeled DNA fragment that indicates complete digestion of the RT-PCR+1 products by *Bam*HI (*Bam*HI cutting control), a 248-bp sequence of CM19m1409 cDNA was amplified with HMF1182 and HMR1430 with the addition of 20 μCi of [α-^{32}P]dATP (3,000 Ci/mmol) (DuPont NEN) to the PCR mixture. To create a radiolabeled *Eco*RI cutting control, an irrelevant 115-bp DNA fragment was first ligated into the *Bam*HI site in exon 2 of the human β-globin gene to create βGIn115. Total cytoplasmic RNA isolated from cells transiently transfected with βGIn115 was reverse transcribed, and the radiolabeled *Eco*RI cutting control was produced by amplification of a 329-bp sequence of βGIn115 cDNA with βGF2 and βG3′Rev with the addition of 20 μCi of [α-^{32}P]dATP (3,000 Ci/mmol) to the PCR mixture. Both the *Bam*HI and *Eco*RI cutting controls have their restriction sites flanked by the same sequence as the RT-PCR+1 products being cut.

The primers and their sequences used in this study are as follows: HMF1182, 5′AAGTCCTGCGCCTCGCAA3′; HMR1430, 5′GCTGTGGCCTCCAGCAG A3′; HMF1269, 5′CCCGAGCCCCTGGTGCTCCAT3′; βGF2, 5′AAGTGCT CGGTGCCTTTAGTGA3′; βG3′Rev, 5′ACACCAGCCACCACTTTCTGA3′; and βGF1, 5′CAAGGGCACCTTTGCCACACT3′.

Differentiation assays and actinomycin D studies of mRNAs in stably transfected cells. Differentiation assays were performed as previously described (49). Briefly, stably transfected C2C12 cells were seeded at subconfluent density into multiple culture plates containing DMEM supplemented with 10% fetal calf serum and antibiotics. Cells were cultured to confluence and then induced to differentiate into multinucleated myotubes by changing the media to DMEM containing 2% horse serum. Total cytoplasmic mRNA was isolated on serial culture days, and mRNA levels were determined by Northern (RNA) analysis using the glyoxal method (33). RNA was electroblotted to Hybond N (Amersham) and UV cross-linked. Hybridizations were carried out by modifications of the method of Church and Gilbert (11) with probes labeled by random priming.

To analyze mRNA decay after actinomycin D treatment, stably transfected cells were seeded into multiple culture plates. After adding actinomycin D (Sigma) to each plate at a final concentration of 10 μg/ml, total cytoplasmic RNA was isolated at defined time points, and mRNA levels were determined by Northern analysis. To examine human *myc* mRNAs, we used a human c-*myc* exon 1 probe (*Xho*I-*Pvu*II fragment); to examine β-globin–*myc* fusion mRNAs, we used a full-length human β-globin cDNA fragment from pSPβκc (gift from Stephen Liebhaber); to examine C2C12 c-*myc* mRNA, we used a murine c-*myc* exon 1 probe (*Bam*HI-*Sac*I fragment) or a human c-*myc* exon 2+3 cDNA probe from pSP65*myc*IIA (45); and to examine rpL32 mRNA, we used a full-length cDNA probe (16). To calculate mRNA half-lives after actinomycin D treatment or downregulation during differentiation, mRNA levels were normalized for RNA loading by using the level of stable rpL32 mRNA. mRNA levels at each time point after actinomycin D treatment relative to the mRNA level in untreated cells were used to generate a best-fit exponential-decay curve by using Cricket Graph (Malvern, Pa.), from which half-lives were calculated. Exceptions to this method of half-life analysis include βGm434SVpA and rpL32 mRNAs, which have long half-lives; their mRNA levels were normalized for RNA loading by ethidium bromide staining of RNA on Hybond N membranes. mRNA levels in differentiating C2C12 cells were compared with mRNA levels in preconfluent cells to determine the fold downregulation.

Southern analysis of plasmid ratios. Southern analysis was used to determine the precise ratio of plasmids in copurified plasmid mixtures and episomal DNA extracted from nuclei of transiently transfected cells (22). Copurified *myc* plasmids, one of which was usually CM19m1409, were digested with *Bgl*II, *Bam*HI, and either *Nsi*I or *Eco*RI. Southern blots of the digests were probed with the 1.3-kb *Bgl*II-*Bam*HI fragment of CM19m1409 in which a *Bam*HI site was engineered at codon 281. Autoradiography reveals a 1.3-kb *Bgl*II-*Bam*HI fragment from CM19m1409, which is easily distinguished from the longer *Bgl*II-*Eco*RI or *Bgl*II-*Nsi*I fragment of the copurified *myc* gene that does not have a codon 281 *Bam*HI site. The relative abundance of copurified β-globin–*myc* fusion genes was determined by Southern analysis following *Bam*HI and *Eco*RI digestion and probing of the blots with the 0.9-kb *Bam*HI-*Eco*RI fragment from the normal β-globin gene. β-globin–*myc* fusion genes containing an *Eco*RI site in β-globin exon 3 produce a 0.9-kb fragment, which is easily distinguished from the longer *Bam*HI-*Eco*RI fragments derived from genes in which the *Eco*RI site in exon 3 was obliterated.

RESULTS

RT-PCR+1 assay for comparing *myc* mRNA levels. mRNA instability plays a major role in determining the steady-state level of c-*myc* mRNA. Although multiple putative *cis*-acting instability elements have been identified (21, 24, 28, 50), the ones that influence steady-state c-*myc* mRNA levels are unknown. To address this issue, we developed a method for identifying *myc* mRNA elements that regulate its steady-state level. Our approach compares the steady-state levels of two human *myc* mRNAs—one a near-normal, reference *myc* mRNA and the other a mutant *myc* mRNA—encoded by two recombinant *myc* genes transiently cotransfected into cells in equimolar amounts. To equalize rates of mRNA transcription and processing, the cotransfected *myc* genes are constructed in identical plasmids and have identical structural features (promoter-enhancers, splicing patterns, and polyadenylation signals, whenever feasible). Under these conditions, equally stable mRNAs will be equally abundant, while removal of an instability determinant in the mutant mRNA will result in a comparatively higher mRNA level. The relative abundance of the two *myc* mRNAs should be proportional to their half-lives, and if the half-life of one is known, the half-life of the other can be deduced. This assay is similar in principle to an assay previously described by Weiss and Liebhaber (47, 48).

To determine which elements in human c-*myc* mRNA are important for regulating its steady-state levels, comparative levels of human *myc* mRNAs were analyzed in proliferating murine C2C12 myoblasts. In these cells, human c-*myc* mRNA has been shown to have a short half-life and is posttranscriptionally downregulated during myogenic differentiation like endogenous murine c-*myc* mRNA (49, 50), making this system suitable for analyzing elements that regulate steady-state levels of human c-*myc* mRNA. C2C12 cells at low density were transiently transfected with essentially normal human c-*myc* genes contained in plasmids CM19 and CM19m1409 (Fig. 1). These two genes, which differ only by a silent point mutation in codon 281 of CM19m1409, were transfected individually and together as a copurified mixture (see Materials and Methods). Cytoplasmic RNA was isolated, and an RT-PCR+1 assay was used to compare the levels of the two human *myc* mRNAs (Fig. 2). After reverse transcription of the RNA, PCR amplification across the *myc* exon 2/3 splice junction with human *myc*-specific primers (HMF1182 and HMR1430) produced a 248-bp fragment from human *myc* cDNA. The point mutation in CM19m1409 generates a *Bam*HI site that distinguishes its RT-PCR product from that of CM19. An additional cycle of amplification with a radiolabeled nested primer, the +1 cycle, ensured that all radiolabeled products were obligate homodimers (9) at the *Bam*HI site if a site is present. After *Bam*HI digestion, the 161-bp radiolabeled nested products derived from CM19 and CM19m1409 mRNAs (Fig. 2B, lanes 1, 3, and 5) were separated by denaturing gel electrophoresis into an uncut 161-bp radiolabeled band from CM19 (Fig. 2B, lanes 2 and 6) and a cut 136-bp radiolabeled band from CM19m1409 (Fig. 2B, lanes 4 and 6), which were quantitated on a PhosphorImager. Completeness of *Bam*HI digestion was monitored with a radiolabeled cutting control added to the reaction (Fig. 2B, lanes 2, 4, and 6 to 8). The primers and PCR conditions used amplified only human and not murine *myc* cDNAs (Fig. 2A and B, compare lane 10 with lanes 1, 3, and 5).

The RT-PCR+1 assay was found to be sensitive to a wide range of mRNA ratios. Following cotransfection of CM19 and CM19m1409 at molar ratios ranging from 1:25 to 17:1, this RT-PCR+1 assay yielded directly proportional mRNA ratios (Fig. 2C), indicating that the assay faithfully reported mRNA ratios over almost a 3-log range. Further, equivalence of the CM19/CM19m1409 input plasmid and output mRNA ratios indicated that the mutation in CM19m1409 did not disturb mRNA stability or processing. This important property of the reference *myc* mRNA was confirmed by showing that CM19m1409 mRNA, like endogenous c-*myc* and CM19 mRNAs (49), decayed with a 20 to 30 min half-life following actinomycin D treatment of stably transfected C2C12 cells (data not shown).

Deletion of the 3′ UTR increases steady-state levels of c-*myc* mRNA. The assay for comparing human *myc* mRNA levels was used to identify c-*myc* mRNA elements that determine its steady-state level. Earlier studies showed that the 3′ UTR of c-*myc* mRNA contains sequences that confer rapid decay following transcriptional inhibition by actinomycin D (21, 24). To test whether these sequences regulate steady-state *myc* mRNA levels, proliferating C2C12 cells were transiently cotransfected with a copurified mixture of *myc*(X/N) and CM19m1409 plasmids present at a 1:4 molar ratio. These two plasmids are identical except for the deletion of *myc* 3′ UTR sequences in *myc*(X/N). By RT-PCR+1 analysis, the level of *myc*(X/N) mRNA was 1.5-fold higher than CM19m1409 mRNA 2 days after transfection (Fig. 3A, lanes 1 and 3; control in lane 5). After normalization for the transfected plasmid ratio, *myc*(X/N) mRNA was sixfold more abundant than CM19m1409 mRNA. Measurements performed 3 days after transfection yielded similar results (Fig. 3A, lanes 2 and 4), indicating that the 6:1 ratio of *myc*(X/N) to CM19m1409 mRNA reflected steady-state levels of the individual mRNAs. Two other copurified plasmid mixtures of *myc*(X/N) and CM19m1409 at molar ratios of 1.6:1 and 3.7:1 were cotransfected into C2C12 cells and produced steady-state *myc*(X/N)/CM19m1409 mRNA levels at ratios of 5.7:1 and 33:1, respectively (Fig. 3A, lanes 6 to 10 and 11 to 15, respectively). After normalization for plasmid transfection ratio, the mRNA ratios

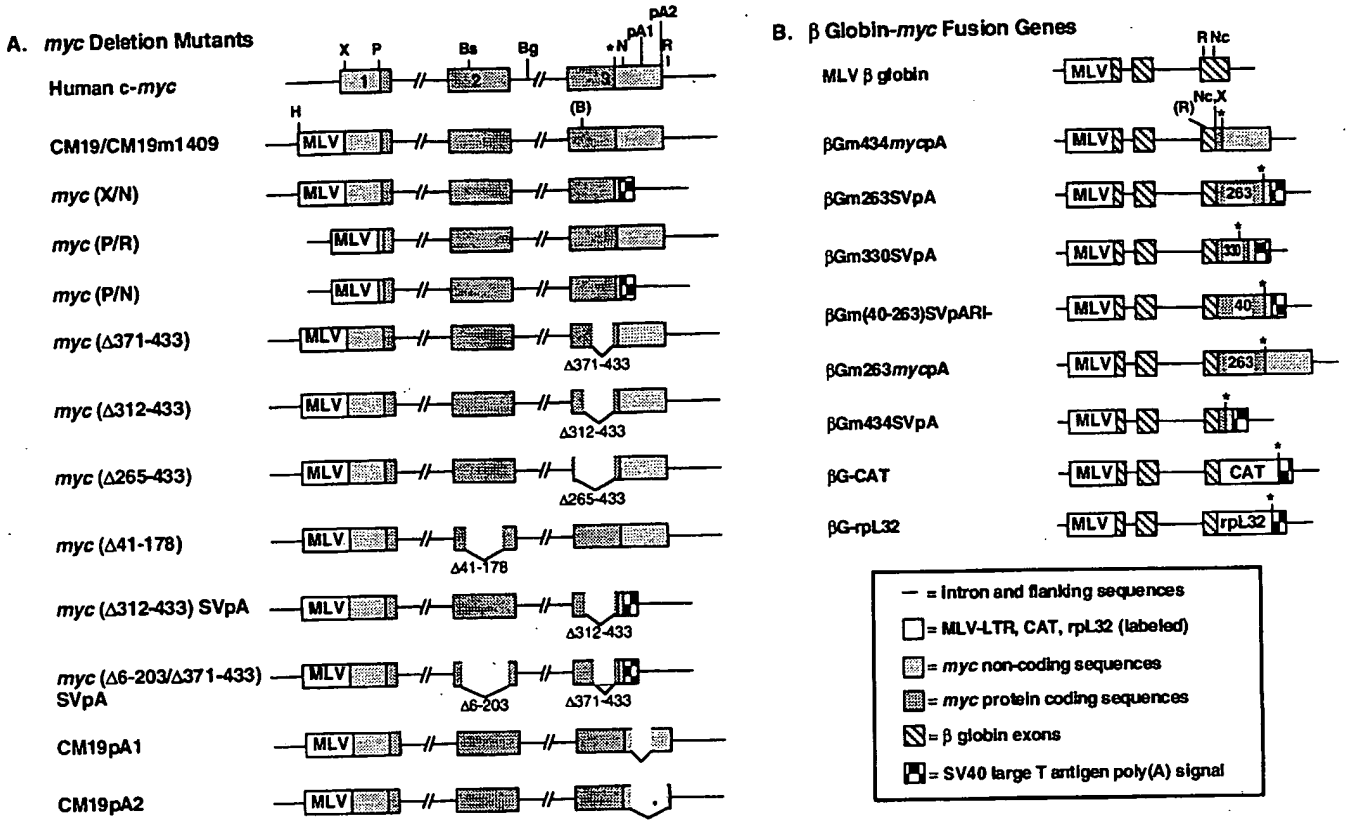

FIG. 1. Schematic diagram of recombinant genes used in this study. The inset box provides a key to introns, flanking sequences, and the shading pattern of exons. The exons in human c-*myc* are numbered. Restriction sites are labeled as follows: B, *Bam*HI; Bg, *Bgl*II; Bs, *Bst*EII; H, *Hin*dIII; N, *Nsi*I; Nc, *Nco*I; P, *Pvu*II; R, *Eco*RI; X, *Xho*I; (B) indicates the *Bam*HI site that is present in CM19m1409 but absent in CM19; (R) indicates the presence of an *Eco*RI site in all globin-*myc* fusion genes not designated RI⁻. pA1 and pA2 designate the first and second *myc* AATAAA polyadenylation signals, respectively, and * denotes the translation termination codon. Deleted sequences are whited out and indicated by a Δ followed by the codons deleted. In globin-*myc* fusion constructs, 263 and 330 indicate that *myc* sequences from codons 263 or 330 to the *Nsi*I site are fused in frame to globin, and 40 indicates that *myc* codons 40 to 263 followed by 11 irrelevant codons are fused in frame to globin. See Materials and Methods for details of construction.

were 3.6 and 8.9. These results confirm that *myc*(X/N) mRNA is about five- to sixfold more abundant than CM19m1409 mRNA at steady state (Table 1).

Potential sources of artifact in our results were excluded by the following experiments. To exclude the possibility that the codon 281 mutation in CM19m1409 mRNA might have influenced the results, we introduced the mutation into *myc*(X/N). Following cotransfection of proliferating C2C12 cells with a mix of *myc*(X/N)m1409 and CM19, the normalized ratio of *myc*(X/N)m1409 to CM19 mRNA was 3.4 (Fig. 3A, lanes 16 to 20), demonstrating that the relative abundance of *myc*(X/N) and CM19 mRNAs was determined by truncation of the *myc* 3′ UTR and not by the codon 281 point mutation. Another potential source of artifact is altered efficiency of 3′-end-processing of *myc*(X/N) mRNA due to substitution of the SV40 polyadenylation signal for the *myc* polyadenylation signals (46). To address this concern, we generated CM19pA1 and CM19pA2 in which *myc* 3′ UTR sequences between the *Nsi*I site and the first or second *myc* polyadenylation signal (3, 27) were deleted: CM19pA1 retains both *myc* polyadenylation signals, and CM19pA2 retains the second, dominant (27) *myc* polyadenylation signal (Fig. 1). CM19pA1 and CM19pA2 were each cotransfected into C2C12 cells with CM19m1409, and their steady-state mRNA levels were found to be 3.0-fold and 3.9-fold more abundant than CM19m1409 mRNA (Fig. 3B; Table 1), similar to the results obtained with *myc*(X/N). Finally to rule out the possibility that a difference in plasmid transfectability or metabolism accounted for these results, the relative levels of the plasmids in the nuclear episomal fraction from transfected cells were determined and found to be identical to those in the transfection mixture. Together, these results demonstrate that the 3′ UTR of c-*myc* mRNA contains a determinant necessary for keeping the steady-state level of c-*myc* mRNA low, and this determinant is positioned between the *Nsi*I site and the 5′ *myc* polyadenylation signal.

Deletion of other *myc* mRNA sequences does not significantly alter steady-state levels. Previous studies have suggested that elements within the 5′ UTR and protein-coding domain may destabilize c-*myc* mRNA (5, 18, 21, 40, 50). To determine if these or other regions regulate steady-state c-*myc* mRNA levels, we used the RT-PCR+1 assay to compare the steady-state levels of CM19m1409 mRNA with those of several mutant *myc* mRNAs: *myc*(P/R) mRNA, which has most of the 5′ UTR deleted; *myc*(Δ41-178) mRNA, which has most of exon 2 deleted; and *myc*(Δ312-433) mRNA, which has most of the exon 3 protein-coding region deleted (Fig. 1). The normalized steady-state levels of *myc*(P/R), *myc*(Δ41-178), and *myc*(Δ312-433) mRNAs were between 1.0 and 1.5 times the level of CM19m1409 mRNA (Table 1), indicating that sequences regulating c-*myc* mRNA steady-state levels in proliferating C2C12 cells do not reside in the deleted portions of these mRNAs. Certain regions of c-*myc* mRNA were not deleted in any of our mutant *myc* mRNAs, because their removal might interfere with splicing (e.g., the ends of exons) or PCR

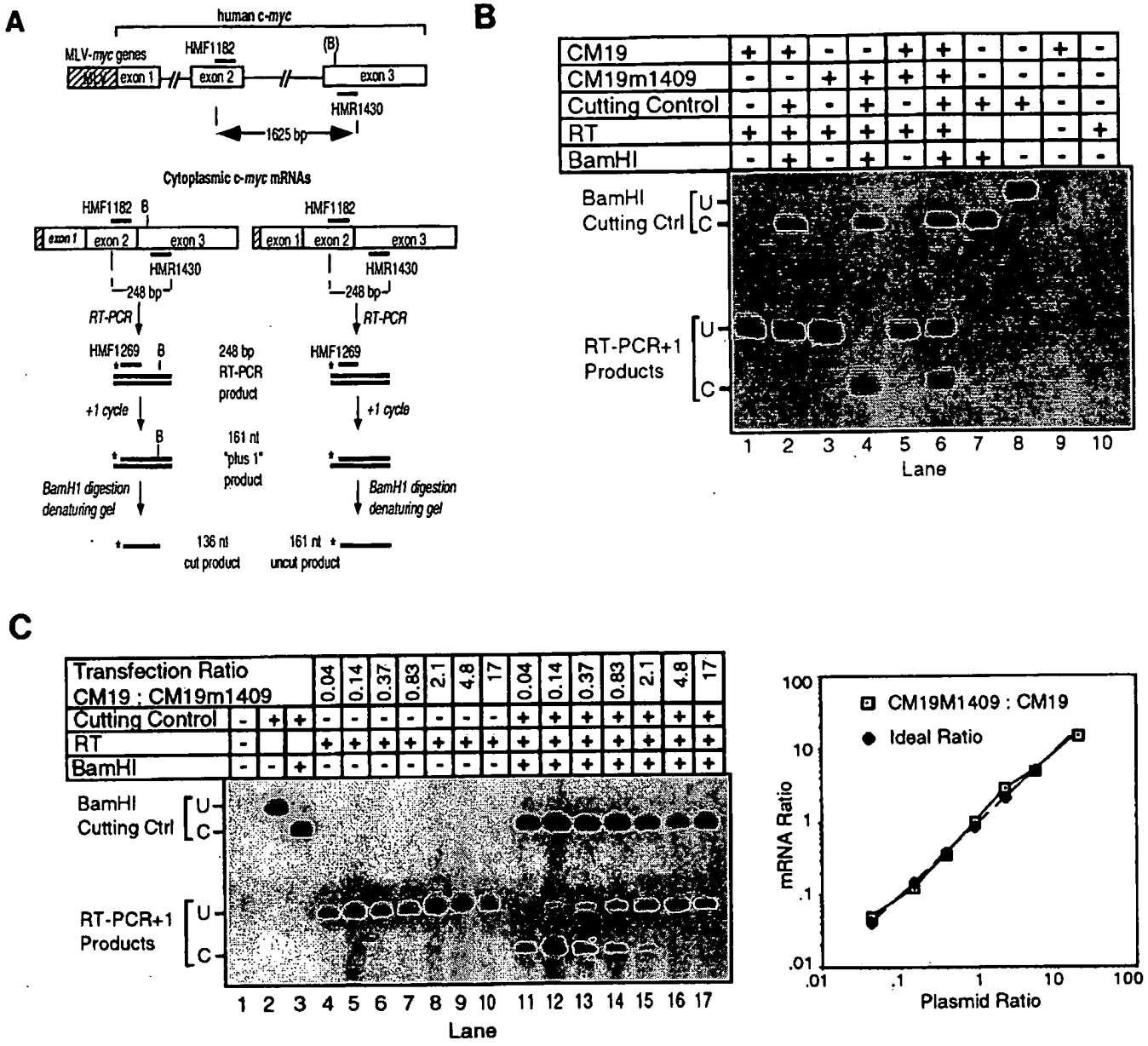

FIG. 2. RT-PCR+1 assay for comparing human *myc* mRNA levels. (A) Schematic diagram of RT-PCR+1 assay. Cytoplasmic RNA isolated from cells cotransfected with an equimolar ratio of two recombinant human c-*myc* genes [distinguished by a *Bam*HI (B) site at codon 281 in one of the genes] was reverse transcribed. A 248-bp sequence of *myc* cDNA spanning the exon 2/3 splice junction was amplified by PCR with a 5′ primer in exon 2 (HMF1182) and a 3′ primer in exon 3 (HMR1430). An additional cycle of amplification with a radiolabeled (*) nested primer (HMF1269) was performed. After restriction with *Bam*HI, the radiolabeled product from the mutated mRNA is 136 nt, while the product from the normal mRNA is 161 nt. (B) RT-PCR+1 analysis of CM19 and CM19m1409 mRNAs. Cytoplasmic RNA was isolated 2 days after C2C12 cells were transiently transfected with CM19, CM19m1409, or both plasmids. Human *myc* mRNAs were amplified by RT-PCR+1, and the products were resolved on a 6% denaturing polyacrylamide gel. The autoradiograph shows the results from cells transfected with the following: CM19 (lanes 1, 2, and 9), CM19m1409 (lanes 3 and 4), an equimolar ratio of CM19 and CM19m1409 (lanes 5 and 6) or pUC19 (lane 10). The products in lanes 1, 3, 5, and 10 are undigested, while those in lanes 2, 4, and 6 were spiked with the *Bam*HI cutting control and digested with *Bam*HI prior to loading. Digested (lane 7) or undigested (lane 8) *Bam*HI cutting control is shown, as is the result of PCR+1 amplification of RNA from CM19-transfected cells that has not been reverse transcribed (lane 9). *Bam*HI cut (C) and uncut (U) products are labeled. (C) Ratio of CM19 to CM19m1409 RT-PCR+1 products from cells transfected with various input plasmid ratios. CM19 and CM19m1409 were copurified at the following molar ratios (CM19/CM19m1409): 0.04, 0.14, 0.37, 0.83, 2.1, 4.8, and 17. Each copurified plasmid mixture was transfected into C2C12 cells, and cytoplasmic RNA was isolated after 2 days. RT-PCR+1 was performed, and the products were resolved on a 6% denaturing polyacrylamide gel. The autoradiograph demonstrates products derived from the copurified plasmid mixtures prior to (lanes 4 to 10) and following (lanes 11 to 17) *Bam*HI digestion; the cut (C) and uncut (U) products are labeled. The PCR+1 product of RNA not reverse transcribed is shown in lane 1, and lanes 2 and 3 show uncut and cut samples of the cutting control added to each *Bam*HI digestion. The results shown in the autoradiograph were quantitated on a PhosphorImager, and CM19m1409/CM19 mRNA ratios (*y* axis) were plotted against the CM19m1409/CM19 plasmid ratios used for transfection (*x* axis). The solid line indicates the actual plot, while the dashed line indicates an ideal plot with mRNA ratios equal to plasmid ratios.

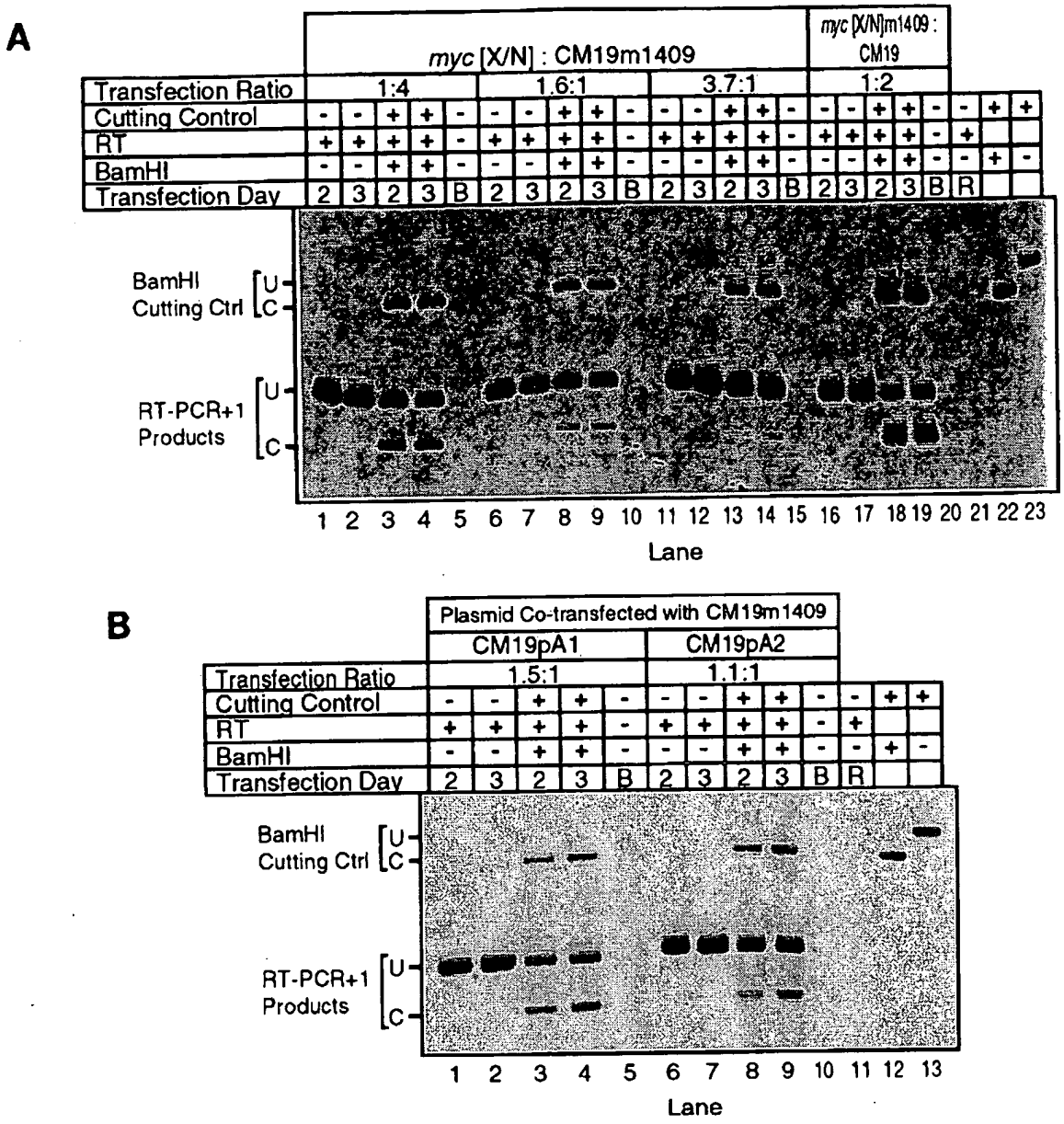

FIG. 3. Steady-state *myc* mRNA levels are increased by deletion of its 3′ UTR. (A) C2C12 cells were transiently cotransfected with 20 μg of *myc*(X/N) and CM19m1409 copurified at a molar ratio of 1:4, 1.6:1, or 3.7:1 or with *myc*(X/N)m1409 and CM19 copurified at a 1:2 molar ratio. At 2 and 3 days, cytoplasmic RNA was isolated, and mRNA levels were determined by the RT-PCR+1 assay. The autoradiograph displays the comparative human *myc* mRNA levels with the lanes labeled as follows: Transfection Ratio, the molar ratio of plasmids transfected; Cutting Control, whether sample was (+) or was not (−) spiked with the *Bam*HI cutting control; RT, product of RT-PCR+1 (+) or PCR+1 without reverse transcription (−); *Bam*HI, whether product was (+) or was not (−) digested with *Bam*HI; Transfection Day, day (2 or 3) of RNA harvest, with "B" indicating a mixture of RNA from days 2 and 3 and "R" indicating RT-PCR+1 reagents alone with no RNA. Uncut (U) and cut (C) *Bam*HI cutting control and RT-PCR+1 products are indicated. (B) C2C12 cells were transiently cotransfected with 20 μg of CM19m1409 copurified with either CM19pA1 or CM19pA2, and cytoplasmic RNA was harvested after 2 or 3 days. The autoradiograph demonstrates the results of RT-PCR+1 analysis of comparative mRNA levels with the lanes labeled as in panel A.

primer binding (from codon 206 in exon 2 to codon 288 in exon 3), so the effect of these sequences on *myc* mRNA levels was not determined. Since none of these regions has been implicated as an instability determinant, we considered it unlikely that these regions contain a determinant of steady-state levels.

From the mRNA stabilization leading to the five- to sixfold-higher steady-state level of *myc* mRNAs missing the 3′ UTR, one would infer that these mRNAs have half-lives of 100 to 150 min, given the 20 to 30 minute half-life of CM19m1409 mRNA. Many mRNAs are even longer lived, raising the possibility that *myc*(X/N) may yet retain other destabilizing elements. Therefore, we determined whether deleting *myc* mRNA sequences in addition to the 3′ UTR further increases *myc* mRNA levels. We examined steady-state levels of *myc*(P/N) mRNA (in which both 5′ and 3′ UTR sequences were deleted), of *myc*(Δ312-433)SVpA mRNA (in which most of the protein-coding sequences of exon 3 and 3′ UTR sequences were deleted), and of *myc*(Δ6-203)(Δ371-433)SVpA mRNA (in which most of exon 2, the sequences at the 3′ end of the exon 3 coding region, and the 3′ UTR were deleted) (Fig. 1). Steady-state levels of these

TABLE 1. Comparative steady-state levels of *myc* mRNA deletion mutants

Cotransfected plasmids		Salient feature of test plasmid[a]	mRNA ratio[b]	No. of determinations
Test plasmid	Reference plasmid			
Single deletion				
myc (X/N)	CM19m1409	Most of *myc* 3′ UTR deleted; SVpA substituted	5.3 ± 2.6	9
CM19pA2	CM19m1409	*myc* 3′ UTR from the *Nsi*I site to the second poly(A) signal deleted	3.9 ± 0.3	4
CM19pA1	CM19m1409	*myc* 3′ UTR from the *Nsi*I site to the first poly(A) signal deleted	3.0 ± 0.9	5
myc (P/R)	CM19m1409	Most of *myc* 5′ UTR deleted	1.0 ± 0.5	7
myc (Δ41-178)	CM19m1409	Most of *myc* exon 2 (codons 41 to 178) deleted	1.3 ± 0.2	2
myc (Δ312-433)	CM19m1409	Most of *myc* exon 3 (codons 312 to 433) deleted	1.5 ± 0.1	4
Multiple deletions				
myc (Δ312-433)SVpA	CM19m1409	3′ end of *myc* exon 3 coding region and 3′ UTR deleted; SVpA substituted	4.8 ± 0.4	4
myc (P/N)	CM19m1409	Most of *myc* 5′ UTR and 3′ UTR deleted	2.6 ± 0.04	2
myc (Δ6-203/371-433) SVpA	CM19m1409	Most of exon 2, 3′ end of *myc* exon 3 coding region, and 3′ UTR deleted; SVpA substituted	5.5 ± 0.5	2
myc (Δ312-433)SVpA	*myc* (X/N)m1409	3′ end of *myc* exon 3 coding region and 3′ UTR deleted; SVpA substituted; most of *myc* 3′ UTR deleted in reference plasmid	1.5 ± 0.3	4

[a] See Materials and Methods for details of plasmid construction.
[b] Test/reference mRNA ratios were determined by RT-PCR+1 ratio, after normalization for the input plasmid ratio as determined by Southern analysis. Values are average mRNA ratios (test/reference) ± standard deviations.

multiply deleted mRNAs were 2.6- to 5.5-fold higher than that of CM19m1409 mRNA (Table 1), i.e., no higher than levels of *myc* mRNAs from which only the 3′ UTR was deleted. Examined another way, *myc*(Δ312-433)SVpA was not significantly (1.5-fold) more abundant than *myc*(X/N)m1409 (Table 1). Thus, none of these three extensively deleted *myc* mRNAs was appreciably more stable than *myc*(X/N) mRNA, suggesting that the *myc* 3′ UTR contains the major instability determinant regulating steady-state c-*myc* mRNA levels in proliferating C2C12 cells.

Sequences in the *myc* 3′ UTR and protein-coding region independently lower steady-state levels of β-globin fusion mRNA. To determine which elements in c-*myc* mRNA can regulate steady-state levels of a heterologous mRNA, we used the principle and design of the *myc* RT-PCR+1 assay to develop a similar assay for comparing levels of mRNAs containing human β-globin sequences. Following cotransfection of a pair of β-globin–*myc* chimeric genes, a 214-bp sequence of globin cDNA was amplified by PCR with primers situated in globin exons 2 and 3. Endogenous globin genes are silent in C2C12 cells, so only globin cDNAs from the transfected genes were amplified (for demonstration of specificity, see Fig. 5). The products of the two fusion mRNAs were distinguished by a C-to-T mutation engineered in globin codon 122 in one of the two genes (designated RI$^-$), which eliminated a naturally occurring *Eco*RI site. Thus, after *Eco*RI digestion and denaturing gel electrophoresis, the RT-PCR+1 product from the mutated mRNA yielded an uncut 168-bp band and that from the unmutated mRNA yielded a cut 119-bp band. A cutting control was added to monitor completeness of digestion. When βGm263SVpA and βGm263SVpARI$^-$ (Fig. 1) were cotransfected into C2C12 cells at 1:100-to-200:1 molar ratios, the globin RT-PCR+1 assay yielded mRNA ratios similar to the plasmid transfection ratio, demonstrating that the assay reports a wide range of mRNA ratios and that the codon 122 mutation in βGm263SVpARI$^-$ does not affect mRNA levels (data not shown).

We anticipated that fusing determinants of *myc* mRNA instability to globin mRNA would lower steady-state levels of the globin-*myc* mRNA, i.e., normally stable globin mRNA should be destabilized. Levels of various globin-*myc* fusion mRNAs were compared with βGm434SVpA (Fig. 1) mRNA, which contains no sequences implicated in *myc* mRNA instability and has a half-life of 10.5 h in C2C12 cells by actinomycin D determinations (Fig. 4A and D). The level of βGm434*myc*pARI$^-$ mRNA (Fig. 1) was found to be 4.3-fold lower than βGm434SVpA mRNA both 2 and 3 days after transfection, demonstrating that the *myc* 3′ UTR lowered steady-state levels of globin mRNA by 4.3-fold (Fig. 5, lanes 1 to 5, and Table 2). Exchanging the construct containing the codon 122 mutation (i.e., βGm434SVpARI$^-$ and βGm434*myc*pA) yielded the same result (Table 2). If this lower steady-state mRNA level was attributable to more rapid mRNA turnover, as our assay was designed to accomplish, βGm434*myc*pA mRNA should be turned over 4.3 times more rapidly than βGm434SVpA mRNA and have a half-life of 2.4 h. Northern analysis of RNA from actinomycin D-treated C2C12 cells stably transfected with βGm434*myc*pA yielded an mRNA half-life of 2.5 h (Fig. 4B and D), suggesting that the lower steady-state level of βGm434*myc*pA mRNA was, in fact, due to mRNA destabilization.

We also examined sequences in the protein-coding regions of *myc* exons 2 and 3 for their ability to reduce levels of chimeric globin mRNAs. Fusion of most of *myc* exon 2 in βGm(40-263)SVpARI$^-$ mRNA (Fig. 1) lowered its abundance 1.7-fold compared with βGm434SVpA mRNA (Fig. 5, lanes 11 to 15, and Table 2). Fusion of *myc* exon 3 sequences from codon 263 to the *Nsi*I site in the 3′ UTR in βGm263SVpARI$^-$ mRNA (Fig. 1) lowered its abundance relative to βGm434SVpA mRNA by a highly significant 4.7-fold (Fig. 5, lanes 6 to 10, and Table 2). As with analysis of the effect of the *myc* 3′ UTR, exchanging the construct containing the codon 122 mutation (i.e., βGm434SVpARI$^-$ and βGm263SVpA) yielded the same result (Table 2). Northern analysis of RNA from actinomycin D-treated C2C12 cells stably transfected with βGm263SVpA yielded a half-life of 1.8 h (Fig. 4C and D), suggesting that the lower steady-state level was due to mRNA destabilization. The destabilization of globin mRNA by *myc* exon 3 protein-coding

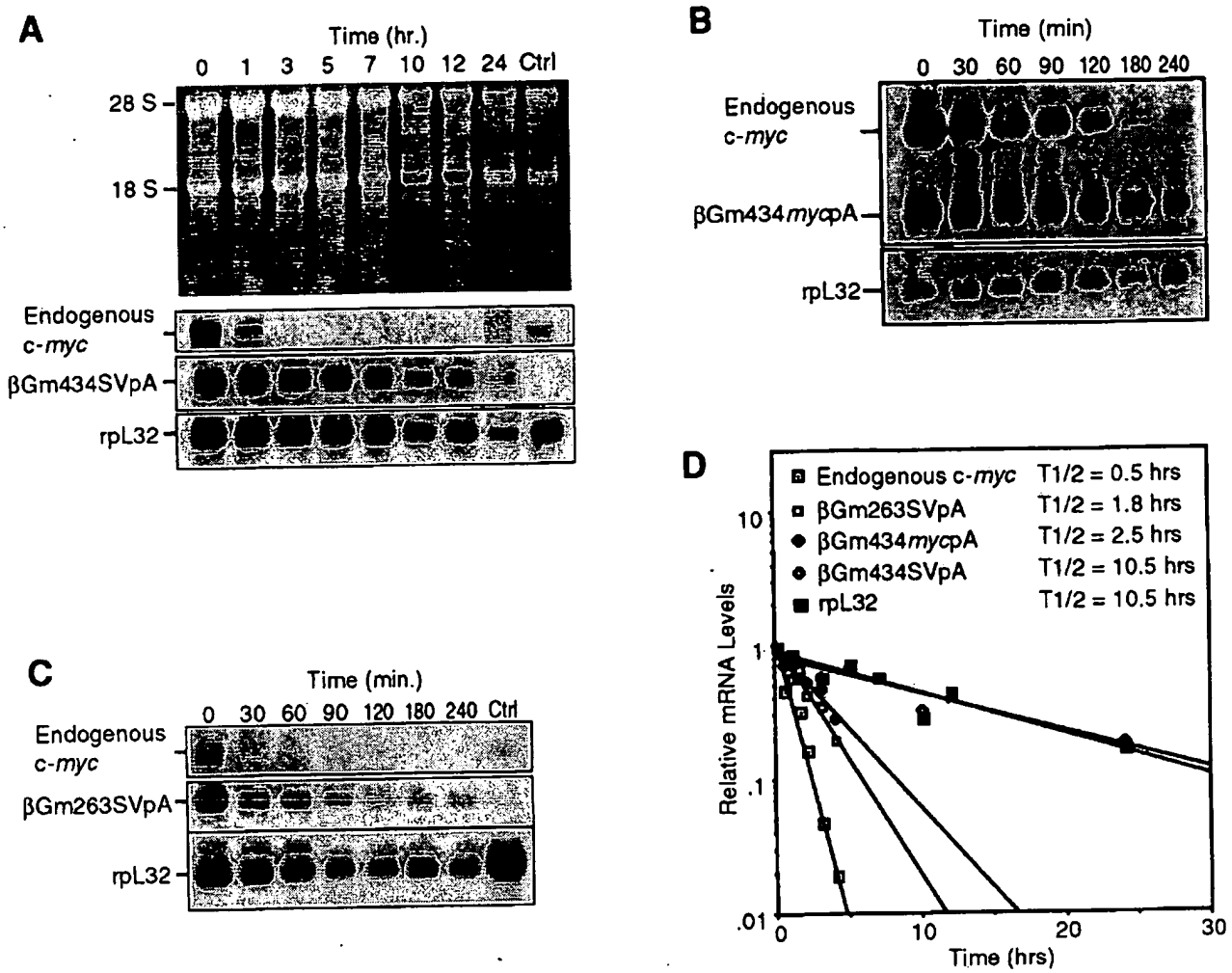

FIG. 4. Decay of globin-*myc* fusion mRNAs after actinomycin D. C2C12 cells were stably transfected with βGm434SVpA, βGm434*myc*pA, or βGm263SVpA and Northern analysis was performed on cytoplasmic RNA isolated at defined times after treatment with actinomycin D (10 μg/ml). mRNAs from transfected genes were detected by using a β-globin cDNA probe with cytoplasmic RNA from untransfected C2C12 cells (Ctrl) used as a negative control. Autoradiographs of blots display the decay of mRNA in cells stably transfected with βGm434SVpA (A), βGm434*myc*pA (B), or βGm263SVpA (C). Endogenous murine c-*myc* and rpL32 mRNAs were detected by using *myc* exon 2/3 and full-length rpL32 probes, respectively. The decay rates of βGm263SVpA and βGm434*myc*pA mRNAs were determined after normalizing for RNA loading by using rpL32 mRNA levels, and the decay rates of βGm434SVpA and rpL32 mRNAs were determined after normalizing for mRNA loading by using ethidium bromide staining. (D) Decay of the various mRNAs with the calculated half-lives indicated.

sequences contrasts with the observation that steady-state *myc* mRNA levels were not significantly increased by deletion of codons 312 to 433. This apparent discrepancy is not explained by the additional *myc* sequences fused to βGm263SVpARI⁻ mRNA compared with those deleted from *myc*(Δ312-433), i.e., *myc* codons 263 to 311 and 434 to 439 and the first 75 nt of the *myc* 3′ UTR. Codons 434 to 439 and the first 75 nt of the *myc* 3′ UTR are present in the reference (βGm434SVpA) mRNA and cannot account for the relative instability of βGm263SV pARI⁻ mRNA. Codons 263 to 311 are unnecessary for destabilization by *myc* exon 3 protein-coding sequences, as steady-state levels of βGm330SVpA and βGm263SVpARI⁻ mRNA were found to be similar (Table 2). Therefore, fusion of *myc* exon 3 protein-coding sequences destabilizes globin mRNA, but their removal from *myc* mRNA does not significantly alter steady-state levels.

To be certain that the destabilization of globin mRNA by fused *myc* sequences is a specific effect, we compared levels of chimeric globin mRNAs in which sequences from other mRNAs were fused at the same position. In-frame fusion of the first 133 codons of normally stable rpL32 mRNA (βG-rpL32) (Fig. 1) resulted in an mRNA with a steady-state level equal to that of βGm434SVpA mRNA (Table 2), indicating that globin mRNA was not destabilized simply by fusion of exogenous mRNA sequences. CAT mRNA has a half-life intermediate between *myc* and globin mRNAs (2, 51). In-frame fusion of 181 codons of CAT mRNA (βG-CAT) (Fig. 1) resulted in an mRNA that was 1.6-fold less abundant than βGm434SVpA mRNA (Fig. 5, lanes 16 to 20, and Table 2), indicating that fusion of *myc* exon 2 sequences was no more destabilizing than fusion of CAT sequences. Compared with the modest destabilization of globin mRNA by CAT or *myc* exon 2 sequences, destabilization by *myc* 3′ UTR or exon 3 protein-coding sequences was marked.

The exon 3 coding region and 3′ UTR together only modestly destabilize β-globin mRNA more than either element alone. The presence of more than one element in *myc* mRNA that can independently destabilize globin mRNA led us to examine whether their effects were additive. We found that the steady-state level of βGm263*myc*pARI⁻ mRNA, which contains most

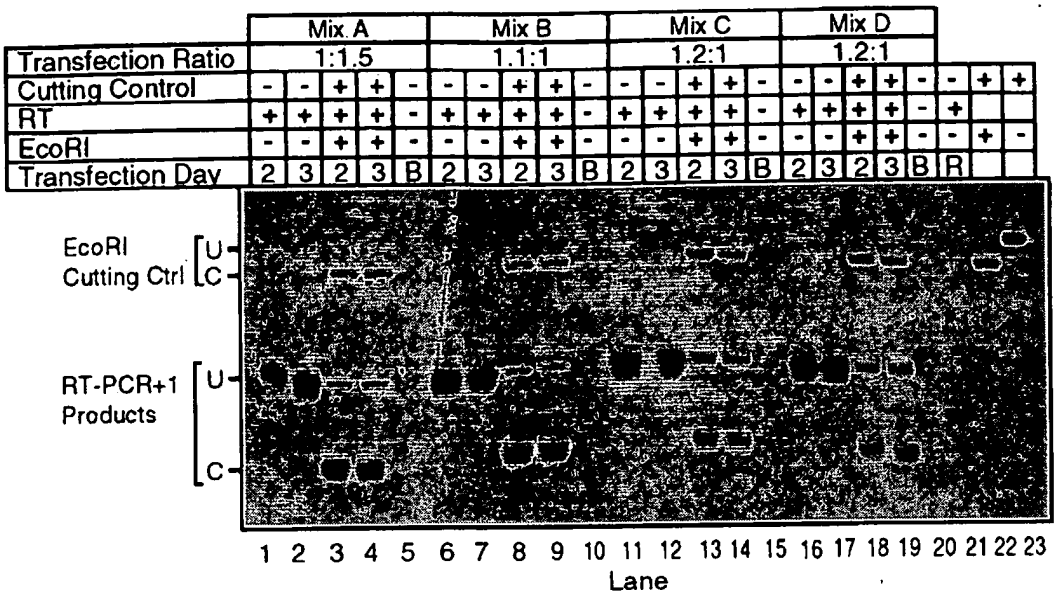

FIG. 5. Fusion of *myc* 3′ UTR or exon 3 sequences lower globin mRNA levels. C2C12 cells were transiently cotransfected with 20 μg of a copurified mixture of βGm434SVpA and βGm434*myc*pARI⁻ (Mix A, lanes 1 to 5), βGm263SVpARI⁻ (Mix B, lanes 6 to 10), βGm(40-263)SVpARI⁻ (Mix C, lanes 11 to 15), or βG-CAT (Mix D, lanes 16 to 20). At 2 and 3 days, cytoplasmic RNA was isolated, and globin fusion mRNA levels were analyzed by RT-PCR+1. The autoradiograph displays the results with the lanes labeled as follows: Transfection Ratio, the molar ratio of plasmids transfected; Cutting Control, whether sample was (+) or was not (−) spiked with the *Eco*RI cutting control; RT, product of RT-PCR+1(+) or PCR+1 without reverse transcription (−); *Eco*RI, whether product was (+) or was not (−) digested with *Eco*RI; Transfection Day, day (2 or 3) of RNA harvest, with "B" indicating a mixture of RNA from days 2 and 3 and "R" indicating reagents alone with no RNA. Uncut (U) and cut (C) *Eco*RI cutting control and RT-PCR+1 products are indicated.

of the protein-coding domain of *myc* exon 3 and the entire 3′ UTR (Fig. 1), was 4.7-fold less than the level of βGm434SVpA mRNA (Table 2). This is similar to the results obtained for globin mRNAs fused to either the protein-coding region of exon 3 or the 3′ UTR, so their effect does not appear to be additive. When we compared βGm263*myc*pARI⁻ and βGm434*myc*pA mRNA levels directly, the former was 1.7-fold less abundant, but the large standard deviation made it difficult to attach significance to this result (Table 2). Direct comparison of βGm263*myc*pARI⁻ and βGm263SVpA mRNA levels revealed that the former was 2.3-fold less abundant, with a reproducibility suggesting that the difference is probably significant (Table 2). Together, these results suggest that the destabilizing effects of the protein-coding region of *myc* exon 3 and the 3′ UTR on β-globin mRNA are not additive and that the effect of the *myc* 3′ UTR may be greater.

Exon 3 coding sequences, but not 3′ UTR sequences, are necessary for downregulation of *myc* mRNA during C2C12 differentiation. C2C12 cells can be induced to differentiate into multinucleated myotubes by culturing them to confluence and changing to mitogen-poor media containing 2% horse serum. During differentiation, the level of C2C12 c-*myc* mRNA decreases 3- to 10-fold over 12 to 24 h through posttranscriptional mechanisms, and mRNA encoded by a stably transfected, MLV-driven, full-length human c-*myc* gene is regulated like the endogenous murine *myc* mRNA (49). Previously, we had shown that sequences in the coding region of human *myc* mRNA were responsible for this downregulation and that se-

TABLE 2. Comparative steady-state levels of chimeric globin mRNAs

Cotransfected plasmids		Salient feature of test plasmid not present in reference plasmid[a]	mRNA ratio[b]	No. of determinations
Reference plasmid	Test plasmid			
βGm434SVpARI⁻	βGm434*myc*pA	Most of *myc* 3′ UTR	4.3 ± 0.1	2
βGm434SVpA	βGm434*myc*pARI⁻	Most of *myc* 3′ UTR	4.3 ± 1.0	12
βGm434SVpA	βGm(40-263)SVpARI⁻	Most of *myc* exon 2 and 5′ end of exon 3 coding region (codons 40 to 263)	1.7 ± 0.7	4
βGm434SVpA	βGm263SVpARI⁻	Most of *myc* exon 3 coding region (codons 263 to 433)	4.7 ± 1.0	4
βGm434SVpARI⁻	βGm263SVpA	Most of *myc* exon 3 coding region (codons 263 to 433)	4.6 ± 0.2	2
βGm434SVpA	βG-CAT	Most of CAT coding region (codons 39 to 219)	1.6 ± 0.7	4
βGm434SVpA	βG-rpL32	Most of rpL32 coding region (codons 1 to 133)	0.8 ± 0.1	2
βGm434SVpA	βGm263*myc*pARI⁻	Most of *myc* exon 3 coding region (codons 263 to 433) and *myc* 3′ UTR	4.7 ± 0.5	2
βGm330SVpA	βGm263SVpARI⁻	*myc* codons 263 to 329; both plasmids contain *myc* sequences from codon 330 to the *Nsi*I site	0.9 ± 0.8	4
βGm263SVpA	βGm263*myc*pARI⁻	Most of *myc* 3′ UTR; both plasmids contain most of *myc* exon 3 coding region	2.3 ± 0.3	3
βGm434*myc*pA	βGm263*myc*pARI⁻	Most of *myc* exon 3 coding region (codons 263 to 433); both contain *myc* 3′ UTR	1.7 ± 0.7	5

[a] See Materials and Methods for details of plasmid construction.

[b] Reference/test mRNA ratios were determined by RT-PCR+1 ratio, after normalization for the input plasmid ratio as determined by Southern analysis. Values are average mRNA ratios (reference/test) ± standard deviations.

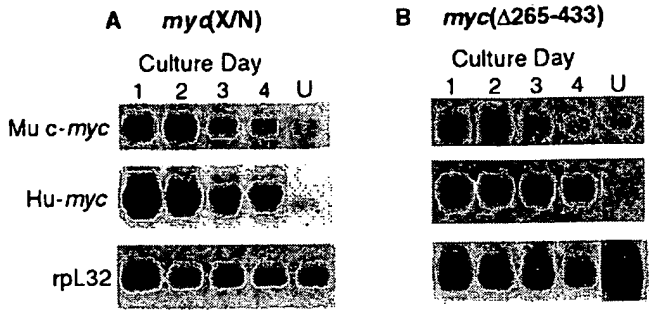

FIG. 6. Deletion of *myc* exon 3 sequences, but not 3′ UTR sequences, abolishes *myc* mRNA downregulation during myoblast differentiation. C2C12 cells stably transfected with *myc* (X/N) or *myc* (Δ265-433) were seeded at low density into multiple culture plates, cultured to confluence, and induced to differentiate by using differentiation media (DM; DMEM containing 2% horse serum). Northern analysis was performed on cytoplasmic RNA isolated on serial days beginning the day after cells were plated. Cells were subconfluent on day 1 and confluent on day 2. The medium was changed to DM on day 2, and days 3 and 4 cells have been exposed to DM for 1 and 2 days, respectively. Autoradiographs of blots display mRNA levels in cells transfected with *myc* (X/N) (A) or *myc* (Δ265-433) (B). mRNA from the transfected gene was detected by using a human (Hu) c-*myc* exon 1 probe (*Xho*I to *Pvu*II fragment); the endogenous murine (Mu) c-*myc* mRNA was detected by using a murine c-*myc* exon 1 probe (*Bam*HI to *Sac*I fragment); and rpL32 mRNA was detected by using a full-length cDNA probe (16). RNA from untransfected C2C12 cells (U) was used to demonstrate specificity of the human c-*myc* exon 1 probe.

quences in the *myc* UTRs were unnecessary (49). We asked whether protein-coding sequences in *myc* exon 3, which confer instability upon β-globin but not *myc* mRNA in proliferating C2C12 cells, might play a role in c-*myc* mRNA downregulation during C2C12 differentiation. Therefore, we stably transfected C2C12 cells with *myc*(X/N) and *myc*(Δ265-433) and determined their mRNA levels during differentiation by Northern analysis. *myc*(X/N) mRNA decreased 3.6-fold, which is similar to the 3.0-fold decrease in endogenous C2C12 c-*myc* mRNA (Fig. 6A) and confirmed that the 3′ UTR is unnecessary for *myc* mRNA downregulation during myoblast differentiation. In contrast, *myc*(Δ265-433) mRNA was not downregulated and even increased about twofold compared with rpL32 mRNA (Fig. 6B). In these cells, endogenous c-*myc* mRNA decreased fourfold (Fig. 6B), demonstrating that c-*myc* mRNA regulatory mechanisms are active and that exon 3 coding sequences are necessary for them to modulate mRNA levels. These results lead to the conclusion that separate elements are important for determining *myc* mRNA levels in proliferating and differentiating C2C12 cells.

DISCUSSION

We describe a strategy for identifying mRNA elements that regulate c-*myc* mRNA levels by comparing steady-state levels of two human *myc* or globin-*myc* fusion mRNAs by using an RT-PCR assay. The assay has been refined so that differences in steady-state mRNA levels may be attributed to differences in mRNA turnover rates. The PCR-based assay offers the advantage of sensitivity and the ability to use transiently transfected cells, which eliminates any influence that sites of gene integration may have on expression. Importantly, this method of analysis determines relative mRNA levels and half-lives without using drugs that perturb important metabolic processes, such as transcription or translation, that can affect mRNA turnover. Avoiding pharmacologic manipulations ensures that mRNA determinants regulating stability and steady-state levels operate in their normal physiologic context and that *trans*-acting factors involved in normal mRNA metabolism are unperturbed. Finally, the nature of the comparative mRNA approach identifies *cis*-acting elements that determine mRNA turnover rates and steady-state levels and that are, by definition, functionally important.

To ensure that factors besides mRNA stability did not differentially affect levels of the two mRNAs, plasmids used in this study were designed and prepared so that their mRNAs would be transcribed and processed identically. Any difference in steady-state levels of the two mRNAs should be attributable, therefore, to differences in mRNA stability. Though one tries to exclude confounding factors that may differentially affect levels of the two mRNAs, they may unknowingly exist when differences between the two genes and mRNAs are large. Thus, minimizing differences between the two genes is desirable, and one has the greatest confidence in drawing conclusions about differential mRNA stability when differences between the mRNAs are minimal. As we developed the comparative mRNA approach, this concern led us to confirm the half-life estimates obtained by this method with half-life estimates obtained by using actinomycin D. Although the latter may be associated with artifacts (35, 43, 50), concurrence of the two estimates lent confidence that our assay is detecting differences in rates of mRNA decay.

Using the RT-PCR+1 assay, we showed that *myc* 3′ UTR removal increases *myc* mRNA half-life to ≥100 min, thereby increasing its steady-state levels four- to eightfold, that its fusion lowers chimeric β-globin–*myc* mRNA steady-state levels four- to fivefold, and therefore, that the *myc* 3′ UTR is necessary and sufficient for maintaining low levels of c-*myc* mRNA in proliferating C2C12 cells. Furthermore, our results suggest that sequences between the *Nsi*I site, 75 nt downstream of the translation termination codon, and the first *myc* AAUAAA are mostly responsible for its effects. This is consistent with previous actinomycin D studies on naturally occurring (1, 23) and recombinant (21, 24) mutant *myc* mRNAs suggesting that the *myc* 3′ UTR functions as an instability element. Interestingly, this region contains two AUUUA elements as well as AU-rich regions thought to be important for the instability of other labile mRNAs (42, 43). However, the importance of the *myc* 3′ UTR for determining *myc* mRNA instability has been clouded by other actinomycin D studies showing that the *myc* 3′ UTR is dispensable for the normal instability of *myc* mRNA (28) and that mutation of the AUUUA pentamers does not affect *myc* mRNA turnover (8). In addition, studies of cycloheximide induction of *myc* mRNA levels suggested that mRNAs missing the normal 3′ UTR are unstable. Rapid, marked induction of *myc* mRNA following inhibition of protein synthesis results mostly from mRNA stabilization and reflects its rapid turnover prior to translation inhibition (32, 50); that mutant *myc* mRNAs, such as *myc*(X/N) mRNA, are rapidly induced (50) argues against the increased stability of 3′ truncated *myc* mRNAs. These discrepancies concerning the role of the *myc* 3′ UTR might be due to drug artifacts in some of these studies or might be reconciled by the presence of two instability determinants, one in the protein-coding region of exon 3 and one in the 3′ UTR. This has been convincingly shown for c-*fos* mRNA (41, 43) and is suggested by studies of *myc* mRNA (5, 21, 50). If there are dual instability determinants, the likelihood that they exert their effects in different cells or under different conditions could explain the discrepancies. This possibility is supported by the observation that deletion of 3′ UTR sequences does not abolish the posttranscriptional downregulation of *myc* mRNA during C2C12 differentiation. In proliferating C2C12 myoblasts, however, only the element in the *myc* 3′ UTR appears to operate.

The other major putative instability determinant identified

in c-*myc* mRNA resides in the protein-coding domain of exon 3. Deletion of this region alone did not increase *myc* mRNA levels in proliferating C2C12 cells, and deletion of exon 3 coding and 3′ UTR sequences did not increase mRNA levels more than deletion of 3′ UTR sequences alone. These data indicate that sequences in the protein-coding domain of *myc* exon 3 do not regulate steady-state *myc* mRNA levels in these cells and are at odds with the results of some other studies (5, 21, 50). Exon 3 coding sequences were initially implicated as a translation-dependent *myc* mRNA instability determinant by cycloheximide induction studies and shown to function as such by decay studies with CAT-*myc* fusion mRNAs transiently transcribed from a c-*fos* serum-inducible promoter (50). Other studies also support the role of this region as an instability determinant (5, 21), and our current study unequivocally shows that it has a destabilizing effect when fused to β-globin mRNA. Comparative β-globin–*myc* mRNA assays showed that fusion of *myc* exon 3 protein-coding sequences lowers the level of β-globin mRNA four- to fivefold, and actinomycin D studies showed that this fusion mRNA decays over five times faster than β-globin mRNA. The apparent discrepancy between the results of the comparative *myc* mRNA and β-globin–*myc* fusion mRNA studies might be explained by an extreme susceptibility of β-globin mRNA to destabilization. An alternative (and not mutually exclusive) explanation might be that the *myc* exon 3 coding region functions as a destabilizing element in special contexts or circumstances and is revealed in proliferating C2C12 cells when fused to β-globin mRNA but not in its normal *myc* mRNA context. The importance of context is highlighted by mRNA decay rates after actinomycin D treatment, which demonstrate that β-globin mRNA is destabilized by *myc* exon 3 coding sequences even in the presence of actinomycin D (this study and reference 21), while the destabilizing function of these sequences in a *myc* context is masked by actinomycin D (50). If this is the case, what is the relevancy of the destabilizing property of the *myc* exon 3 coding region? We do not have a definitive answer to this question at this time, but during C2C12 myogenic differentiation, exon 3 coding sequences are necessary for normal posttranscriptional downregulation of c-*myc* mRNA. This contrasts with *myc* 3′ UTR sequences which, though clearly important for maintaining steady-state levels in proliferating C2C12 cells, are dispensable for downregulation during differentiation. Thus, in its normal *myc* mRNA context in C2C12 myoblasts, exon 3 coding sequences may not function as an instability determinant in proliferating cells but may do so in differentiating cells. Further study should reveal whether *myc* exon 3 coding sequences, while critical for the overall normal regulation of c-*myc* mRNA, function as an instability element in proliferating C2C12 cells only when fused to β-globin mRNA.

Other *myc* mRNA sequences do not appear to have a role in regulating steady-state levels in proliferating C2C12 cells. We were unable to demonstrate any destabilizing effect of *myc* exon 2 sequences in the normal *myc* context, and their effect in a heterologous globin context is so slight as to be of questionable significance. Lavenu et al. (30) demonstrated that exon 2 sequences are important for posttranscriptional determination of c-*myc* mRNA levels in the normal and regenerating liver. The variance with our results obtained in C2C12 myoblasts may be due to tissue specificity of the exon 2 effect. Exon 1 has also been implicated as a c-*myc* mRNA instability determinant on the basis of the finding that *myc* transcripts missing exon 1 sequences from translocated alleles in B-cell lymphomas have prolonged half-lives (18, 37, 40). Another explanation is that these mRNAs are more stable because their leader contains unusual sequences brought in by translocation. Our studies favor the latter explanation because a mutant *myc* mRNA missing most of exon 1 and not containing novel leader sequences is found at the same level as a near-normal *myc* mRNA containing almost all of exon 1.

In conclusion, we have used a method for accurately comparing steady-state mRNA levels of mutant *myc* and globin-*myc* fusion mRNAs to determine which *cis*-acting elements in c-*myc* mRNA function as instability determinants and regulate steady-state mRNA levels. Our data demonstrate that *myc* 3′ UTR sequences are necessary and sufficient for this function. We also demonstrate that an element in the protein-coding domain of exon 3 can act independently to destabilize a heterologous mRNA but is unimportant for maintaining normal steady-state *myc* mRNA levels in proliferating myoblasts. We further demonstrate that these exon 3 coding sequences, but not *myc* 3′ UTR sequences, are necessary for the normal posttranscriptional downregulation of c-*myc* mRNA during myoblast differentiation. Ongoing work will further localize the 3′ UTR element(s) regulating steady-state *myc* mRNA levels and characterize the different functional roles of the exon 3 coding region and 3′ UTR sequences.

ACKNOWLEDGMENTS

We thank Stephen Liebhaber for providing the β-globin cDNA clone and Xinkang Wang for providing rpL32. We also thank Eric Russell, Holly Kurzawa, and Christina M. Coughlin for critical reading of the manuscript.

This work was supported by a National Research Service Award GM16261-01 (N.M.Y.), a Clinical Investigator Award AR01956 (N.M.Y.), and a U.S. Public Health Service grant GM47147 (W.M.F.L.) from the National Institutes of Health, and by an American Cancer Society Faculty Research Award FRA-406 (W.M.F.L.).

REFERENCES

1. **Aghib, D. F., J. M. Bishop, S. Ottolenghi, A. Guerrasio, A. Serra, and G. Saglio.** 1990. A 3′ truncation of MYC caused by chromosomal translocation in a human T-cell leukemia increases mRNA stability. Oncogene 5:707–711.
2. **Amara, F. M., F. Y. Chen, and J. A. Wright.** 1994. Phorbol ester modulation of a novel cytoplasmic protein binding activity at the 3′-untranslated region of mammalian ribonucleotide reductase R2 mRNA and role in message stability. J. Biol. Chem. 269:6709–6715.
3. **Battey, J., C. Moulding, R. Taub, W. Murphy, T. Stewart, H. Potter, G. Lenoir, and P. Leder.** 1983. The human c-*myc* oncogene: structural consequences of translocation into the IgH locus in Burkitt lymphoma. Cell 34: 779–787.
4. **Bentley, D. L., and M. Groudine.** 1986. A block to elongation is largely responsible for decreased transcription of c-*myc* in differentiated HL60 cells. Nature (London) 321:702–706.
5. **Bernstein, P. L., D. J. Herrick, R. D. Prokipcak, and J. Ross.** 1992. Control of c-*myc* mRNA half-life in vitro by a protein capable of binding to a coding region stability determinant. Genes Dev. 6:642–654.
6. **Blanchard, J. M., M. Piechaczyk, C. Dani, J. C. Chambard, A. Franchi, J. Pouyssegur, and P. Jeanteur.** 1985. c-*myc* gene is transcribed at high rate in G0-arrested fibroblasts and is post-transcriptionally regulated in response to growth factors. Nature (London) 317:443–445.
7. **Blau, H. M., G. K. Pavlath, E. C. Hardeman, C.-P. Chiu, L. Silberstein, S. G. Webster, S. C. Miller, and C. Webster.** 1985. Plasticity of the differentiated state. Science 230:758–766.
8. **Bonnieu, A., P. Roux, L. Marty, P. Jeanteur, and M. Piechaczyk.** 1990. AUUUA motifs are dispensable for rapid degradation of the mouse c-*myc* RNA. Oncogene 5:1585–1588.
9. **Borriello, F., and K. S. Krauter.** 1990. Reactive site polymorphism in the murine protease inhibitor gene family is delineated using a modification of the PCR reaction (PCR+1). Nucleic Acids Res. 18:5481–5487.
10. **Caput, D., B. Beutler, K. Hartog, R. Thayer, S. Brown-Shimer, and A. Cerami.** 1986. Identification of a common nucleotide sequence in the 3′-untranslated region of mRNA molecules specifying inflammatory mediators. Proc. Natl. Acad. Sci. USA 83:1670–1674.
11. **Church, G. M., and W. Gilbert.** 1984. Genomic sequencing. Proc. Natl. Acad. Sci. USA 81:1991–1995.
12. **Dani, C., J. M. Blanchard, M. Piechaczyk, S. El Sabouty, L. Marty, and P. Jeanteur.** 1984. Extreme instability of *myc* mRNA in normal and transformed human cells. Proc. Natl. Acad. Sci. USA 81:7046–7050.
13. **Dean, M., R. A. Levine, and J. Campisi.** 1986. c-*myc* regulation during

retinoic acid-induced differentiation of F9 cells is posttranscriptional and associated with growth arrest. Mol. Cell. Biol. 6:518–524.
14. **Dean, M., R. A. Levine, W. Ran, M. S. Kindy, G. E. Sonenshein, and J. Campisi.** 1986. Regulation of c-*myc* transcription and mRNA abundance by serum growth factors and cell contact. J. Biol. Chem. 261:9161–9166.
15. **Dony, C., M. Kessel, and P. Gruss.** 1985. Post-transcriptional control of *myc* and *p53* expression during differentiation of the embryonal carcinoma cell line F9. Nature (London) 317:637–639.
16. **Dudov, K. P., and R. P. Perry.** 1984. The gene family encoding the mouse ribosomal protein L32 contains a uniquely expressed intron-containing gene and an unmutated processed gene. Cell 37:457–458.
17. **Eick, D., and G. W. Bornkamm.** 1986. Transcriptional arrest within the first exon is a fast control mechanism in c-*myc* gene expression. Nucleic Acids Res. 14:8331–8346.
18. **Eick, D., M. Piechaczyk, B. Henglein, J. M. Blanchard, R. Traub, E. Koffler, S. Wiest, G. M. Lenoir, and G. W. Bornkamm.** 1985. Aberrant c-*myc* mRNAs of Burkitt's lymphoma have longer half-lives. EMBO J. 4:3717–3725.
19. **Greenberg, M. E., and E. B. Ziff.** 1984. Stimulation of 3T3 cells induces transcription of the c-*fos* proto-oncogene. Nature (London) 311:433–438.
20. **Grosso, L. E., and H. C. Pitot.** 1985. Transcriptional regulation of c-*myc* during chemically induced differentiation of HL-60 cultures. Cancer Res. 45:847–850.
21. **Herrick, D. J., and J. Ross.** 1994. The half-life of c-*myc* mRNA in growing and serum-stimulated cells: influence of the coding and 3' untranslated regions and role of ribosome translocation. Mol. Cell. Biol. 14:2119–2128.
22. **Hirt, B.** 1967. Selective extraction of polyoma DNA from infected mouse cell cultures. J. Mol. Biol. 26:365–369.
23. **Hollis, G. F., A. F. Gazdar, V. Bertness, and I. R. Kirsch.** 1988. Complex translocation disrupts c-*myc* regulation in a human plasma cell myeloma. Mol. Cell. Biol. 8:124–129.
24. **Jones, T. R., and M. D. Cole.** 1987. Rapid cytoplasmic turnover of c-*myc* mRNA: requirement of 3' untranslated sequences. Mol. Cell. Biol. 7:4513–4521.
25. **Knight, E., Jr., E. D. Anton, D. Fahey, B. K. Friedland, and G. J. Jonak.** 1985. Interferon regulates c-*myc* gene expression in Daudi cells at the post-transcriptional level. Proc. Natl. Acad. Sci. USA 82:1151–1154.
26. **Krystal, G., M. Birrer, J. Way, M. Nau, E. Sausville, C. Thompson, J. Minna, and J. Battey.** 1988. Multiple mechanisms for transcriptional regulation of the *myc* gene family in small-cell lung cancer. Mol. Cell. Biol. 8:3373–3381.
27. **Laird-Offringa, I. A., P. Elfferich, H. J. Knaken, J. de Ruiter, and A. J. van der Eb.** 1989. Analysis of polyadenylation site usage of the c-*myc* oncogene. Nucleic Acids Res. 17:6499–6514.
28. **Laird-Offringa, I. A., P. Elfferich, and A. J. van der Eb.** 1991. Rapid c-*myc* mRNA degradation does not require (A + U)-rich sequences or complete translation of the mRNA. Nucleic Acids Res. 19:2387–2394.
29. **Laski, F. A., B. Alzner-DeWeerd, U. L. RajBhandary, and P. A. Sharp.** 1982. Expression of a *X. laevis* $tRNA^{Tyr}$ gene in mammalian cells. Nucleic Acids Res. 10:4609–4626.
30. **Lavenu, A., S. Pistoi, S. Pournin, C. Babinet, and D. Morello.** 1995. Both coding exons of the c-*myc* gene contribute to its posttranscriptional regulation in the quiescent liver and regenerating liver and after protein synthesis inhibition. Mol. Cell. Biol. 15:4410–4419.
31. **Levine, R. A., J. E. McCormack, A. Buckler, and G. E. Sonenshein.** 1986. Transcriptional and posttranscriptional control of c-*myc* gene expression in WEHI 231 cells. Mol. Cell. Biol. 6:4112–4116.
32. **Linial, M., N. Gunderson, and M. Groudine.** 1985. Enhanced transcription of c-*myc* in bursal lymphoma cells requires continuous protein synthesis. Science 230:1126–1132.
33. **McMaster, G. K., and G. C. Carmichael.** 1977. Analysis of single- and double-stranded nucleic acids on polyacrylamide and agarose gels by using glyoxal and acridine orange. Proc. Natl. Acad. Sci. USA 74:4835–4838.
34. **Mechti, N., M. Piechaczyk, J. M. Blanchard, L. Marty, A. Bonnieu, P. Jeanteur, and B. Lebleu.** 1986. Transcriptional and post-transcriptional regulation of c-*myc* expression during the differentiation of murine erythroleukemia Friend cells. Nucleic Acids Res. 14:9653–9666.
35. **Mullner, E. W., and L. C. Kuhn.** 1988. A stem-loop in the 3' untranslated region mediates iron-dependent regulation of transferrin receptor mRNA in the cytoplasm. Cell 53:815–825.
36. **Nepveu, A., and K. B. Marcu.** 1986. Intragenic pausing and anti-sense transcription within the murine c-*myc* locus. EMBO J. 5:2859–2865.
37. **Piechaczyk, M., A. Bonnieu, D. Eick, E. Remmers, J. Q. Yang, K. Marcu, P. Jeanteur, and J. M. Blanchard.** 1986. Altered c-*myc* RNA metabolism in Burkitt's lymphomas and mouse plasmacytomas. Curr. Top. Microbiol. Immunol. 132:331–338.
38. **Piechaczyk, M., J. Q. Yang, J. M. Blanchard, P. Jeanteur, and K. B. Marcu.** 1985. Posttranscriptional mechanisms are responsible for accumulation of truncated c-*myc* RNAs in murine plasma cell tumors. Cell 42:589–597.
39. **Pontecorvi, A., J. R. Tata, M. Phyillaier, and J. Robbins.** 1988. Selective degradation of mRNA: the role of short-lived proteins in differential destabilization of insulin-induced creatine phosphokinase and myosin heavy chain mRNAs during rat skeletal muscle L6 cell differentiation. EMBO J. 7:1489–1495.
40. **Rabbitts, P. H., A. Forster, M. A. Stinson, and T. H. Rabbitts.** 1985. Truncation of exon 1 from the c-*myc* gene results in prolonged c-*myc* mRNA stability. EMBO J. 4:3727–3733.
41. **Schiavi, S. C., C. L. Wellington, A. B. Shyu, C. Y. Chen, M. E. Greenberg, and J. G. Belasco.** 1994. Multiple elements in the c-*fos* protein-coding region facilitate mRNA deadenylation and decay by a mechanism coupled to translation. J. Biol. Chem. 269:3441–3448.
42. **Shaw, G., and R. Kamen.** 1986. A conserved AU sequence from the 3' untranslated region of GM-CSF mRNA mediates selective mRNA degradation. Cell 46:659–667.
43. **Shyu, A.-B., M. E. Greenberg, and J. G. Belasco.** 1989. The c-*fos* transcript is targeted for rapid decay by two distinct mRNA degradation pathways. Genes Dev. 3:60–72.
44. **Siebenlist, U., P. Bressler, and K. Kelly.** 1988. Two distinct mechanisms of transcriptional control operate on c-*myc* during differentiation of HL60 cells. Mol. Cell. Biol. 8:867–874.
45. **Stone, J., T. de Lange, G. Ramsay, E. Jakobovits, J. M. Bishop, H. Varmus, and W. Lee.** 1987. Definition of regions in human c-*myc* that are involved in transformation and nuclear localization. Mol. Cell. Biol. 7:1697–1709.
46. **van den Hoff, M. J., W. T. Labruyere, A. F. Moorman, and W. H. Lamers.** 1993. Mammalian gene expression is improved by use of a longer SV40 early polyadenylation cassette. Nucleic Acids Res. 21:4987–4988.
47. **Weiss, I. M., and S. A. Liebhaber.** 1994. Erythroid cell-specific determinants of α-globin mRNA stability. Mol. Cell. Biol. 14:8123–8132.
48. **Weiss, I. M., and S. A. Liebhaber.** 1995. Erythroid cell-specific mRNA stability elements in the α2-globin 3' nontranslated region. Mol. Cell. Biol. 15:2457–2465.
49. **Wisdom, R., and W. Lee.** 1990. Translation of c-*myc* mRNA is required for its post-transcriptional regulation during myogenesis. J. Biol. Chem. 265: 19015–19021.
50. **Wisdom, R., and W. Lee.** 1991. The protein-coding region of c-*myc* mRNA contains a sequence that specifies rapid mRNA turnover and induction by protein synthesis inhibitors. Genes Dev. 5:232–243.

BIOCHEMICAL AND BIOPHYSICAL RESEARCH COMMUNICATIONS 227, 707–711 (1996)
ARTICLE NO. 1573

An Enhanced Green Fluorescent Protein Allows Sensitive Detection of Gene Transfer in Mammalian Cells

Guohong Zhang,[1] Vanessa Gurtu, and Steven R. Kain

Clontech Laboratories, Inc., 1020 East Meadow Circle, Palo Alto, California 94303

Received August 27, 1996

The green fluorescent protein (GFP) from the jellyfish *Aequorea victoria* has become an important marker of gene expression. However, the sensitivity of wild-type GFP has been below that of standard reporter proteins, such as β-galactosidase, which utilize enzymatic amplification. To improve the detection of GFP in transfected mammalian cells, we have constructed a unique GFP variant which contains chromophore mutations that make the protein 35 times brighter than wild-type GFP, and is codon-optimized for higher expression in mammalian cells. These changes in the GFP coding sequence provide an enhanced GFP (EGFP) that greatly increases the sensitivity of the reporter protein. We show that the EGFP expression vector delivered into mammalian cells gives rise to bright fluorescence that is readily detectable following a 16-24 hr transfection interval. Visual detection of transfected cells with EGFP appears to be more sensitive than equivalent measurements with β-galactosidase catalyzed conversion of the X-gal substrate. We conclude that EGFP allows sensitive and convenient detection of gene transfer in mammalian cells.

The introduction of a foreign gene into a cell is of great interest both for basic research and gene therapy. For example, transient transfection of plasmid DNA is a commonly used method to investigate transcriptional regulation and gene expression (1). Transfection of cultured cells is also a common model system in gene therapy applications to develop DNA delivery systems. In many cases, transfection efficiency is measured in order to monitor whether the gene of interest is efficiently delivered into cells, and/or to normalize transcriptional activity (1, 2).

There are a number of *in vitro* reporter genes, such as secreted alkaline phosphatase [SEAP; (3, 4)], β-galactosidase [β-gal; (5)], firefly luciferase (6), and chloramphenicol acetyltransferase [CAT; (7)], available for quantifying transfection efficiencies. However, these reporter activities assayed in conditioned medium or cellular extracts of transfected cells provide a somewhat indirect measurement of the efficiency of gene transfer. *In vivo* reporter assays, such as *in situ* β-gal staining (5), *in situ* β-glucuronidase [GUS; (9)] and *in situ* luciferase (10) assays are also available for detecting gene transfer in either fixed cells or tissue sections. These procedures allow visualization of transfected cells following staining with enzymatic substrates or antibodies (8). Among these procedures, *in situ* β-gal staining following expression of the *E. coli LacZ* gene is a widely used method because of its simplicity and sensitivity. In this procedure, reaction of β-gal with the X-gal substrate produces a rich blue color that can be easily visualized under a light microscope, and therefore, provides a direct assessment of transfection efficiency (1, 18). However, in this assay transfected cultures need to be fixed and reacted with substrates

[1] Corresponding author. Fax: (415) 354-0776.

Abbreviations used: GFP, green fluorescent protein; wtGFP, wild-type GFP; EGFP, enhanced GFP; β-gal, β-galactosidase; SEAP, secreted alkaline phosphatase; CAT, chloramphenicol acetyltransferase; GUS, β-glucuronidase; CMV, cytomegalovirus; MCS, multiple cloning site.

0006-291X/96 $18.00

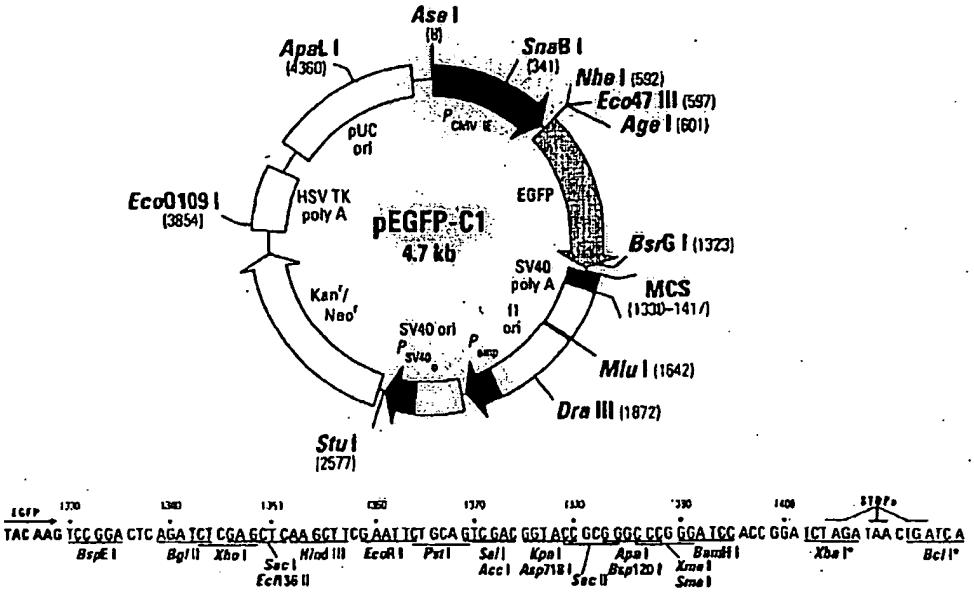

FIG. 1. Map of pEGFP-C1 and Multiple Cloning Site (MCS). The vector pEGFP-C1 (CLONTECH) contains the immediate early promoter of human CMV and SV40 polyadenylation signals to drive expression of the EGFP gene in mammalian cells. This vector contains a multiple cloning site (MCS) on the 3' end of the egfp gene, and can be used to create in-frame fusions to the C-terminus of EGFP. The egfp gene of pEGFP-C1 encodes a variant chromophore sequence, and has been codon-optimized for maximal expression and fluorescence intensity in mammalian cells.

to detect transfected cells. Thus, the cultures used for β-gal staining experiments must be produced separately from those utilized to analyze the specific gene of interest.

The green fluorescent protein (GFP) from the jellyfish *Aequorea victoria* has become an important reporter for monitoring gene expression and protein localization in a variety of cells and organisms (11, 12). GFP expressed in eukaryotic cells yields green fluorescence when cells are excited by ultraviolet (UV) or blue light. The chromophore in GFP is intrinsic to the primary structure of the protein, and fluorescence from GFP does not require additional cofactors, substrates, or additional gene products (11, 13). Moreover, GFP fluorescence is stable, species-independent, and can be monitored noninvasively using techniques of fluorescence microscopy, flow cytometry, and macroscopic imaging (11, 12, 14). Therefore, GFP provides an attractive means for direct measurement of transfection efficiency in transient transfection assays.

Wild-type GFP has several undesirable properties including low fluorescent intensity when excited by blue light, a lag in the development of fluorescence after protein synthesis, and poor expression in several mammalian cell types (13, 15, 20). Thus, the sensitivity of wild-type GFP has been below that of standard reporter proteins, such as β-gal, which utilize enzymatic amplification. To improve the detection of GFP in transfected mammalian cells, we have constructed a unique GFP variant (EGFP) which contains chromophore mutations that make the protein 35 times brighter than wild-type GFP (16). The EGFP variant is also codon-optimized by using the favored codons of highly expressed human proteins in place of the corresponding "jellyfish" codons for higher expression in mammalian cells (17). We found that these changes in the GFP coding sequence greatly increases the sensitivity of the reporter

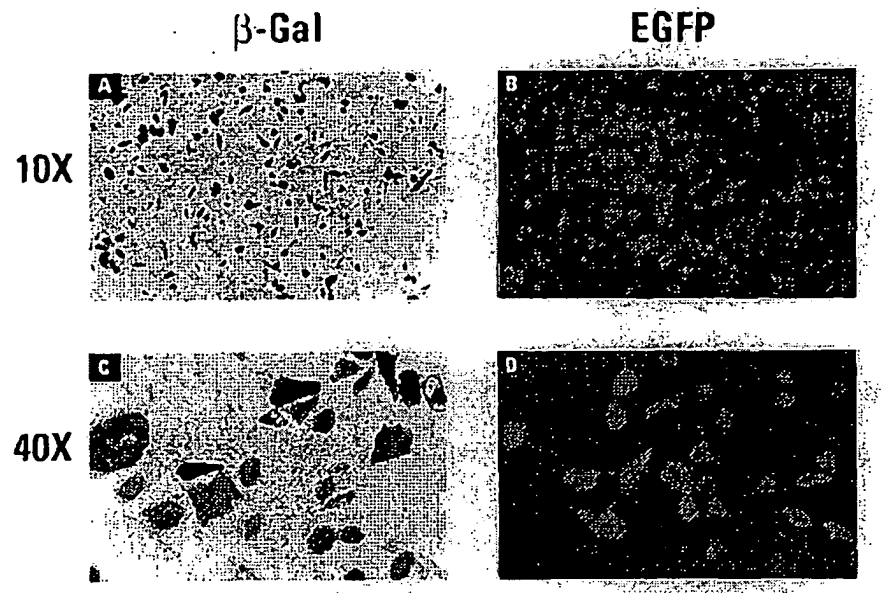

FIG. 2. Visualization of EGFP and β-Gal Expression in CHO-K1 Cells. CHO-K1 Cells were transfected with pCMVβ (A, C) and pEGFP-C1 (B, D) using CLONfectin. At 24 hour post-transfection, EGFP fluorescence was visualized and photographed directly under a Zeiss fluorescence microscope (B, D). Blue-colored β-gal positive cells were visualized and photographed at the same time point with a Leica light microscope following fixation and staining of the cells with X-gal substrate as described in Methods (A, C). A and B, 10× magnification; C and D, 40× magnification.

protein. Here, we demonstrate the utility of pEGFP as a non-invasive, sensitive and convenient marker for direct measurement of transfection efficiency in transient transfection assays.

MATERIALS AND METHODS

Cell culture and reagents. CHO-K1 cells were cultured in Ham's F-12 medium supplemented with 10% fetal bovine serum (FBS). BHK-21, COS-1 and HeLa cells were cultured in DMEM medium supplemented with 10% FBS. All cell lines were obtained from ATCC (Rockville, MD, USA). Media for all cultures routinely included 100 units/ml of penicillin and 100 μg/ml of streptomycin. All media, sera, and other supplements were purchased from Sigma Chemical Co. (St. Louis, MO). Cultures were maintained at 37°C with 5% CO_2/95% air.

Transfection reagents and methods. CLONfectin transfection reagent is from CLONTECH Laboratories, Inc. (Palo Alto, CA, USA), and is used according to the manufacturer's protocol. For each of the mammalian cell lines used in these studies, 8×10^5 cells per well were seeded in 60-mm tissue culture plates one day prior to transfections, and grown in the appropriate medium supplemented with serum. The cultures were 60-80% confluent at the time of transfection. Cells were transfected with 6 μg plasmid DNA per plate.

Plasmid vectors and assays. pEGFP-C1 expression vector was constructed (Fig. 1; see Results below for detail) and used to evaluate the feasibility of using EGFP expression as a sensitive marker for transfection. The vector contains an immediate early promoter of human cytomegalovirus (CMV) to drive expression of the EGFP gene in mammalian cells. For determining the actual transfection efficiencies, both fluorescent and non-fluorescent cells were scored in 4-6 representative fields at 40× magnification using a Zeiss Axioskop fluorescence microscope equipped with a fluorescein or GFP filter set (Chroma Technology, Inc., Brattleboro, VT). For comparison studies, we also transfected pCMVβ (CLONTECH) encoding the *E. coli LacZ* gene, also driven by the CMV immediate early promoter. The β-galactosidase expression was detected by *in situ* staining using the X-gal substrate as described previously (5, 18). Briefly, 24 hrs after transfection, cells were rinsed in phosphate-buffered saline (PBS), fixed in 2% formaldehyde and 0.2% glutaraldehyde in PBS, rinsed twice with PBS, and stained for 2 hours with 0.1% X-gal in PBS containing 5 mM potassium ferricyanide and 2 mM $MgCl_2$. Cells were photographed on a Leica Leitz light Microscope (Leica Inc., Foster City, CA).

TABLE I
Comparison of Transfection Efficiencies Detected by EGFP Fluorescence and β-Gal Staining

Cell lines	%EGFP Positive cells	%β-Gal Positive cells
CHO-K1	66.8 ± 16.4	39.8 ± 3.8
COS-1	63.5 ± 21.1	35.9 ± 5.4
HeLa	25.4 ± 6.3	14.0 ± 6.0
BHK-21	51.8 ± 14.6	59.8 ± 5.1

Note. Cells were transfected with pEGFP-C1 and pCMVβ, individually, using CLONfectin transfection reagent as described in Methods. EGFP fluorescent cells were counted directly using a Zeiss fluorescence microscope 24 hours following transfection. β-gal positive cells were scored at the same time point using a Leica light microscope following fixation and staining with X-gal substrate as described in Methods. The total cell number was determined by phase contrast. 4–6 representative fields were scored for each transfection and data represent the mean ± standard deviations.

RESULTS AND DISCUSSION

Wild type GFP exhibits lower fluorescence intensity which is hard to detect in several mammalian cell types (13, 15, 20). To improve upon these qualities, we have constructed the vector pEGFP-C1 (Fig. 1) which encodes a variant GFP protein described as GFPmut1 (16). This variant contains two point mutations in the GFP chromophore: Ser65 to Thr and Phe64 to Leu. The GFPmut1 variant generates approximately 35 fold brighter fluorescence relative to wild type GFP when excited by blue light, and has improved solubility, and more efficient protein folding characteristics (16). In addition, we have used the favored codons that are highly expressed in human proteins to replace the corresponding "jellyfish" codons to further improve the expression of the GFP variant in mammalian cells. These changes greatly increases the sensitivity of the reporter protein.

In situ β-gal staining is a commonly used and well accepted procedure for monitoring the actual efficiency of gene transfer (5, 8, 18). However, the procedure involves fixation and staining steps which require separate cultures and additional time and effort before the actual transfected cells are visualized. To determine whether pEGFP-C1 expression vector can be used effectively as a direct marker for gene transfer, we performed side-by-side transfections with pCMVβ and pEGFP-C1 expression vectors in CHO-K1 cells. Fig. 2 shows the representative fields of transfected cultures for both β-gal staining (Panel A, C) and EGFP fluorescence (Panel B, D) at low (A, B) and high (C, D) magnifications. Cells transfected with pEGFP gave rise to bright fluorescence that are directly detected under a fluorescence microscope. Cells transfected with pCMVβ were fixed and stained with the X-gal substrate before they were visualized under a light microscope. Both pEGFP-C1 and pCMVβ transfected cultures were visualized 24 hours following transfections. We observed that 40% of the cells are β-gal positive, whereas 60% of cells are EGFP positive. These data suggest that detection of EGFP expression provides better sensitivity than detection of β-gal expression using X-gal as a substrate.

To evaluate whether EGFP can be used to effectively monitor gene transfer and expression in a variety of mammalian cells, we transfected a number of additional mammalian cell lines

each with pCMVβ and pEGFP-C1. pEGFP-C1 expression was readily detectable in all cell lines tested, including CHO-K1, COS-1, HeLa, and BHK-21 cells. Table I summarizes the transfection efficiency monitored by both β-gal staining and EGFP expression. For each of these cell lines tested, we scored β-gal and EGFP positive cells as well as total cells in 4-6 representative fields of the transfected cultures. Data show that transfections with pCMVβ and pEGFP-C1 expression vectors detected comparable transfection efficiencies in BHK-21 cells, whereas in CHO-K1, COS-1 and HeLa cell lines, we visualized a higher percentage of cells positive for EGFP than for β-gal detection (Table I). These results indicate that visual detection of transfected cells with EGFP appears to be more sensitive than equivalent measurements with β-gal catalized conversion of the X-gal substrate. We have also noted that the signal-to-noise ratio for the EGFP expression is excellent for visual detection.

The use of EGFP has several advantages over the existing reporter markers, such as the *in situ* β-gal assay. First, EGFP requires no additional cofactors, substrates or additional gene products to fluoresce (11, 14, 19). Thus, it is superior to the β-gal enzyme which requires X-gal as a substrate to detect transfected cells. Second, since EGFP can be visualized directly under a fluorescence microscope without killing the cells, use of the EGFP allows researchers to analyze specific genes of interest in the same cultures that are used to monitor transfection efficiency. Third, since no extra steps or addition of reagents are required to produce EGFP fluorescence following transfection, use of EGFP to monitor gene transfer saves time and effort. Therefore, we conclude that EGFP provides a sensitive and convenient marker for direct measurement of transfection efficiency in transient transfection assays.

ACKNOWLEDGMENTS

We express our appreciation to Dr. Paul Kitts for helpful information on construction of the pEGFP-C1 vector. We also thank Theresa Provost for the preparation of the figures. We greatly acknowledge Dr. Paul Diehl and Nicola Zahl for careful reading of the manuscript and useful discussion.

REFERENCES

1. Ausubel, F. M., Brent, R., Kingston, R. E., Moore, D. D., Seidman, J. G., Smith, J. A., and Struhl, K. (1994) *in* Current Protocols in Molecular Biology, Vol. 1, Ch. 9, John Wiley & Sons, Inc., NY.
2. Felgner, P. L., and Ringold, G. M. (1989) *Nature* 337, 387–388.
3. Berger, J., Hauber, J., Hauber, R., Geiger, R., and Cullen, B. R. (1988) *Gene* 66, 1–10.
4. Kain, S. R. *in* Methods of Molecular Biology Series: Expression and Detection of Recombinant Genes (Tuan, R. S., Ed.), Humana Press, New Jersey, in press.
5. Alam, J., and L., c. J. (1990) *Anal. Biochem.* 188, 245–254.
6. de Wet, J. R., Wood, K. V., DeLuca, M., Helinski, D. R., and Subramani, S. (1987) *Mol. Cell. Biol.* 7, 725–737.
7. Gorman, C. M., Moffat, L. G., and Howard, B. H. (1982) *Mol. Cell. Biol.* 2, 1044–1051.
8. Kain, S. R., and Ganguly, S. (1995) *in* Current Protocols in Molecular Biology, John Wiley & Sons, New York.
9. Jefferson, R. A., Kavanagh, T. A., and Bevan, M. W. (1987) *EMBO J.* 6, 3901–3907.
10. Bronstein, I., Fortin, J., Stanley, P. E., Stewart, G. S., and Kricka, L. J. (1994) *Anal. Biochem.* 219, 169–181.
11. Chalfie, M., Tu, Y., Euskirchen, G., Ward, W. W., and Prasher, D. C. (1994) *Science* 263, 802–805.
12. Kain, S. R., Adams, M., Kondepudi, A., Yang, T. T., Ward, W. W., and Kitts, P. (1995) *BioTechniques* 19, 650–655.
13. Stearns, T. (1995) *Current Biology* 5, 262–264.
14. Inouye, S., and Tsuji, F. I. (1994) *FEBS Letters* 341, 277–280.
15. Haas, J., Park, E. C., and Seed, B. (1996) *Current Biology* 6, 315–324.
16. Cormack, B. P., Valdivia, R., and Falkow, S. (1996) *Gene* 173, 33–38.
17. Chiu, W. L., Niwa, Y., Zeng, W., Hirano, T., Kobayashi, H., and Sheen, J. (1996) *Current Biology* 6, 325–330.
18. Zhang, G., and Kain, S. R. (1996) *BioTechniques*, in press.
19. Cody, C. W., Prasher, D. C., Westler, W. M., Prendergast, F. G., and Ward, W. W. (1993) *Biochemistry* 32, 1212–1218.
20. Heim, R., Cubitt, A. B., and Tsien, R. Y. (1995) *Nature* 373, 663–664.